PHYSICAL CHEMISTRY OF THE REACTIONS OF SOME METALS WITH MOLTEN NITRATES

A thesis

submitted for the

Degree of Doctor of Philosophy

in the University of London

by

Brian David Bond, A.R.C.S., B.Sc.

Chemistry Department,
Imperial College,
London, S.W.7.

June, 1963.

ABSTRACT.

A kinetic study of the thermal decomposition of sodium nitrate and of magnesium-sodium nitrate mixtures has been made by means of thermogravimetry and self-heating measurements. The replacement of magnesium in the mixtures by other metals and metallic oxides (e.g. Al, MgO and Al_2O_3) has been investigated, as was the thermogravimetry of sodium nitrite.

The decomposition of sodium nitrate was found to occur in two stages: (i) decomposition of the nitrate to sodium nitrite, and (ii) the subsequent breakdown of the nitrite to sodium oxide. However, in the decomposition of the magnesium-sodium nitrate mixtures, separate steps in the reaction were not observed. The mechanism of these reactions is considered in some detail.

The effect of variations in the surrounding atmosphere on the mechanism of these reactions was studied by performing thermogravimetric and self-heating measurements in an atmosphere of argon.

ACKNOWLEDGMENTS.

I wish to express my gratitude to my supervisor, Dr. P.W.M. Jacobs, for his constant advice and interest throughout this work, and invaluable guidance during the preparation of this thesis. I also wish to thank Professor R.M. Barrer, F.R.S., for the provision of laboratory facilities. I would like to thank the War Office for the award of a bursary and the Pyrotechnics Research Section of A.R.D.E., Langhurst, for their helpful co-operation throughout the period of this research.

INDEX

		Page
1.	Introduction	1
1.1.	Pyrotechny	1
1.1.1.	General	1
1.1.2.	Experimental techniques for the study of pyrotechnic compositions	2
1.2.	Thermal decomposition of nitrates	6
1.2.1.	Ammonium nitrate	7
1.2.2.	Lead nitrate	8
1.2.3.	Potassium nitrate	9
1.3.	Thermal decomposition of sodium nitrate	9
1.4.	Thermal decomposition of magnesium-sodium nitrate mixtures	14
2.	Experimental	16
2.1.	Apparatus for the study of thermal decomposition by weight loss measurements	16
2.2.	Apparatus to measure self-heating	17
2.3.	Materials and preparation of the samples	20
3.	Results	21
3.1.	Thermogravimetry in air	21
3.1.1.	Thermal decomposition of sodium nitrate	21
3.1.2.	Thermal decomposition of the mixture 4.45% Mg + 95.55% $NaNO_3$	25
3.1.3.	Thermal decomposition of the mixture 11.12% Mg + 88.88% $NaNO_3$	25
3.1.4.	Thermal decomposition of the mixture 15.57% Mg + 84.43% $NaNO_3$	28
3.1.5.	Thermal decomposition of the mixture 22.25% Mg + 77.75% $NaNO_3$	29
3.1.6.	The effect of variation in the magnesium content of the mixture at constant temperature	30

Page

3.2. Thermogravimetry in argon 31

3.2.1. Thermal decomposition of sodium nitrate 31

3.2.2. Thermal decomposition of the mixture 11.12% Mg + 88.88% $NaNO_3$ 33

3.2.3. Thermal decomposition of the mixture 22.25% Mg + 77.75% $NaNO_3$ 34

3.3. Thermogravimetry involving other additives 35

3.4. Measurement of self-heating in the thermal decomposition of sodium nitrate and magnesium + sodium nitrate mixtures 38

3.4.1. Treatment of the data 38

3.4.2. Variation of temperature 40

3.4.2.1. Runs performed at atmospheric pressure 40

3.4.2.2. Runs performed at 10^{-4} mm Hg pressure 44

3.4.3. Variation of pressure 45

3.4.4. Variation of magnesium content 48

3.4.5. Variation in atmosphere 53

4. Discussion 56

4.1. Thermogravimetry 56

4.1.1. Avrami-Erofeyev equation 56

4.1.2. "Contracting area" equation 59

4.1.3. Thermal decomposition of sodium nitrate and magnesium-sodium nitrate mixtures 60

4.2. Self-heating 66

4.3. Reaction mechanisms 70

4.3.1. Mechanism of the decomposition of sodium nitrate 70

4.3.2. Mechanism of the decomposition of magnesium-sodium nitrate mixtures 75

References 79

1. INTRODUCTION

1.1 Pyrotechny.

1.1.1. General.

Pyrotechnics are a part of a group of highly exothermic compositions which also include explosives and propellants. The speed of a chemical reaction usually depends upon temperature and upon the intimacy with which the reactants can be brought together. This is particularly relevant to the category of reactions under consideration. If this chemical reaction evolves heat which cannot be dissipated rapidly, then, since chemical reactions accelerate with temperature, self-heating and auto-acceleration tend to occur.

Among these highly exothermic compositions, are on the one hand, compositions such as a very intimately compounded mixture of charcoal, potassium nitrate and sulphur, commonly called 'gunpowder', in which, in addition to being very exothermic, the gaseous volume of the products is large and, hence, an explosive reaction results. In contrast to this, there are the compositions which, although they evolve a considerable amount of heat, do not explode as the products of the reaction are practically non-gaseous. It is this latter category which are termed pyrotechnics; classically they were known as "gas-less, exothermic compositions". In all cases, the exothermicity

is sufficiently great to cause ignition to take place.

Most pyrotechnic compositions devised for military purposes were developed empirically without a knowledge of the reaction mechanisms involved in the propagative ignition. There have been, subsequently, investigations of some of these compositions, particularly by Gordon and his associates in the U.S.A. and by Hill and co-workers in this country, to determine the thermal parameters of ignition and propagative burning, and to elucidate the reaction mechanisms taking place during both the pre-ignition and ignition reactions. The particular techniques mainly used in these studies have been differential thermal analysis, thermogravimetry, time-to-ignition measurements, temperature-profile studies, and, to a lesser extent, heats of combustion and self-heating measurements.

1.1.2. Experimental techniques for the study of pyrotechnic compositions.

Among the first pyrotechnic compositions to be studied by the Gordon school was a pyrotechnic smoke containing zinc, hexachlorobenzene and potassium perchlorate (Gordon and Campbell, 1954). Compositions with various proportions of the three ingredients have also included additives, such as aluminium powder, to modify the burning characteristics. However, the basic ternary pyrotechnic was the composition primarily studied. The differential

thermal analysis apparatus was described in detail in this paper (Gordon and Campbell, 1954) and it has been used in the subsequent work with only minor modifications (Gordon and Campbell, 1955 ; Hogan and Gordon, 1958, 1959a, 1960). The usefulness of differential thermal analysis (DTA) as a tool in the field of pyrotechnics, explosives, etc. can be seen at its best in conjunction with thermogravimetry. A Comparative study of the endothermic and exothermic peak temperatures obtained from the differential thermal analysis curve and those temperatures in thermogravimetry at which weight changes occur (in the field of pyrotechnics these will be, essentially, loss of weight) can yield detailed information about the reaction mechanisms. For the most accurate results, DTA requires a high furnace heating rate, of the order of 10-15°C per minute, whereas thermogravimetry needs a comparatively slow heating rate, of the order of 4°C per minute. Therefore a compromise heating rate is necessary because, for the comparison between the techniques to be satisfactory, the same heating rate for each is required (Garn, 1961).

Thermogravimetry was introduced into the study of pyrotechnics by Gordon in the investigation of the potassium perchlorate-aluminium-barium nitrate compositions (Hogan, Gordon and Campbell, 1957) and the barium peroxide-magnesium-calcium resinate standard pyrotechnic

igniter composition (Hogan and Gordon, 1957). The apparatus used was that described by Gordon (Gordon and Campbell, 1956).

The time-to-ignition measurements apparatus described by Gordon and Campbell (1954) was based on earlier work on explosives (Henkin and McGill, 1952) and this method provides a means of determining the activation energy for the ignition reaction.

The study of the temperature profiles of burning compositions has been very useful, particularly when studying slow-burning materials. As stated by Hill (1954), a temperature profile is, strictly, a curve formed by projecting the temperature distribution in the reaction zone on to a plane parallel to the direction of propagation; but the term may usefully be applied to temperature-time curves, which are easier to measure, obtained by recording the temperature at one particular point with a thermo-couple. Temperature profiles obtained in this manner have been used to decide the mechanism of propagation and the type of reaction (Hill et al, 1950). During this work, it was found that it was sometimes impossible to make useful measurements because of the high temperatures and vigour of some of the reactions. Consequently, Hill in his later work restricted his study of temperature profiles to relatively cool, slow burning compositions such as iron

and potassium permanganate (Hill, 1954; 1957) and molybdenum and potassium permanganate (Hill and Welsh, 1959).

That the temperature profile method is inapplicable to the more vigorous compositions was confirmed during work on delay powders (Nakahara and Hikita, 1959). They showed that where the volume of gaseous products evolved is great the combustion pressure is high and the fine thermocouples which are necessary for accurate profiles, are frequently broken. Hence this method is only applicable to compositions which burn slowly and do not have too high a flame temperature.

Another technique which is often used for studying exothermic reactions is that of determining self-heating temperatures. This may be used to provide purely qualitative information, although the mathematical theory is well developed; summaries have been given by Gray and Harper (1959), and Jacobs and Kureishy (1963).

In self-heating measurements, the reaction mixture is raised to the furnace temperature (T_0) as rapidly as possible and the progress of the reaction is followed by measuring $T(t)$. In DTA, the reactants are heated continuously at a much slower, and usually linear, rate.

1.2 Thermal decomposition of nitrates.

The classical theory of the decomposition of nitrates divides metallic nitrates into three definite groups. The first group contains the more electropositive metals such as sodium and potassium, the second group consists of most metals other than the alkali metals and are typified by copper and zinc. The noble metals, silver and gold, make up the final group. Classical chemistry gives a separate decomposition reaction for each of the groups.

Sodium nitrate, as typical of the more electropositive alkali metals, was believed to decompose on heating to yield sodium nitrite:

$$2NaNO_3 \longrightarrow 2NaNO_2 + O_2$$

The decomposition of the second group metal nitrates was shown to proceed further than the nitrite and the final product was the oxide:

$$2Cu(NO_3)_2 \longrightarrow 2CuO + 4NO_2 + O_2$$

The noble metal nitrate decomposition was complete, the final product being the metal itself:

$$2AgNO_3 \longrightarrow 2Ag + 2NO_2 + O_2$$

Ammonium nitrate, which is a constituent of explosives, has three stages of decomposition. Firstly at lower temperatures

$$NH_4NO_3 \longrightarrow N_2O + 2H_2O$$

then at temperatures above 250°C, it deflagrates with a yellow flame:

$$2NH_4NO_3 \longrightarrow N_2 + 2NO + 4H_2O$$

but at yet higher temperatures it detonates

$$2NH_4NO_3 \longrightarrow 2N_2 + O_2 + 4H_2O$$

The study of the decomposition of nitrates has not been very comprehensive, but the information which has been obtained is summarised in the following paragraphs.

1.2.1. Ammonium nitrate.

As ammonium nitrate is a constituent of several explosive compositions, it has been the most widely studied (Kummer 1947; Feick and Hainer, 1954; Cook and Taylor Abegg, 1956; Kerdivarenko et al, 1957, 1960; Keenan and Dimitriades, 1961, 1962). Kummer showed that the nitrous oxide formed during the decomposition reaction is formed by bond-formation between two nitrogen atoms from the two different groups present in ammonium nitrate rather than by interaction between nitrogen atoms in two similar groups. The decomposition reaction was shown to be first order (Cook et al, 1956) and it was found that, in molten ammonium nitrate, a steady-state temperature is reached as a result of the irreversible exothermic decomposition to nitrous oxide (g) and water (g), and the reversible endothermic dissociation to ammonia (g) and nitric acid (g) (Feick and Hainer, 1954). Kerdivarenko and his associates found an

activation energy of 39.0 kcal/mole for the decomposition reaction in the temperature range 169-230°C (1957). In a later paper (1960) they found an induction period of one hour at 170°C and about one minute at 195°C. However Keenan and Dimitriades (1961), who used the differential rate method to determine the reaction kinetics, found an activation energy of 49.5 kcal/mole in the temperature range 230-265°C.

1.2.2. Lead nitrate.

The decomposition of lead nitrate has been studied by measuring the loss of weight as a function of temperature (Nicol, 1948). It was found that this could be resolved into four stages, with the loss of weight in the first stage being equal to the total loss of the other three, which had equal weight losses. Assuming that each molecule of lead nitrate liberated two molecules of nitrogen dioxide and half a molecule of oxygen, the following products were identified:

(1) at 445°C; $PbO.Pb(NO_3)_2$

(2) 445-455°C; $4PbO.Pb(NO_3)_2$

(3) 455-470°C; $5PbO.Pb(NO_3)_2$

(4) above 470°C; a mixture of PbO and Pb_3O_4.

1.2.3. Potassium nitrate.

In the early studies of alkali nitrates, potassium nitrate was considered along with sodium nitrate (Robinson et al, 1926; Butkov, 1936; Leschewski and Dagenhard, 1939). This work was primarily concerned with identifying the products of the decomposition reaction and the determination of the temperature for the onset of such decomposition. Subsequent work (Freeman, 1957) has shown that the activation energy for the decomposition reaction of potassium nitrate is 65.6 kcal $mole^{-1}$. Leschewski found that, studying the decomposition in a glass reaction vessel, potassium nitrite formation begins at about 286°C and that potassium peroxide is detectable at about 850°C, the final product being potassium oxide.

1.3 Thermal decomposition of sodium nitrate.

Due to the extensive use of alkali nitrates in pyrotechnics, explosives and rocket ignitors as well as in metallurgical heat treating, there is considerable interest in the high-temperature behaviour of these salts. The early investigations of molten sodium nitrate were primarily concerned with the identification of the reaction products and the determination of its decomposition temperature. (Robinson et al, 1926; Butkov, 1936; Leschewski and Dagenhard, 1939). Leschewski found that, with increasing temperature, sodium nitrate formed the nitrite first,

then the peroxide and finally the oxide. He first observed the formation of sodium nitrite, in a glass reaction vessel, at about 255°C and the peroxide was detectable at about 750°C. The colour of the melt was observed to change from light brown at 600°C to dark brown, almost black, at 900-1000°C. The unvapourised residue on cooling was yellowish, owing to the peroxide, or colourless, if a high reaction temperature (above 800°C) was used due to the formation of the oxide. In a later paper, (Leschewski and Zulla, 1944) it was shown that sodium nitrate, when heated above 800°C, decomposes rapidly with foaming leaving the alkali oxide and forming only a little peroxide.

Osipov investigated the thermal decomposition of sodium nitrate at 1000°C (Osipov and Ievinš, 1954) and he found that the oxides of nitrogen formed corresponded to 19-23% of the available nitric acid, however, in the presence of water vapour the yield was 80%. In a later paper (Osipov and Ievinš, 1956) the thermal decomposition was studied in the presence of ferric oxide and the following reaction occurred,

$$2NaNO_3 + Fe_2O_3 = Na_2O.Fe_2O_3 + 2NO_2 + \tfrac{1}{2}O_2$$

and the yield of oxides of nitrogen corresponded to 84.4% nitric acid as compared with a maximum of 29% nitric acid for sodium nitrate alone. They also found that at lower temperatures (below 800°C) slow heating favoured the release of nitrogen dioxide.

Bartos and Musgrave (1956) heated sodium nitrate in gold boats at temperatures up to 865°C and the gaseous decomposition products formed were studied by analysing themmass spectrographically and recording their absorption spectra.

In the absorption spectra, the gaseous nitric oxide molecule began to appear very faintly at 700°C and with increasing intensity at 775°C, 825°C and 865°C. In the mass spectrograph at 800°C, large amounts of nitric oxide, nitrogen and oxygen were present, the oxygen peak being twice as intense as the nitrogen peak, which was approximately equivalent to the nitric oxide peak. Nitrogen dioxide and possibly nitrous oxide were also detectable. At 400-600°C only nitrogen and oxygen were found to be present and nitric oxide was again first detected at 700°C. However they are uncertain as to whether nitric oxide is a primary product or nitrogen dioxide is the primary product and then decomposes thermally. It would appear that the former possibility is the more likely as the absorption spectra showed no trace whatsoever of nitrogen dioxide bands and the nitrogen dioxide observed by the mass spectrograph could have resulted from the combination of nitric oxide and oxygen in the sample bulbs.

The thermal decomposition of sodium nitrate has been studied thermogravimetrically and the rate of reaction followed by measuring volume changes as a function of time, at constant pressure (Freeman, 1956). The thermogravimetric study of sodium nitrate in air was performed with a furnace heating rate of 15°C per minute. The total loss of weight corresponded to the final product of sodium oxide. The discrepancy between the observed and the theoretical values was 2.3%. Freeman found that decomposition, as indicated by loss of weight by the sample, began slowly at 600°C, was rapid at temperatures exceeding 756°C, and was complete at 910°C. He also analysed the gaseous products formed in the temperature range 650°C to 780°C during decomposition in an atmosphere of argon and detected the presence of oxygen, nitrogen and small quantities of nitrogen dioxide. At 650°C, the ratio of oxygen, nitrogen and nitrogen dioxide in the gaseous products is 100 : 8 : 1 respectively, whereas at 780°C it is 100 : 37 : 9 respectively. That, in the initial stages of the reaction, oxygen is the principal gas formed indicates that the primary stage of the decomposition of sodium nitrate involves predominantly the formation of sodium nitrite and oxygen. Casonova and his associates (Chrétien, 1956; Casonova, 1959) also draw the same conclusion about the decomposition of sodium nitrate,

but they regard the reaction as occurring in two distinct stages, not completely separated but quite separable.

In view of this decomposition to sodium nitrite with the subsequent breakdown of the nitrite to sodium oxide, it is important to consider the investigations of the thermal decomposition of sodium nitrite.

In the thermal decomposition of sodium nitrite, nitric oxide is observed as a product at temperatures up to 600°C but nitrogen dioxide is absent (Butkov and Chassovenny, 1936).

A thermogravimetric study of sodium nitrite in air (Freeman, 1956) showed that at approximately 620°C the oxidation of sodium nitrite by oxygen becomes apparent as indicated by increases in the sample weight, the maximum weight being attained at 740°C. Further increase in the temperature resulted in loss of weight, which was rapid above 780°C and complete at 920°C. The total loss of weight corresponded to the formation of sodium oxide and the difference between the observed and theoretical values is 2.2%. Freeman found that the gaseous products of the thermal decomposition of sodium nitrite in argon over the temperature range 650°C to 780°C were nitrogen and oxygen. During the initial stages of the reaction, nitrogen was the predominant gas formed, but as the reaction progressed, so the relative quantity of oxygen increased.

Oza and Walawalkar (1945) found the gaseous products of the decomposition of sodium nitrite to be nitric oxide, nitrogen dioxide and nitrogen and stated that the decomposition reaction appears to be homogeneous, occurring only in the molten mass.

1.4 Thermal decomposition of magnesium-sodium nitrate mixtures.

The system 54% magnesium + 36% sodium nitrate + 10% laminac, which approximates to an empirically developed standard pyrotechnic illuminant composition has been studied (Hogan and Gordon, 1959b) as have the systems magnesium-lithium nitrate and magnesium-sodium nitrate (Freeman and Gordon, 1956). In the ternary system, laminac, which is a polyester resin crosslinked with styrene, acts as a binder.

The experimental techniques used in these studies were thermogravimetry, differential thermal analysis and determinations of the time-to-ignition as a function of temperature. The binary mixtures of magnesium and sodium nitrate studied by Hogan and Gordon were 22.2% magnesium + 77.8% sodium nitrate, which is stoichiometric for the reaction,

$$Mg + NaNO_3 \longrightarrow MgO + NaNO_2$$

and 60% magnesium + 40% sodium nitrate, which is equivalent in proportion to the ternary pyrotechnic composition quoted earlier.

The higher magnesium content mixture was found to ignite at 560°C in the DTA study, whereas the 22.2% magnesium + 77.8% sodium nitrate mixture ignited at 613°C. The activation energies for these reactions were 37 kcal/mole and 28 kcal/mole for the 22.2% magnesium + 77.8% sodium nitrate mixture and the 60% magnesium + 40% sodium nitrate mixture respectively.

In the time-to-ignition studies of both Hogan and Gordon, and Freeman and Gordon the minimum ignition temperature was found to be 570°C.

The ternary pyrotechnic composition combustion was found to proceed via a pre-ignition reaction between molten sodium nitrate and some thermal degradation product of laminac. This reaction furnishes sufficient heat to ensure ignition and combustion of the magnesium and sodium nitrate, which is the light-producing reaction.

2. EXPERIMENTAL

2.1. Apparatus for the study of thermal decomposition by weight loss measurements

The apparatus used was a Stanton automatically-recording thermobalance. The furnace was nichrome wound with a maximum temperature of 1,000°C, and was programmed to give a uniform increase in temperature of 250°C per hour. By switching off the programming cam when the required temperature had been reached, that particular temperature could be held (variation < 1°C) for any required length of time. Thus a series of runs could be performed in which the temperature was held at various values.

The instrument operated at the ambient pressure but, by means of a sheath fitted inside the furnace, it was possible to change the ambient gas. Argon was the only other atmosphere used, the gas being introduced through a plug fitted to the bottom of the sheath, at a rate of ca. 100 ml per minute. The gas escaped both through the top of the sheath and through the hole in the plug through which the crucible support passes from the furnace into the balance.

The weighing mechanism of the balance automatically arrests every five minutes. This served two purposes: firstly it calibrated the weight change graph with respect to time, and it also provided a check on the zero of the

balance.

The required amount of the sample under study was weighed out into a porcelain crucible which was placed on the silica support. The thermobalance was counterpoised for the weight of the crucible and its contents and then put into operation.

As the furnace temperature was recorded by a platinum/platinum-13% rhodium thermocouple positioned against the furnace wall, it was necessary to calibrate the crucible temperature against the furnace temperature, and this was done by means of another platinum/platinum-13% rhodium thermocouple positioned in the crucible. The calibration was performed in both an atmosphere of air and of argon and the data obtained is shown in diagrams 1 and 2. Repeat calibrations were performed to check the reproducibility and it was found that, in air, the accuracy was $\pm 1^{\circ}$. In argon, the accuracy was $\pm 2^{\circ}$ up to 600°C and $\pm 4^{\circ}$ above that temperature.

2.2. Apparatus to measure self-heating

This apparatus is shown in diagram 3. The reaction tube R was connected to the main pumping system by means of a length of pressure tubing D, the connections of which to the system were made vacuum tight by picein wax. The use of pressure tubing was necessary to allow the reaction tube

to be lowered into the molten metal bath B when required. As the self-heating only lasted for times of the order of ten minutes it was possible for a pressure of 10^{-4} mm Hg to be held in the system despite the use of pressure tubing.

An electric furnace, F, was used to heat the reaction zone. Its heating elements were so adjusted as to give a uniform temperature zone (to within $\pm 1°C$) about 4 cm long. In order to facilitate heat transfer to the reaction tube when it was plunged into the reaction zone, a cylindrical iron vessel B containing a melt M of either lead (m.p. 327°C) for the high temperature work or a 67% Sn, 33% Pb alloy ("Plumbers' solder" - m.p. 180°C) for the lower temperatures was placed inside the furnace. In both cases nitrogen gas was passed continuously over the surface of the melt with the result that oxidation of the alloy was eliminated and that of the lead kept to the minimum. To make the heat transfer even more efficient the top of the furnace was fitted with a Syndanyo plug P ($1\frac{1}{2}$" thick) with four holes drilled in it to pass the thermocouples T_1 and T_3, the reaction tube and the tube carrying the nitrogen stream into the furnace.

The sample S was in powder form with one junction of thermocouple T_2, so positioned that it reached the bottom of the reaction tube and hence was completely surrounded by the powder. This thermocouple was intro-

duced into the reaction tube by means of metal-soda glass seals; the soda glass was connected to the system via the ground glass joint J_1. The reaction tube, which, because of the high temperatures involved, was made of transparent silica, was connected to the vacuum line via the joint J_2.

The thermocouples T_2 and T_3, the wires of which were insulated from each other by the use of twin-bore alumina tubing, were connected in opposition and the difference in e.m.f. was applied across a previously calibrated galvanometer G through a variable series resistance. Thus the difference in temperature between the powder (T_2) and the bath (T_3), ΔT, could be measured. The optimum setting for the variable resistance was $R = 6 \times 10^3$ ohms which gave a ΔT reading accurate to $\pm 0.3^\circ C$. The thermocouples T_2 and T_3 were constructed from platinum -platinum/13% rhodium wires (0.3 mm diam.) and thermocouple T_1, which recorded the temperature of the heating bath T_0, was a calibrated chromel-alumel thermocouple.

The pressure of the system was adjusted to that required for the run and when the temperature of the heating bath had stabilised at the required value, the reaction tube was quickly introduced into the furnace up to a fixed mark so that the sample, and thermocouples, T_1 and T_3 were all at the same level. It was found that the heating bath came to thermal equilibrium 4-10°C below

the original temperature within 2 min., the extent of the fall depending on the original temperature. Readings of ΔT were taken at regular intervals by recording the galvanometer deflection.

2.3. Materials and preparation of the samples

The magnesium and sodium nitrate used were provided by A.R.D.E., Langhurst, and were used without further purification. The magnesium powder had a specification of a minimum of 98% free metallic magnesium with the possible impurities being other metals (e.g. Fe, Mn, Zn, Ca) and their compounds. The grade of the magnesium was 3B, which is "blown" or "atomised" magnesium and its particle size distribution is:

All pass B.S. sieve No. 72.

$\not>$ 7% retained B.S. sieve No. 100.

$\not>$ 15% pass B.S. sieve No. 240.

The particle distribution was further restricted by using only the fraction which passed a B.S. sieve No. 120 ($<107\mu$).

Similarly the sodium nitrate all passed a B.S. sieve No. 120 and its specification was:

Cl^-: 0.2% max.; $SO_4^=$: 0.25% max.;

ClO_3^-: 0.2% max.; NO_2^-: 0.15% max; $NaNO_3$: 98% min.

The materials used in the various mixtures were dried in an oven at 110°C overnight prior to the making of

the compositions. The mixtures, which are given in wt. %, were made by weighing the required amounts of the two materials and shaking them together in a sample tube fitted with a rubber bung, for approximately 15 minutes until the mixture appeared to be uniform.

3. RESULTS

3.1. Thermogravimetry in air

3.1.1 Thermal decomposition of sodium nitrate

The thermal decomposition of sodium nitrate in the form of powder was studied in the temperature range 570-760°C. Using the thermobalance, 100 mg samples of the salt were decomposed isothermally after being heated to the required temperature at a rate of 250°/hr, and the changes in weight of the sample were automatically recorded on the chart. From the resultant charts α-t graphs were constructed, where α is the fraction decomposed at time t (based on t=0 at 450°C). Typical examples of these α-t graphs are shown in Figure 1. The loss of weight corresponding to α=1.0 was equivalent to decomposition from sodium nitrate to sodium oxide (±5%) and this reaction, as shown in Figure 1, divides into two distinct parts. The loss of weight for a reaction from sodium nitrate to sodium

nitrite is equivalent to $\alpha = 0.295$ and this corresponds to the break in the α-t graphs for the total decomposition of sodium nitrate (Fig. 1). The kinetics of the reaction were therefore analysed in two parts corresponding to:

(a) the decomposition of sodium nitrate to form sodium nitrite;

(b) the subsequent decomposition of the sodium nitrite to form sodium oxide.

Typical α-t graphs of the separated parts of the reaction are shown in Fig. 3. The separation was effected by taking $\alpha = 0.295$ from the original α-t graph (Fig. 1) as corresponding to $\alpha=1$ for the sodium nitrate $\rightarrow$ sodium nitrite reaction and as $\alpha=0$ for the sodium nitrite $\rightarrow$ sodium oxide reaction. Hence the initial part of the kinetics curve was extrapolated up to the value $\alpha = 0.295$ and then, by subtraction from the original (total) α-t graph, the second part of the curve was extrapolated back to $\alpha = 0.295$ (Fig. 2).

Both the first and the second reaction obey an Avrami-Erofeyev type of equation (Avrami 1939,1940,1941; Erofeyev 1946)

$$\left[-\log(1-\alpha)\right]^{\frac{1}{n}} = kt \qquad (1)$$

with $n=3$. Fig. 4 shows a typical plot of the function $\left[-\log(1-\alpha)\right]^{\frac{1}{3}}$ vs t for each part of the reaction. In Tables 1 and 2 the values of k and the range of α, over

which the equation holds, are given for all the runs in this series. Figs. 5 and 6 are plots of log k vs $^{1}/_{T}$ from which activation energies and pre-exponential factors may be calculated (Table 3).

TABLE 1

Thermal decomposition of sodium nitrate.
(a) Sodium nitrate ⟶ sodium nitrite.
Rate constants determined from the Avrami-Erofeyev equation

Run	Temp. °C	$10^3/T°K$	$k(min^{-1})$	log k	α-range
N8	575	1.179	0.00082	$\bar{4}.9138$	0.05- 0.9
N11	599	1.147	0.00198	$\bar{3}.2967$	0.1 - 0.9
N13	628	1.110	0.00343	$\bar{3}.5353$	0.3 - 0.9
N12	649	1.085	0.00485	$\bar{3}.6857$	0.3 → 0.9
N10	650	1.083	0.00542	$\bar{3}.7340$	0.1 → 0.9
N9	673	1.057	0.00854	$\bar{3}.9315$	0.05→0.9
N16	698	1.030	0.01682	$\bar{2}.2258$	0.05→0.9
N7	728	0.999	0.04325	$\bar{2}.6360$	0.2 → 0.9

TABLE 2

Thermal decomposition of sodium nitrate.
(b) Sodium nitrite → sodium oxide.
Rate constants determined from the Avrami-Erofeyev Equation.

Run	Temp.°C	$10^3/T°K$	$k(min^{-1})$	log k	α-range
N8	575	1.179	0.000434	$\bar{4}.6375$	0.2 → 0.6*
N11	599	1.147	0.000844	$\bar{4}.9263$	0.05→0.8
N13	628	1.110	0.00193	$\bar{3}.2856$	0.05→0.9
N12	649	1.085	0.00391	$\bar{3}.5922$	0.05→0.9
N10	658	1.074	0.00411	$\bar{3}.6138$	0.05→0.9
N9	673	1.057	0.00534	$\bar{3}.7275$	0.2→ 0.9
N16	698	1.030	0.00754	$\bar{3}.8774$	0.05→0.9
N7	728	0.999	0.02940	$\bar{2}.4683$	0.05→0.9

* unfinished.

TABLE 3

Activation energies and pre-exponential factors for the thermal decomposition of sodium nitrate.

Reaction	E(kcal/mole)	log A
$NaNO_3 \rightarrow NaNO_2$	41.6	7.56
$NaNO_2 \rightarrow Na_2O$	40.1	6.84

3.1.2. Thermal decomposition of the mixture 4.45% Mg + 95.55% $NaNO_3$

A thermogravimetric study of the decomposition reaction of the mixture 4.45% Mg + 95.55% $NaNO_3$ was undertaken in a manner similar to that previously described (3.1.1) for sodium nitrate. The total loss of weight in the mixture corresponded (to within ±5%) to final products of magnesium oxide and sodium oxide. Typical examples of the resultant α-t graphs are shown in Fig. 7. In this mixture there is no separation of the α-t curve into two parts and the kinetics of the whole reaction fit the "contracting area" equation (Jacobs and Tompkins, 1955):

$$1 - (1 - \alpha)^{\frac{1}{2}} = kt \qquad (2)$$

Fig. 8 shows a typical plot of $1 - (1 - \alpha)^{\frac{1}{2}}$ vs t, and in Table 4 the values of k and the range of α, over which the equation holds, are given for the runs performed with this mixture. Fig. 9 is a plot of log k vs 1/T from which an activation energy of 38.2 kcal/mole and a pre-exponential factor (log A) of 6.52 may be calculated.

3.1.3. Thermal decomposition of the mixture 11.12% Mg + 88.88% $NaNO_3$

The total loss of weight in the mixture during its thermogravimetric decomposition corresponded (±5%) to final products of magnesium oxide and sodium oxide. Using

TABLE 4

Thermal decomposition of the mixture 4.45% Mg + 95.55% $NaNO_3$.
Rate constants determined from the "contracting area" equation.

Run	Temp°C	$10^3/T°K$	$k(min^{-1})$	log k	α-range
P61	600	1.145	0.000864	$\bar{4}.9365$	0.15-0.85
P60	624	1.115	0.00179	$\bar{3}.2529$	0.05-0.95
P59	648	1.086	0.00294	$\bar{3}.4683$	0.05-0.9
P39	674	1.056	0.00411	$\bar{3}.6138$	0.05-0.95
P64	700	1.028	0.00745	$\bar{3}.8722$	0.1→0.95
P62	728	0.999	0.01470	$\bar{2}.1673$	0.15-0.9
P63	757	0.971	0.03490	$\bar{2}.5428$	0.45-0.95

the total loss of weight, α-t graphs were constructed for the decompositions at the various temperatures employed (Fig. 10). As with the 4.45% Mg mixture, the reaction obeys the "contracting area" equation (Fig. 11) and table 5 shows the values of k and the range of α, over which the equation holds, for the runs performed with this mixture. From a plot of log k vs 1/T (Fig. 12) values for the activation energy (47.9 kcal/mole) and the pre-exponential factor (8.56) can be calculated.

TABLE 5

Thermal decomposition of the mixture 11.12% Mg + 88.88% $NaNO_3$. Rate constants determined from the "contracting area" equation.

Run	Temp°C	$10^3/T°K$	$k(min^{-1})$	log k	α-range
P33	631	1.106	0.00104	$\bar{3}.0170$	0.1 -0.95
P32	650	1.083	0.00156	$\bar{3}.1931$	0.15-0.95
P30	665	1.066	0.00266	$\bar{3}.4249$	0.05-0.95
P52	676	1.054	0.00323	$\bar{3}.5092$	0.1→0.95
P31	699	1.029	0.00603	$\bar{3}.7803$	0.1 -0.95
P34	728	0.999	0.01320	$\bar{2}.1206$	0.2 -0.95
P28	758	0.970	0.02610	$\bar{2}.4166$	0.3 -0.9

3.1.4. Thermal decomposition of the mixture 15.57% Mg + 84.43% $NaNO_3$

Reaction products consisting of magnesium oxide and sodium oxide are equivalent to the loss of weight observed (±5%) during the thermogravimetric decomposition of this mixture. The resultant α-t graphs are typified in Fig. 13; they also obey the "contracting area" kinetic law (Fig. 14).

Table 6 summarises the data obtained from the application of this law, and from an Arrhenius plot (Fig. 15) an activation energy of 40.2 kcal/mole and a pre-exponential factor (log A) of 6.80 were calculated.

TABLE 6

Thermal decomposition of the mixture 15.57% Mg + 84.43% $NaNO_3$. Rate constants determined from the "contracting area" equation.

Run	Temp°C	$10^3/T°K$	$k(min^{-1})$	log k	α-range
P67	599	1.147	0.000519	$\bar{4}.7152$	0.1 -0.95
P70	625	1.114	0,000958	$\bar{4}.9814$	0.05-0.95
P65	648	1.086	0.00179	$\bar{3}.2529$	0.1 -0.95
P45	673	1.058	0.00307	$\bar{3}.4871$	0.1 -0.95
P68	699	1.029	0.00550	$\bar{3}.7404$	0.05-0.95
P66	728	0.999	0.01050	$\bar{2}.0212$	0.1 -0.95
P69	758	0.970	0.01830	$\bar{2}.2625$	0.15-0.95

3.1.5. Thermal decomposition of the mixture 22.25% Mg + 77.75% $NaNO_3$

The mixture 22.25% Mg + 77.75% $NaNO_3$ is stoichiometric for the reaction:

$$Mg + NaNO_3 = MgO + NaNO_2$$

However the total loss of weight observed during the thermogravimetric reaction again corresponded ($\pm$5%) to final products of magnesium oxide and sodium oxide. Typical α-t graphs are shown in Fig. 16. The kinetics of the reaction obeyed the "contracting area" equation (Fig. 17). Table 7 summarises the data calculated, giving values of k and the range of α over which the equation holds. Fig. 18 is a plot of log k vs 1/T and from this an activation energy of 34.5 kcal/mole and a pre-exponential factor (log A) of 5.54 were calculated.

TABLE 7

Thermal decomposition of the mixture 22.25% Mg + 77.75% $NaNO_3$. Rate constants determined from the "contracting area" equation.

Run	Temp°C	$10^3/T°K$	$k(min^{-1})$	log k	α-range*
P53	598	1.148	0.000383	$\bar{4}.5832$	0.05-0.95
P55	625	1.114	0.00175	$\bar{3}.2430$	0.45-0.95
P50	639	1.096	0.00252	$\bar{3}.4014$	0.35-0.85
P37	650	1.083	0.00252	$\bar{3}.4014$	0.2 -0.9
P73	673	1.057	0.00340	$\bar{3}.5315$	0.45-0.95
P54	700	1.028	0.00659	$\bar{3}.8189$	0.35-0.95
P58	728	0.999	0.01140	$\bar{2}.0569$	0.7 -0.95

* Where the α-range is low, this is due to ignition of the mixture during which as much as 40% decomposition could occur.

3.1.6. The effect of variation in the magnesium content of the mixture at constant temperature.

A series of thermogravimetric runs were performed in air at 674±2°C in which the magnesium content was varied from a 0.1:1 mixture (2.22% Mg + 97.78% $NaNO_3$) to a 1:1 mixture (22.25% Mg + 77.75% $NaNO_3$). (The ratio of the two components of the mixture was based on a weight to weight ratio for the stoichiometric reaction $Mg+NaNO_3 = MgO+NaNO_3$).

The total loss of weight corresponded (±5%) to final products of magnesium oxide and sodium oxide and, in each case, the "contracting area" equation was obeyed. In Table 8 there is a summary of the kinetic data obtained.

TABLE 8

The effect of variation in the magnesium content of the mixture at constant temperature.

Run	% Mg	k(min^{-1})	α-range
P38	2.22	0.00538	0.35-0.9
P39	4.45	0.00411	0.05-0.95
P40	6.67	0.00454	0.1 -0.95
P41	8.90	0.00464	0.1 -0.95
P52	11.12	0.00323	0.1 -0.95
P43	13.35	0.00425	0.1 -0.95
P45	15.57	0.00307	0.1 -0.95
P46	17.80	0.00398	0.05-0.95
P48	20.02	0.00412	0.4 -0.95
P73	22.25	0.00340	0.45-0.95

3.2. Thermogravimetry in Argon.

3.2.1. Thermal decomposition of sodium nitrate.

The thermal decomposition of sodium nitrate in argon was studied in the temperature range 630-760°C.

The method of treatment of the results in argon was identical to that applied to those results obtained in air. The loss of weight observed corresponded ($\pm 5\%$) to a final product of sodium oxide. Typical kinetic graphs are shown in Fig. 19, and it can be seen that the thermal decomposition of sodium nitrate in argon can be divided into two parts in a similar manner to the thermal decomposition of sodium nitrate in air:

(a) the decomposition of sodium nitrate to form sodium nitrite,

(b) the subsequent decomposition of the sodium nitrite to form sodium oxide.

Typical kinetic plots of the separated parts of the reaction are shown in Fig. 20.

Both parts of the reaction obey an Avrami-Erofeyev type of equation:

$$\left[-\log(1 - \alpha)\right]^{\frac{1}{n}} = kt \qquad (1)$$

with n=3. Fig. 21 shows a typical plot of the function $\left[-\log(1 - \alpha)\right]^{\frac{1}{n}}$ vs t for each part of the reaction. In Tables 9 and 10 the values of k and the range of α over

which the equation holds, are given for all the runs in this series. Fig. 22 is an Arrhenius plot for the first part of the reaction - the decomposition of sodium nitrate to form sodium nitrite - and from this an activation energy of 41.6 kcal/mole and a pre-exponential factor (log A) of 7.61 can be calculated. Similarly Fig. 23 is an Arrhenius plot for the second part of the reaction - the decomposition of sodium nitrite to form sodium oxide - and from this an activation energy of 38.9 kcal/mole and a pre-exponential factor (log A) of 6.79 can be calculated.

TABLE 9

Thermal decomposition of sodium nitrate.
(a) Sodium nitrate $\longrightarrow$ sodium nitrite.
Rate constants determined from the Avrami-Erofeyev equation.

Run	Temp°C	$10^3/T°K$	$k(min^{-1})$	log k	α-range
AN5	630	1.107	0.00334	$\bar{3}.5237$	0.05-0.9
AN4	655	1.078	0.00822	$\bar{3}.9149$	0.05-0.9
AN6	676	1.054	0.01146	$\bar{2}.0592$	0.05-0.8
AN3	697	1.031	0.01950	$\bar{2}.2900$	0.05-0.9
AN7	723	1.004	0.02855	$\bar{2}.4556$	0.1 -0.9
AN2	753	0.975	0.03465	$\bar{2}.5397$	0.1 -0.9

TABLE 10

Thermal decomposition of sodium nitrate.
(b) Sodium nitrite → sodium oxide.
Rate constants determined from the Avrami-Erofeyev equation.

Run	Temp°C	$10^3/T°K$	$k(min^{-1})$	log k	α-range
AN5	636	1.100	0.00279	$\bar{3}.4456$	0.1 -0.8
AN4	655	1.078	0.00456	$\bar{3}.6590$	0.05-0.8
AN6	676	1.054	0.00585	$\bar{3}.7672$	0.05-0.8
AN3	697	1.031	0.00996	$\bar{3}.9983$	0.05-0.8
AN7	723	1.004	0.01820	$\bar{2}.2601$	0.05-0.9
AN2	755	0.973	0.03755	$\bar{2}.5746$	0.05-0.9

3.2.2. Thermal decomposition of the mixture 11.12% Mg + 88.88% $NaNO_3$.

The total loss of weight observed corresponded (±5%) to final products of magnesium oxide and sodium oxide. Typical kinetic plots of this reaction are shown in Fig. 24 and the "contracting area" equation was obeyed by the reaction (Fig. 25).

Table 11 summarises the data obtained from the application of the "contracting area" equation and Fig. 26 is an Arrhenius plot and from this an activation energy of 48.5 kcal/mole and a pre-exponential factor (log A) of 8.68 can be calculated.

TABLE 11

Thermal decomposition of the mixture 11.12% Mg + 88.88% $NaNO_3$. Rate constants determined from the "contracting area" equation.

Run	Temp°C	$10^3/T°K$	$k(min^{-1})$	log k	α-range
AP6	650	1.083	0.00159	$\bar{3}.2014$	0.05-0.85
AP3	677	1.053	0.00285	$\bar{3}.4548$	0.05-0.95
AP5	699	1.029	0.00598	$\bar{3}.7767$	0.05-0.95
AP4	723	1.004	0.01236	$\bar{2}.0920$	0.1-0.9
AP7	746	0.981	0.01849	$\bar{2}.2669$	0.2-0.85

3.2.3. Thermal decomposition of the mixture 22.25% Mg + 77.75% $NaNO_3$

This series of thermogravimetric runs gave a total loss of weight which corresponded ($\pm$5%) to final products of magnesium oxide and sodium oxide. Fig. 27 gives examples of the α-t graphs obtained from this reaction and the kinetics of the reaction obeyed the "contracting area" equation (Fig. 28).

The values of k and the range of α, over which the equation holds, obtained from application of this law are given in Table 12 and an Arrhenius plot (Fig. 29) of log k vs I/T was constructed. From this graph an activation energy of 36.0 kcal/mole and a pre-exponential factor

(log A) of 5.51 can be calculated.

TABLE 12

Thermal decomposition of the mixture 22.25% Mg + 77.75% $NaNO_3$. Rate constants determined from the "contracting area" equation.

Run	Temp°C	$10^3/T°K$	$k(min^{-1})$	log k	α-range
AP12	655	1.078	0.00102	$\bar{3}.0086$	0.4 -0.95
AP11	677	1.053	0.00135	$\bar{3}.1303$	0.45-0.95
AP9	699	1.029	0.00273	$\bar{3}.4362$	0.2 -0.9
AP10	722	1.005	0.00475	$\bar{3}.6767$	0.15-0.95
AP8	747	0.980	0.00608	$\bar{3}.7839$	0.2 -0.9

3.3. Thermogravimetry involving other additives.

All the runs described in this section were done in air.

(a) Replacing magnesium by magnesium oxide: Two magnesium oxide/sodium nitrate mixtures were studied thermogravimetrically. The mixtures used were 7.17% MgO + 92.83% $NaNO_3$ (which was equivalent in magnesium content to the 4.45% Mg, 95.55% $NaNO_3$) and 22.25% MgO + 77.75% $NaNO_3$. Typical kinetic plots are shown in Figs. 30 and 31. The loss of weight observed corresponded ($\pm$5%) to final products of magnesium oxide and sodium oxide.

(b) Replacing magnesium by aluminium or by aluminium oxide: The mixtures investigated were 17.46% Al + 82.54% $NaNO_3$, which is the stoichiometric mixture for the reaction:

$$2Al + 3NaNO_3 \rightleftharpoons Al_2O_3 + 3NaNO_2$$

and 6.59% Al_2O_3 + 93.41% $NaNO_3$, which corresponds to the mixture 7.17% MgO + 92.83% $NaNO_3$.

In each case the thermal decomposition was identical with that observed for sodium nitrate alone. In Table 13 a comparison is given of the kinetic data obtained from runs performed at a constant rate of heating (250°C/hr.).

(c) Thermal decomposition of sodium nitrite: Table 14 shows the comparison between the decomposition of sodium nitrite and that of sodium nitrate at a constant rate of heating (250°C/hr.).

(d) Thermogravimetry of magnesium: A series of runs at a constant rate of heating (250°C/hr.) was performed using varying amounts of magnesium. From this it was found that oxidation in air began at 405±5°C and that ignition occurred at 605±5°C.

TABLE 13

Comparison of the thermal decomposition of (1) sodium nitrate; (2) 6.59% Al_2O_3 + 93.41% $NaNO_3$; and (3) 17.46% Al + 82.54% $NaNO_3$.

Time (mins)

α	(1)	(2)	(3)	Temp(°C)
0	0	0	0	450
0.1	33	32.5	31	588
0.2	39	38	39	612
0.3	43.5	42.5	43.5	629
0.4	46	46	46	642
0.5	49	48.5	49	656
0.6	51	50.5	50	660
0.7	52	51.5	52	666
0.8	53.5	53	53.5	673
0.9	55	56	55	679
1.0	65	65	65	721

TABLE 14

Comparison of the thermal decomposition of sodium nitrate and sodium nitrite.

Time (mins)

α	$NaNO_3$	$NaNO_2$	Temp(°C)
0	0	-18*	450
0.1	32	35.5	584
0.2	38	41	608
0.3	42.5	44	625
0.4	45	46.5	638
0.5	48	48.5	652
0.6	50	50	656
0.7	51	51	662
0.8	52.5	52.5	669
0.9	54	54	675
1.0	65	65	721

* The time scale has been adjusted to give t=0 at 450°C and in the case of sodium nitrite slight decomposition had occurred before 450°C.

3.4. Measurement of self-heating in the thermal decomposition of sodium nitrate and magnesium + sodium nitrate mixtures.

All the work described in this section was performed in the apparatus shown in Diagram 3.

3.4.1. Treatment of the data.

Because self-heating of the sample began before the temperature of the reaction tube had reached that of the furnace, it was necessary to calibrate the system, by means of some reference, so that the extent of the self-heating could be determined accurately. The melting of sodium nitrate at 308°C meant that it was difficult to find a suitable inert reference material owing to the change in thermal characteristics which accompany the phase change. The required characteristic for the reference material is that no decomposition should take place so that the equation applicable is:

$$Cm \frac{dT}{dt} = \chi S(T_o - T)^n \qquad (1)$$

where C, the heat capacity, m the mass, S the surface area, and χ the surface heat transfer coefficient. Then

$$\frac{Cm}{\chi S} \frac{dT}{(T_o - T)^n} = dt \qquad (2)$$

Integrating with n=1 we have

$$\frac{Cm}{\chi S} \left[-\ell n(T_o - T)\right] = t + K \qquad (3)$$

Applying the boundary condition that at t=0, $T = T_R$, where T_R is the initial temperature of the reaction tube, gives

$$\frac{Cm}{\chi S}\left[-\ell n(T_o - T_R)\right] = K \qquad (4)$$

Combining (3) and (4)

$$\frac{Cm}{\chi S}\ell n\left[\frac{T_o - T_R}{T_o - T}\right] = t \qquad (5)$$

so that

$$\frac{T_o - T_R}{T_o - T} = e^{\left(\frac{\chi S}{Cm}\right)t} \qquad (6)$$

Therefore

$$T_o - T = \Delta T = (T_o - T_R)e^{-\frac{\chi S}{Cm}t} \qquad (7)$$

Therefore a plot of $\log_{10} \Delta T$ against t for a non-reacting material should be linear. Sodium nitrate and magnesium-sodium nitrate mixtures at temperatures below that at which self-heating starts did yield a series of straight line plots for log ΔT vs t (Fig. 32). Equation (1) was also integrated for n=2, 3 and 4. Fig. 33 shows a test of the equations obtained. In no case was a linear plot found. In Fig. 34 there is a comparison between the plots when n=1 and those obtained for the heat-up of a typical inert reference material - kaolin - at the same temperature.

From Fig. 34 it can be seen that the heat transfer coefficient of sodium nitrate is greater than that for kaolin and therefore calibration using the normal inert reference material is no use in this particular study. However a comparison of the plots of log ΔT vs t for the

thermal decomposition of sodium nitrate and magnesium-sodium nitrate mixtures over a wide temperature range shows that, when self-heating occurred, the initial portion of the plots was a straight line parallel to the lines obtained at lower temperatures where self-heating was negligible (Fig. 35). Hence the self-heating temperatures can be calculated by constructing graphs of log ΔT vs t and extrapolating the initial straight-line portion of the graph. This line would then correspond to the heat-up of the composition had no self-heating occurred. Therefore the extent of the self-heating can be ascertained by determining the difference in temperature, at any particular time, between the actual self-heating run and that of the extrapolated linear portion.

This method of determining the self-heating temperatures has been employed in the subsequent sections.

3.4.2. Variation of temperature.

A detailed study was made of the effect of the variation of temperature on the extent of self-heating produced during the thermal decomposition of sodium nitrate and also of the 22.25% Mg + 77.75% $NaNO_3$ mixture in the temperature range 250-600°C. In all the self-heating experiments performed the mass of sample taken was 180 ± 1 mg.

3.4.2.1. Runs performed at atmospheric pressure.

At the lower temperatures (250°C, 300°C, and 320°C) around

the melting point of sodium nitrate (308°C), no self-heating was observed for either sodium nitrate or the 22.25% Mg + 77.75% $NaNO_3$ mixture. In Fig. 32 is shown the linearity of the log ΔT vs t plots for sodium nitrate at 250°C and 300°C. Fig. 36 shows the remaining log ΔT vs t plots for sodium nitrate at 320°C and those for the 22.25% Mg + 77.75% $NaNO_3$ mixture at all three temperatures.

At all the other temperatures studied self-heating was observed and Fig. 35 shows a typical plot of log ΔT vs t for a decomposition run with self-heating. From such plots the self-heating involved in the thermal decomposition of sodium nitrate and the mixture 22.25% Mg + 77.75% $NaNO_3$ were calculated. Typical data obtained is shown in Figs. 37 and 38, and the results are given in detail in Tables 15 and 16.

TABLE 15

Self-heating temperatures (in °C) of the thermal decomposition of sodium nitrate at various temperatures and atmospheric pressure.

Time (mins)	410°C	450°C	500°C	535°C	600°C
0	0	0	0	0	0
0.25	0	0	0	0	32
0.5	56	73	74	62	120
0.75	82	81	92	82	112
1.0	69	71	87	73	89
1.25	53	55	66	59	68
1.5	40	42	50	47	50
1.75	29	32	39	36	36
2.0	21	24	30	28	25
2.5	12	11	17	19	13
3.0	6	5	9.5	9	7.5
3.5	3	2.5	5	5	4
4.0	1.5	2.5	2	3	1.5
4.5	0.5	1.5	0.5	2	0.5
5.0	0	1	0	0.5	0

TABLE 16

Self-heating temperatures (in °C) of the thermal decomposition of the mixture 22.25% Mg + 77.75% $NaNO_3$ at various temperatures and atmospheric pressure.

Time (mins)	410°C	450°C	500°C	535°C	600°C
0	0	0	0	0	0
0.25	0	0	0	0	23
0.5	67	66	73	106	325*
0.75	81	110	80	109	190
1.0	71	103	67	87	118
1.25	55	87	55	69	77
1.5	41	70	43	54	51
1.75	28	56	34	43	34
2.0	19	44	26	35	23
2.5	10	26	18	25	10
3.0	5	15	9	19	4.5
3.5	2.5	9	5	16	2
4.0	1	5	3	14	1
4.5	0.5	3	3	12	0.5
5.0	0	1.5	3	11	0

* Ignition occurred after 0 mins. 28 secs.

3.4.2.2. Runs performed at 10^{-4}mm Hg pressure.

No self-heating was observed for either sodium nitrate or the mixture 22.25% Mg + 77.75% $NaNO_3$ at the lower temperatures studied (250°C, 300°C and 320°C). However, as in the atmospheric pressure runs, self-heating was observed at all other temperatures and examples of the self-heating temperature plots are given in Figs. 39 and 40. The data obtained at 10^{-4} mm Hg pressure is summarised in Tables 17 and 18.

TABLE 17

Self-heating temperatures (in °C) of the thermal decomposition of sodium nitrate at various temperatures and 10^{-4}mm Hg pressure.

Time (min)	410°C	450°C	500°C	535°C	600°C
0	0	0	0	0	0
0.25	0	0	0	88	235
0.5	114	65	154	176	248
0.75	155	104	120	136	177
1.0	124	95	89	100	123
1.25	99	89	64	71	82
1.5	79	74	46	50	57
1.75	63	60	33	35	40
2.0	50	49	24	25	28
2.5	31	31	13	13	15
3.0	19	20	6.5	6	8
3.5	12	13	3.5	3	5
4.0	7	8	1.5	1	3
4.5	4.5	5	1	1	3
5.0	3	2	1	0.5	2.5

TABLE 18

Self-heating temperatures (in °C) of the thermal decomposition of the mixture 22.25% Mg + 77.75% $NaNO_3$ at various temperatures and 10^{-4}mm Hg pressure.

Time (min)	410°C	450°C	500°C	535°C	600°C
0	0	0	0	0	0
0.25	0	114	114	152	195
0.5	2	221	165	177	210
0.75	156	193	144	149	157
1.0	161	161	118	116	108
1.25	134	130	93	87	77
1.5	110	104	73	63	60
1.75	91	83	57	47	44
2.0	75	66	43	35	*
2.5	51	43	25	18	23
3.0	34	28	16	11	6
3.5	22	18	10.5	5	2
4.0	15	11	7	3	1.5
4.5	10	7	5	3	1
5.0	6.5	4.5	4	2.5	0.5

* Ignition occurred after 1m 58s.

3.4.3. Variation of pressure.

In addition to the study of the thermal decomposition of sodium nitrate and the mixture 22.25% Mg + 77.75% $NaNO_3$ at both atmospheric pressure and 10^{-4}mm Hg pressure, the effect of pressure variation was also examined at one partic-

ular temperature. The temperature selected for this study was 410°C and the data obtained has been tabulated (Tables 19 and 20).

TABLE 19

Self-heating temperatures (in °C) for the thermal decomposition of sodium nitrate at 410°C and various pressures.

Time (min)	380mm Hg	100mm Hg	10mm Hg
0	0	0	0
0.25	0	16	0
0.5	54	74	70
0.75	80	83	97
1.0	66	69	68
1.25	52	54	49
1.5	39	41	38
1.75	29	30	27
2.0	21	21	20
2.5	10	11	10
3.0	5	5	5
3.5	2.5	2.5	2.5
4.0	1	1	1
4.5	0.5	0.5	0.5
5.0	0	0	0

TABLE 20

Self-heating temperatures (in °C) for the thermal decomposition of the mixture 22.25% Mg + 77.75% $NaNO_3$ at 410°C and various pressures.

Time (min)	380mm Hg	100mm Hg	10mm Hg
0	0	0	0
0.25	4	9	0
0.5	72	49	33
0.75	82	69	101
1.0	73	66	80
1.25	57	54	59
1.5	42	41	43
1.75	30	30	30
2.0	22	21	21
2.5	11	10	11
3.0	5	5	5
3.5	2.5	2.5	2.5
4.0	1	1	1
4.5	0.5	0.5	0.5
5.0	0	0	0

3.4.4. Variation of magnesium content.

A study of the effect of varying the magnesium proportion of the magnesium-sodium nitrate mixtures was made at ambient pressure at two temperatures - 410°C and 600°C (Tables 21 and 22). A series was also performed at 600°C and 10^{-4}mm Hg pressure (Table 23).

Table 24 shows the effect of the magnesium content on the time to ignition during thermal decomposition at 600°C and ambient pressure. At 600°C and 10^{-4}mm Hg pressure, the only mixture to ignite was 22.25%Mg + 77.75% $NaNO_3$ which ignited after 118 secs, although there was an acceleration without ignition after 100 secs during the thermal decomposition of 15.57% Mg + 84.43% $NaNO_3$.

TABLE 21

Self-heating temperatures (in °C) for the thermal decomposition of various mixtures at 410°C and ambient pressure.

Time (min)	0% Mg	2.22% Mg	4.45% Mg	11.12% Mg	13.35% Mg	15.57% Mg
0	0	0	0	0	0	0
0.25	0	11	20	53	32	24
0.5	56	71	57	73	64	70
0.75	82	75	78	76	71	71
1.0	69	66	64	67	72	70
1.25	53	52	50	54	54	53
1.5	40	38	37	41	39	38
1.75	29	28	27	27	28	29
2.0	21	20	19	22	19	19
2.5	12	10	10	10	10	10
3.0	6	4.5	4.5	4.5	4.5	4.5
3.5	3	2	2	2	2	2
4.0	1.5	1	1	1	1	1
4.5	0.5	0.5	0.5	0.5	0.5	0.5
5.0	0	0	0	0	0	0

TABLE 21 (contd.)

Time (min)	17.80% Mg	20.02% Mg	22.25% Mg	100% Mg
0	0	0	0	0
0.25	24	42	4	17
0.5	63	68	72	23
0.75	75	79	82	18
1.0	68	69	73	15
1.25	53	56	57	19
1.5	40	39	42	19
1.75	29	27	30	17
2.0	21	22	22	13
2.5	11	10	11	8
3.0	4.5	4.5	5	4.5
3.5	2	2	2.5	2
4.0	1	1	1	1
4.5	0.5	0.5	0.5	0.5
5.0	0	0	0	0

TABLE 22.

Self-heating temperatures (in °C) for the thermal decomposition of various mixtures at 600°C and ambient pressure.

Time (min)	0% Mg	2.22% Mg	4.45% Mg	6.67% Mg	8.90% Mg	11.12% Mg
0	0	0	0	0	0	0
0.25	32	23	104	46	97	23
0.5	120	98	151	113	158	106
0.75	112	94	125	101	139	- *
1.0	89	72	94	82	180*	152
1.25	68	50	68	115*	85	81
1.5	50	36	47	57	49	49
1.75	36	25	32	33	31	30
2.0	25	17	23	21	21	21
2.5	13	8	11	9	9	9
3.0	7.5	4	5.5	3.5	4	4
3.5	4	1.5	3	1.5	1.5	1.5
4.0	1.5	1	2	0.5	1	1
4.5	0.5	0.5	1.5	0	0.5	0.5
5.0	0	0	1	0	0	0

* Ignition occurred between this reading and the previous one.

contd.

TABLE 22 (contd.)

Time (mins)	13.35% Mg	15.57% Mg	17.80% Mg	20.02% Mg	22.25% Mg
0	0	0	0	0	0
0.25	38	129	27	168	23
0.5	143	210	122	235	325*
0.75	- *	235*	222*	241*	190
1.0	167	130	128	133	118
1.25	94	83	82	83	77
1.5	55	54	53	53	51
1.75	33	35	33	34	34
2.0	21	22	21	22	23
2.5	9	10	9	9	10
3.0	4.5	4.5	4	4	4.5
3.5	2	2.5	1.5	2	2
4.0	1	1.5	1	1	1
4.5	0.5	1	0.5	0.5	0.5
5.0	0	0.5	0	0	0

* Ignition occurred between this reading and the previous one.

TABLE 23

Self-heating temperatures (in °C) for the thermal decomposition of various mixtures at 600°C and 10^{-4}mm Hg pressure.

Time(min)	4.45% Mg	11.12% Mg	15.57% Mg	22.25% Mg
0	0	0	0	0
0.25	95	206	130	195
0.5	196	213	178	210
0.75	154	155	141	157
1.0	106	106	98	108
1.25	72	71	66	77
1.5	49	47	45	60
1.75	33	31	75/	44
2.0	22	20	39	- *
2.5	10	9	10	23
3.0	5	4	3	6
3.5	2	1.5	0.5	2
4.0	1	1	0	1.5
4.5	0.5	0.5	0	1
5.0	0	0	0	0

* Ignition occurred after 118 sec.

/ Acceleration without ignition occurred after 100 sec.

TABLE 24

Variation in the times to ignition with magnesium content for various mixtures at 600°C and ambient pressure.

% Mg in mixture	Time to ignition (sec.)
0	d. n. i.
2.22	d. n. i.
4.45	d. n. i.
6.67	62
8.90	47
11.12	42
13.35	44
15.57	33.5
17.80	31
20.02	32.5
22.25	28

d. n. i. - did not ignite.

3.4.5. Variation in atmosphere.

A series of self-heating runs was performed at 600°C on various compositions of the magnesium-sodium nitrate mixture in an atmosphere of argon. (Table 25).

Table 26 shows the effect of the magnesium content on the time to ignition during thermal decomposition under these conditions.

TABLE 25

Self-heating temperatures (in °C) for the thermal decomposition of various mixtures at 600°C and one atmosphere pressure of argon.

Time (min)	0% Mg	4.45% Mg	11.12% Mg	15.57% Mg	28.25% Mg
0	0	0	0	0	0
0.25	99	42	102	49	89
0.5	117	145	136	220*	237*
0.75	96	121	118	170	145
1.0	73	89	- *	104	97
1.25	52	64	120	67	63
1.5	35	44	63	43	41
1.75	23	30	38	27	26
2.0	15	19	24	17	16
2.5	5	7	10	6	4
3.0	1.5	2	4	1	0.5
3.5	0	1.5	2	0	0
4.0		1	1		
4.5		0.5	0.5		
5.0		0	0		

* Ignition occurred between this reading and the previous one.

TABLE 26

Variation in the times to ignition of various mixtures at 600°C and one atmosphere pressure of argon with respect to magnesium content.

% Mg in mixture	Time to ignition (sec.)
0	d. n. i.
4.45	d. n. i.
11.12	59
15.57	29
22.25	20

d. n. i. - did not ignite.

4. DISCUSSION.

4.1 Thermogravimetry.

The kinetic data obtained from the thermogravimetric study of the thermal decomposition of sodium nitrate and the magnesium-sodium nitrate mixtures are summarised in Table 27. However, before discussing the significance of these results, the applicability of the equations to the kinetics will be considered.

4.1.1. Avrami-Erofeyev equation.

It was found that an equation of the Avrami-Erofeyev type:

$$\left[-\log(1 - \alpha)\right]^{1/n} = kt \qquad (1)$$

fitted the kinetic data obtained from the thermal decomposition of sodium nitrate, the value of n being 3. In solid state decompositions, the Avrami-Erofeyev equation holds for random nucleation followed by three-dimensional growth. However, the thermal decomposition of sodium nitrate occurs in a melt. The concept of nucleation taking place in the melt is not an easy one to visualise and the equation could, in this case, be purely empirical. Nevertheless the initial acceleratory period of the α - t graph implies the presence of some co-operative effect. In molten sodium nitrate at 314°C, the peak energy for

TABLE 27.

(a) Variation of activation energy (in kcal/mole) with magnesium content for the thermal decomposition of magnesium-sodium nitrate mixtures in air and argon.

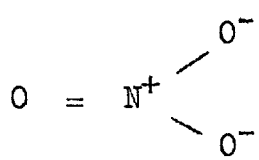
% Mg	Air	Argon
0* (i) $NaNO_3 \rightarrow NaNO_2$	41.6	41.6
(ii) $NaNO_2 \rightarrow \frac{1}{2}Na_2O$	40.1	38.9
4.45	38.2	-
11.12	47.9	48.5
15.57	40.2	-
22.25	34.5	36.0

(b) Variation of the pre-exponential factor ($\log_{10}$ A).

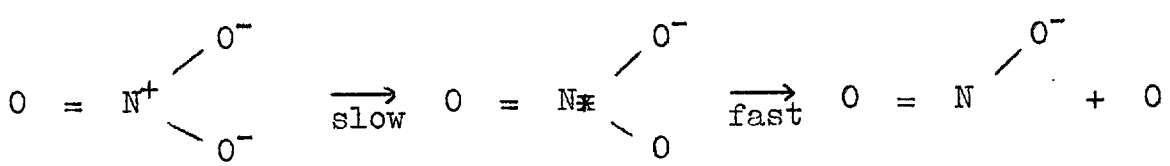
% Mg	Air	Argon
0* (i) $NaNO_3 \rightarrow NaNO_2$	7.56	7.61
(ii) $NaNO_2 \rightarrow \frac{1}{2}Na_2O$	6.84	6.79
4.45	6.52	-
11.12	8.56	8.68
15.57	6.80	-
22.25	5.54	5.51

*from the Avrami-Erofeyev equation; "contracting area" equation applied in the other cases.

the absorption band at 298 mμ obtained by ultra-violet spectroscopy, due to an internal transition in the nitrate ion, is about 4.15 eV (Smith and Boston, 1961). Since the optical value will be much greater than the thermal energy required to effect this transition, it is quite probable that the thermal activation energy of the reaction is due to this transition. The nitrate ion has been shown in X-ray studies to be a flat, equilateral triangle with the nitrogen in the centre, the three oxygens at the vertices and N-O bond lengths of 1.27Å (Cartmell and Fowles, 1956). Elliott (1937) postulated the basic structure



Thus the thermal transition could be:



excited state

It is difficult to formulate any precise analogy in the melt for the nucleation and growth stages, which occur in solids, for this chemical reaction. The acceleratory section of the reaction could be due quite generally to autocatalysis and the subsequent decay section due to the consumption of the reactants. The possibility of autocatalysis will be discussed later.

4.1.2. "Contracting area" equation.

As the magnesium content in the pyrotechnic mixture is increased, so the initial acceleratory period of the α-t graph disappears and the "contracting area" equation

$$1 - (1 - \alpha)^{\frac{1}{2}} = kt \qquad (2)$$

fits the results.

The implication of both the "contracting area" and the "contracting volume" equation,

$$\left[1 - (1 - \alpha)^{\frac{1}{3}} = kt\right]$$

is that of surface reactions. In solid state decompositions, the "contracting area" equation can be interpreted by considering the reaction as being initiated at one corner or edge and spreading two-dimensionally over the surface. Similarly the "contracting volume" equation can be interpreted by considering the reaction as being initiated entirely over the surface and penetrating into the body of the solid. The decomposition of magnesium-sodium nitrate mixtures occurs in a melt, or more precisely in a heterogeneous system comprising a distribution of magnesium particles through a melt of sodium nitrate.

Due to surface tension effects, the pyrotechnic melt forms a concave-shaped melt in the crucible and during the course of the decomposition the melt gradually reduces in size due to a loss of weight. Thus the reaction tends

to proceed by reaction at edges of the meniscus where the melt is in contact with the walls of the crucible and hence the "contracting area" equation fits the results (see Diagram 4). However, as the magnesium content is increased, which means that the mixture is becoming more "solid", the surface tension effects become less marked and the decomposition should tend towards that described by the "contracting volume" equation. This is borne out experimentally, as the "contracting volume" equation shows an improved fit as the magnesium content increases and for the 22.25% Mg + 77.75% $NaNO_3$ mixture the fit is as good as that for the "contracting area" equation.

4.1.3. Thermal decomposition of sodium nitrate and magnesium-sodium nitrate mixtures.

The most significant point to be drawn from Table 27 is that the activation energies for thermal decomposition in air are in good agreement with those obtained for thermal decomposition in argon. In both cases, the weight changes correspond to final products of magnesium oxide and sodium oxide, therefore the formation of magnesium oxide under an atmosphere of argon must be the result of some reaction in the melt. It can therefore be concluded that aerial oxidation of magnesium plays no part in the reaction mechanism. Discussion of the activation energies, and the corresponding pre-exponential factors, will now be restricted to those obtained for thermal decomposition in

air, but the same conclusions may be drawn for thermal decomposition in argon.

Previous work on the kinetics of the thermal decomposition of sodium nitrate and magnesium-sodium nitrate mixtures has been somewhat limited. Freeman (1956), who considered the decomposition reaction of sodium nitrate as one unit, calculated an activation energy of 44.7 kcal $mole^{-1}$, which is a slightly higher figure than those activation energies obtained in this work for the two separate parts of the reaction. In a similar investigation on potassium nitrate, Freeman (1957) determined an activation energy of 65.6 kcal $mole^{-1}$ for the decomposition reaction. He attributes the lower activation energy for sodium nitrate to the more extensive polarising power of the sodium ion.

During work on the pyrotechnic mixture magnesium-sodium nitrate-laminac, the 22% Mg +78% $NaNO_3$ mixture was studied and an activation energy of 37 kcal $mole^{-1}$ was determined (Hogan and Gordon, 1959b), a figure comparable, within experimental error, to that found in this work.

Although different kinetic equations have been applied to the decomposition of sodium nitrate and the decomposition of the magnesium-sodium nitrate mixtures, the activation energies can be compared because both the Avrami-Erofeyev equation and the "contracting area" equation

have been used in the form

$$F(\alpha) = kt$$

and the units of k are the same in each case, viz. min^{-1}. However, the pre-exponential factors for sodium nitrate and the magnesium-sodium nitrate mixtures cannot be compared quantitatively. Figure 41 shows a plot of activation energy against magnesium content and Fig. 42 is a similar plot for the pre-exponential factor.

That the division into two parts of the thermal decomposition kinetics for sodium nitrate does not occur when various proportions of magnesium are added to the sodium nitrate is also very significant. This implies that the presence of magnesium has a definite acceleratory effect on the decomposition of sodium nitrate in so far as it causes the reaction to proceed as one unit. The addition of magnesium to the sodium nitrate also has the effect of lowering the temperature at which decomposition begins. Sodium nitrate decomposition begins at 570°C, whereas mixtures containing magnesium start to decompose at 450°C.

Increasing the magnesium content of the mixture has an effect on the ignition temperature (Fig. 43) and the mixture of lowest magnesium content which would ignite was 4.45% Mg + 95.55% $NaNO_3$. It can be seen from this graph that as the magnesium content is increased the ignition

temperature approaches a constant value; the ignition temperature of pure magnesium is 605 ± 5°C.

The lowering of the temperature at which decomposition begins implies the possibility that the decomposition of sodium nitrate is being catalysed and among the possible catalysts are magnesium itself, magnesium oxide and a reaction product of the decomposition such as sodium nitrite. In order to investigate this possibility, two mixtures were made up in which the magnesium content was replaced by magnesium oxide. The thermal decomposition of sodium nitrite was also studied.

The results of the latter experiment are shown in Table 14; from $\alpha = 0.5$ to complete decomposition the kinetics of the thermal decomposition of sodium nitrite are identical with sodium nitrate. This is considerable evidence in favour of the theory postulated previously (cf. 3.1.1.) that the decomposition of sodium nitrate occurs in two distinct phases viz. decomposition to the nitrite with subsequent decomposition of the nitrite to the oxide. However, the initial decomposition rate for sodium nitrite is slower than that for sodium nitrate and, therefore, a steady-state concentration of sodium nitrite could exist in a decomposing melt of sodium nitrate. When magnesium is replaced by magnesium oxide, the α - t graphs show the same form but although magnesium oxide does have an effect on the decomposition of sodium nitrate this is not as marked

as it is for magnesium. This is shown by the temperature at which decomposition starts. As stated previously this is 570°C for sodium nitrate and 450°C for magnesium-sodium nitrate mixtures whereas for magnesium oxide-sodium nitrate mixtures it lies between these two temperatures at 510°C. Thus, while the possibility of some catalytic activity of magnesium oxide in the decomposition of magnesium-sodium nitrate mixture cannot be ruled out, this evidence suggests that it is the magnesium itself which is the active constituent.

When magnesium was replaced in the mixture by aluminium, it was found that this metal played no part in the decomposition of the sodium nitrate (Table 13) as the decomposition rate for sodium nitrate and the 17.46% Al + 82.54% $NaNO_3$ mixture were identical. In both cases sodium oxide was a product but in the mixture, the aluminium was unchanged when the decomposition of the sodium nitrate was complete and it was only oxidised when the temperature became high enough for aerial oxidation to occur (800°C).

Similarly, when magnesium was replaced in the mixture by aluminium oxide, no difference was observed between the decomposition rate for sodium nitrate and for the 6.59% Al_2O_3 + 93.41% $NaNO_3$ mixture.

It is of interest here to consider the work of Markowitz and Boryta (1961) on magnesium and aluminium

metal-gas reactions. Working with a thermogravimetric furnace heating rate of 600°C/hr, they gave the onset of magnesium oxidation in air as 450°C and for aluminium, 900°C. That Markowitz and Boryta's figures are higher than those obtained in this work (400°C for magnesium and 800°C for aluminium) can be accounted for by the much slower furnace heating rate used in this work. Thus these figures are more reliable than those of Markowitz and Boryta. As magnesium (651°C) and aluminium (660°C) have comparable melting-points, the oxidation of magnesium can take place in the solid phase whereas aluminium oxidation only occurs well above its melting point. This lack of reactivity of aluminium as compared with magnesium accounts for its non-participation in the decomposition of sodium nitrate. However, the temperatures involved in the ignition of pyrotechnic mixtures are high enough to enable aluminium to participate in the reaction when such a flare is fired.

Several workers have investigated the oxidation of magnesium (Gulbransen, 1945; Leontis and Rhines, 1946; Gregg and Jepson, 1958; Mikhail and Gouda, 1960; Freeman and Campbell, 1963) though only Campbell used magnesium powder. However, in all cases, the activation energy found for the reaction lay in the range 48-51 kcal/mole. This value is significantly higher than all the values of E in Table 27, except those for the 11.12% Mg mixture.

For the decomposition of magnesium-sodium nitrate mixtures in air, the possibility of the formation of magnesium nitride must be considered. Belin (1962) studied the nitridation of magnesium over the temperature range 500-600°C and found the activation energy to be 26.0 kcal/mole (cf. Table 27). Markowitz and Boryta (1961) also studied the magnesium-nitrogen reaction and they found that the onset of rapid reaction occurred at a higher temperature than reaction with oxygen. Thus, although it is quite likely that some magnesium nitride is formed as a secondary reaction during the decomposition of magnesium-sodium nitrate mixtures in air, the nitridation of magnesium does not play a significant part in the reaction mechanism.

4.2. Self-heating.

It is important to compare the conditions under which the self-heating experiments were performed with those prevailing for thermogravimetry. In the latter experiment, the heating rate was 250°C/hr, while in the self-heating runs it was of the order of 250°C/minute. The slow rate of heating employed in the thermogravimetric study meant that, during the kinetic runs, self-heating was negligible. As shown by the data (Tables 15-25) there is virtually no induction period before the onset of self-heating during the decomposition of sodium nitrate and magnesium-

sodium nitrate mixtures and the magnitude of the resultant self-heating temperatures is, in part due to the rapid heating rate. However, although the extent of self-heating may be slightly exaggerated, the general form of the self-heating curve gives an accurate picture of the exothermicity of the reactions.

The lowest temperature at which self-heating was studied was 410°C. All mixtures were studied under one atmosphere pressure of air, and, in addition, sodium nitrate and the 22.25% Mg + 77.75% $NaNO_3$ mixture were studied at a series of pressures. At atmospheric pressure, the extent of self-heating was independent of magnesium content for all mixtures and the degree of self-heating in pure magnesium at this temperature was comparatively low (Table 21). Hence, it can be deduced that the initial amount of self-heating in the decomposition of sodium nitrate and magnesium-sodium nitrate mixtures is due to the decomposition of the nitrate ion, probably the first stage of its decomposition, to the nitrite ion. That the self-heating is the result of reaction involving sodium nitrate is further confirmed by the self-heating data obtained at other pressures, as the extent of the self-heating for sodium nitrate and the 22.25% Mg + 77.75% $NaNO_3$ mixture at various pressures is comparable.

The next temperature used was 450°C and the decomposition of sodium nitrate and the 22.25% Mg + 77.75% $NaNO_3$ mixture were studied at atmospheric pressure and 10^{-4} mm Hg pressure (Tables 15-18). The self-heating temperatures observed at this temperature show that magnesium has now begun to play a significant role. The 22.25% Mg + 77.75% $NaNO_3$ mixture showed a self-heating temperature maximum at atmospheric pressure one third as great again as that found for sodium nitrate and at 10^{-4} mm Hg pressure it was approximately twice as great. The conclusion that magnesium begins to play a reactive part in the decomposition at 450°C is consistent with the thermogravimetric data for it is at this temperature that mixtures containing magnesium start to lose weight.

The self-heating data obtained at both 500°C and 535°C (Tables 15-18) confirms this conclusion for in all cases the 22.25% Mg + 77.75% $NaNO_3$ mixture produced more self-heating than sodium nitrate.

Some qualitative evidence obtained at 570°C shows that at this temperature, a further reaction may be initiated in sodium nitrate as there is a definite increase in the extent of self-heating. It is significant that this temperature is the one at which, in the thermogravimetric study, it was found that sodium nitrate began to lose weight.

The highest temperature studied was 600°C, the only temperature at which ignition occurred. A detailed study was made at this temperature and this included all mixtures under one atmosphere of air and several mixtures at 10^{-4} mm Hg pressure (Tables 22-24). A study was also made of several mixtures under an atmosphere of an inert gas namely argon (Tables 25 and 26).

The general overall conclusion to be drawn from the work at 600°C is that the increase in the self-heating of sodium nitrate observed at 570°C has meant that the self-heating at this higher temperature is, in broad terms, independent of the composition of the mixture.

Table 25 confirms the conclusion drawn from the thermogravimetric study that a change of atmosphere from air to argon involves no change in the reaction as the extent of self-heating in argon is comparable with that obtained in air. Hence it can be concluded that aerial oxidation of magnesium is not part of the reaction mechanism.

Tables 24 and 26 show the variation of times to ignition with magnesium content in both air and argon at 600°C. Table 24 shows that, within experimental error, there is a steady decrease in the time to ignition as the magnesium content is increased. It is also found (Table 26) that not only are self-heating temperatures in argon comparable but so are the times to ignition.

In comparison with thermogravimetry, again a high degree of correlation is obtained. Figure 43 shows the variation of ignition temperature with magnesium content obtained thermogravimetrically. The sole difference between this and the self-heating data is that the 4.45% Mg + 95.55% $NaNO_3$ mixture was found to ignite in the thermogravimetric study but not in the self-heating study. However this difference can be explained by this mixture being on the ignition limit with regard to magnesium content and also that the 4.45% Mg + 95.55% $NaNO_3$ mixture has a high ignition temperature (approx. 650°C) and this temperature was not attained during the self-heating runs at 600°C.

4.3 Reaction mechanisms.

4.3.1. Mechanism of the decomposition of sodium nitrate.

In the thermogravimetric study, it was shown that the decomposition of sodium nitrate takes place in two stages, the initial formation of the nitrite by loss of oxygen with the subsequent decomposition of the nitrite to sodium oxide. Casonova (1959) alone among other workers in this field, has also reported this two-stage decomposition. He states that sodium nitrate undergoes rapid decomposition to the nitrite which is followed by the decomposition of the sodium nitrite according to the reaction:

$$2NaNO_2 \longrightarrow Na_2O + N_2 + \tfrac{3}{2}O_2$$

but that this overall reaction results from the combination of two reactions:

(i) $2NaNO_2 \longrightarrow Na_2O + 2NO + \tfrac{1}{2}O_2$

(ii) $Na_2O + 3NO \longrightarrow 2NaNO_2 + \tfrac{1}{2}N_2$

which are both rapid but have opposite effects.

In earlier work, Casonova and his associates (Chrétien et al, 1956) found that at temperatures not above 500°C reaction (ii) occurs and that the sodium nitrite formed begins to decompose at 550°C. At 600°C, sodium nitrite is oxidised by nitric oxide but this oxidation is limited by the equilibrium

$$2NaNO_3 \rightleftharpoons 2NaNO_2 + O_2$$

However, Oza and Walawalkar (1945), who studied the thermal decomposition of sodium nitrite, stated that the basic decomposition reaction is

$$2NaNO_2 \longrightarrow Na_2O + NO + NO_2$$

They also state that the nitr gen dioxide formed in this initial reaction reacts simultaneously with the alkali oxide produced and the nitrite in the melt

$$Na_2O + 2NO_2 \longrightarrow NaNO_2 + NaNO_3$$

$$2NaNO_2 + NO_2 \longrightarrow NaNO_3 + NO$$

Reaction between nitric oxide and sodium nitrite also occurs:

$$2NaNO_2 + 2NO \longrightarrow 2NaNO_3 + N_2$$

Thus the gaseous products, according to Oza and Walwalkar, are nitric oxide, nitrogen dioxide and nitrogen.

A further conclusion drawn by these workers is that the decomposition of alkali nitrites appears to be a case of homogeneous reactions proceeding to a very considerable extent, only in the molten mass. This viewpoint is confirmed by the present work where the comparable activation energies obtained for the decomposition of sodium nitrate in air and in argon constitute strong evidence for homogeneous reaction in the melt.

The initial decomposition of the nitrate to the nitrite proceeds by the removal of one oxygen atom from the nitrate ion to form the nitrite ion:

$$NaNO_3 \rightleftharpoons [Na^+] + [NO_3^-] \rightleftharpoons [Na^+] + [NO_2^-] + O$$

However, the nitrate ion can also dissociate into the nitronium ion and an oxide ion:

$$[NO_3^-] \rightleftharpoons [NO_2^+] + [O^{2-}]$$

The existence of the nitronium ion was first confirmed by Ingold and his associates (Gillespie et al, 1946) during their studies on nitric acid (see also Goddard et al, 1946; Ingold et al, 1946).

The extent of nitronium ion formation is quite small and the mole-fraction of $[NO_2^+]$ in anhydrous nitric acid is of the order of 0.01 in the temperature range 0-20°C (Lee and Millen, 1956).

Subsequently Duke and co-workers (1958, 1959) showed the presence of the nitronium ion in molten alkali nitrates. In mixtures of molten alkali nitrates with dichromates and pyrosulphates the following reactions occur.

$$[Cr_2O_7^{2-}] + [NO_3^-] \rightleftharpoons [NO_2^+] + 2[CrO_4^{2-}]$$

followed by the slow step

$$[NO_3^-] + [NO_2^+] \longrightarrow \text{decomposition products.}$$

The initial reaction actually takes place in two stages:

$$[Cr_2O_7^{2-}] + 2[NO_3^-] \rightleftharpoons N_2O_5 + 2[CrO_4^{2-}]$$

Then $$N_2O_5 \rightleftharpoons [NO_3^-] + [NO_2^+]$$

Similarly

$$[S_2O_7^{2-}] + [NO_3^-] \rightleftharpoons [NO_2^+] + 2[SO_4^{2-}]$$

$$[NO_3^-] + [NO_2^+] \underset{\text{slow}}{\rightleftharpoons} 2NO_2 + O$$

Thus the following equilibria occur in molten sodium nitrate:

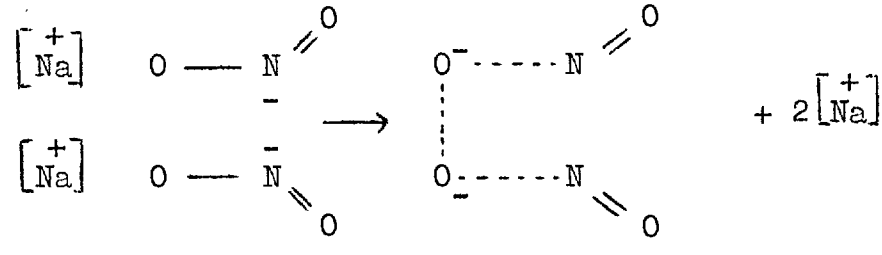
(i) $$NaNO_3 \rightleftharpoons [Na^+] + [NO_3^-] \rightleftharpoons [Na^+] + [NO_2^-] + \tfrac{1}{2}O_2$$

(ii) $$NaNO_3 \rightleftharpoons [Na^+] + [NO_2^+] + [O^{2-}]$$

However, the extent of nitronium ion formation is small and in the absence of any definite evidence in favour of its participation in the decomposition of sodium nitrate, we must assume that it does not play a major part. Presumably it will participate to some extent in side reactions.

The second stage in the decomposition of sodium nitrate - the decomposition of sodium nitrite to give sodium oxide - begins slowly as is shown in the two-stage α - t graph for the reaction (Figs. 1 and 2). Though the breakdown of the nitrite ion begins before the nitrate-nitrite reaction is complete, it is sufficiently slow in the early stages to imply that a build-up of nitrite ion concentration is required for the reaction to proceed. Thus a binary reaction between nitrite ions is indicated.

X-ray and Raman data (Langseth and Walles, 1934) indicate a non-linear structure for the nitrite ion, the N-O bond distance being 1.13Å and the O-N-O bond angle approximately 125°. Therefore such a binary reaction may be formulated as follows:



$$\longrightarrow \begin{array}{c} O^- \\ | \\ O^- \end{array} + 2NO + 2\left[\overset{-}{\underset{+}{Na}}\right]$$

Thus an intermediate in the decomposition reaction is sodium peroxide; however, at the temperatures involved the peroxide ion breaks down to the oxide and oxygen. The existence of sodium peroxide as an intermediate in the decomposition of sodium nitrate has been confirmed (Leschewski and Dagenhard, 1939).

$$\begin{array}{c} O^- \\ | \\ O^- \end{array} \longrightarrow O^{=} + \tfrac{1}{2}O_2$$

Therefore the overall reaction in the decomposition of sodium nitrate is:

$$2NaNO_3 \longrightarrow Na_2O + 2NO + \tfrac{3}{2}O_2$$

During the self-heating experiments nitrogen dioxide was observed in the cold parts of the reaction vessel and this would be due to the combination of nitric oxide and oxygen molecules at these lower temperatures.

4.3.2. Mechanism of the decomposition of magnesium-sodium nitrate mixtures.

The only significant difference between the reaction kinetics for the thermal decomposition of sodium nitrate and magnesium-sodium nitrate mixtures is that the

presence of magnesium removes the two-stage reaction and the reaction proceeds in one stage.

The activation energies obtained for the thermal decomposition of sodium nitrate and the magnesium-sodium nitrate mixtures (Table 27a) are comparable and combining this with the evidence that the self-heating of the mixtures at 410°C is independent of magnesium content (0-22.25%) it can be inferred that the initial reaction in magnesium-sodium nitrate mixtures is the same as that occurring in sodium nitrate alone, namely the formation of sodium nitrite:

$$2NaNO_3 \longrightarrow 2NaNO_2 + 2O$$

At this point, magnesium begins to take part in the reaction.

That the reaction takes place as one kinetic unit, as opposed to two for sodium nitrate, implies that a build-up of the nitrite ion concentration is not required for the reaction to proceed. The oxygen liberated during the nitrite formation will oxidise the magnesium. However, the nitrite decomposition will begin immediately after formation and hence at this stage the oxidation of magnesium by the liberated oxygen is by no means complete, particularly in the high magnesium content mixtures. The following reaction can therefore occur:

$$Mg + NO_2^- \longrightarrow [Mg^+] + NO + O^=,$$

followed by the reaction of $[Mg^+]$ with a further nitrite ion

$$[Mg^+] + NO_2^- \longrightarrow Mg^{2+} + O^{2-} + NO$$

Hence the reaction of magnesium with sodium nitrite is

$$Mg + 2NaNO_2 \longrightarrow MgO + Na_2O + 2NO \qquad (1)$$

and therefore the overall reaction of the magnesium-sodium nitrate mixtures is

$$2Mg + 2NaNO_3 \longrightarrow 2MgO + Na_2O + 2NO + \tfrac{1}{2}O_2 \qquad (2)$$

Reaction (2) shows that the stoichiometric composition is a 1 : 1 mixture, which corresponds to 22.25% Mg + 77.75% $NaNO_3$. This mixture has conventionally been assumed to be the stoichiometric mixture but for the wrong reasons as it was based on the reaction

$$Mg + NaNO_3 \longrightarrow MgO + NaNO_2$$

Reaction (1) shows that for complete reaction with magnesium participation, the minimum magnesium ratio is 0.5 : 1, which corresponds to 11.12% Mg + 88.88% $NaNO_3$. For mixtures of smaller magnesium content, there is excess sodium nitrate and hence sodium nitrite and this must decompose by the mechanism discussed previously for pure sodium nitrate (4.31). This would explain why,

in the study of 4.45% Mg + 95.55% $NaNO_3$ mixture, it was observed that there was a tendency for the reaction to divide into two stages as the build-up of nitrite ion concentration would be required for the decomposition of the excess sodium nitrate.

As with sodium nitrate, nitrogen dioxide was observed in the cold part of the reaction vessel during the self-heating experiments involving magnesium-sodium nitrate mixtures. As before this is due to the combination of nitric oxide and oxygen but the presence of nitrogen dioxide is only observed when there is no ignition. If ignition does occur, the temperatures involved are great enough to effect the dissociation of the nitric oxide molecules into the permanent gases - nitrogen and oxygen.

Therefore if there is non-ignition the gaseous products are nitric oxide and oxygen, with nitrogen dioxide formed as a by-product, but after ignition nitrogen and oxygen are the gaseous products. Magnesium oxide and sodium oxide are the other products in either case.

REFERENCES.

Avrami, M., 1939, J. Chem. Phys., 7, 1103.

Avrami, M., 1940, J. Chem. Phys., 8, 212.

Avrami, M., 1941, J. Chem. Phys., 9, 177.

Bartos, H.R. and Musgrave, J.L., 1956, J. Phys. Chem., 60, 256.

Belin, P., 1962, Compt. Rend., 255, 3164.

Butkov, K., 1936, Acta Physicochim. U.R.S.S., 5, 137.

Butkov, K. and Chassovenny, V., 1936, Acta Physicochim. U.R.S.S., 5, 645.

Cartmell, E. and Fowles, G.W.A., 1956, "Valency and Molecular Structure", (Butterworths, London), p. 164.

Casonova, J.C., 1959, Bull. Soc. Chim. France, 429.

Chédin, J. and Fénéant, S., 1947, Compt. Rend., 224, 1008.

Chrétien, A., Heubel, J. and Casonova, J.C., 1956, Compt. Rend., 242, 1479.

Cook, M.A. and Taylor Abegg, M., 1956, Ind. Eng. Chem., 48, 1090.

Duke, F.R. and Iverson, M.L., 1958, J.A.C.S., 80, 5061.

Duke, F.R. and Yamamoto, S., 1959, J.A.C.S., 81, 6378.

Elliott, N., 1937, J.A.C.S., 59, 1380.

Erofeyev, B.V., 1946, C.R. Acad. Sci. U.R.S.S., 52, 511.

Feick, G. and Hainer, R.M., 1954, J.A.C.S., 76, 5860.

Freeman, E.S., 1956, J. Phys. Chem., 60, 1487.

Freeman, E.S., 1957, J.A.C.S., 79, 838.

Freeman, E.S. and Campbell, C., 1963, Trans. Faraday Soc., 59, 165.

Freeman, E.S. and Gordon, S., 1956, J. Phys. Chem., 60, 867.

Garn, P.D., 1961, Anal. Chem., 33, 1247.

Gillespie, R.J., Graham, J., Hughes, E.D., Ingold, C.K. and Peeling, E.R.A., 1946, Nature, 158, 480.

Goddard, D.R., Hughes, E.D. and Ingold, C.K., 1946, Nature, 158, 481.

Gordon, S. and Campbell, C., 1954, Fifth Symposium (International) on Combustion, 277.

Gordon, S. and Campbell, C., 1955, Anal. Chem., 27, 1102.

Gordon, S. and Campbell, C., 1956, Anal. Chem., 28, 124.

Gray, P. and Harper, M.J., 1959, Trans. Faraday Soc., 55, 581.

Gregg, S.J. and Jepson, W.B., 1958, J. Inst. Met., 87, 187.

Gulbransen, E.A., 1945, Trans. Electrochem. Soc., 87, 589.

Henkin, H. and McGill, R., 1952, Ind. Eng. Chem., 44, 1391.

Hill, R.A.W., 1954, Proc. Roy. Soc., A226, 455.

Hill, R.A.W., 1957, Trans. Faraday Soc., 53, 1136.

Hill, R.A.W., Sutton, L.E., Temple, R.B. and White, A., 1950, Research, 3, 569.

Hill, R.A.W. and Welsh, J.N., 1959, Trans. Faraday Soc., 55, 299.

Hogan, V.D. and Gordon, S., 1957, J. Phys. Chem., 61, 1401.

Hogan, V.D. and Gordon, S., 1958, J. Phys. Chem., 62, 1433.

Hogan, V.D. and Gordon, S., 1959a, J. Phys. Chem., 63, 93.

Hogan, V.D. and Gordon, S., 1959b, Combustion and Flame, 3, 3.

Hogan, V.D. and Gordon, S., 1960, J. Phys. Chem., 64, 172.

Hogan, V.D., Gordon, S. and Campbell, C., 1957, Anal. Chem., 29, 306.

Ingold, C.K., Millen, D.J. and Poole, H.G., 1946, Nature, 158, 481.

Jacobs, P.W.M. and Kureishy, A.R.T., 1963, Ninth Symposium (International) on Combustion.

Jacobs, P.W.M. and Tompkins, F.C., 1955, "Chemistry of the Solid State", (Butterworths, London), Chapter 7.

Keenan, A.G. and Dimitriades, 1961, Trans. Faraday Soc., 57, 1019.

Keenan, A.G. and Dimitriades, 1962, J. Chem. Phys., 37, 1583.

Kerdivarenko, A.M. and Davidovich, R.L., 1957, Uchenye Zapiski Kishinev Univ., 27, 169.

Kerdivarenko, A.M. and Fainshtein, L.B., 1960, Uchenye Zapiski Kishinev Gosudarst. Univ., 56, 203.

Kummer, J.T., 1947, J.A.C.S., 69, 2559.

Langseth, A. and Walles, E., 1934, Z. Physik. Chem., 27B, 209.

Lee, W.H. and Millen, D.J., 1956, J.C.S., 4463.

Leontis, T.E. and Rhines, F.N., 1946, Trans. Amer. Inst. in. Met. Eng., 166, 265.

Leschewski, K. and Dagenhard, W., 1939, Ber., 72B, 1763.

Leschewski, K. and Zulla, G., 1944, Chem. Zentr., I, 743.

Markowitz, M.M. and Boryta, D.A., 1961, Anal. Chem., 33, 949.

Mikhail, R. Sh. and Gouda, V.K., 1960, J. Appl. Chem., 10, 384.

Nakahara, S. and Hikita, T., 1959, J. Ind. Expl. Soc. Japan, 20, 275.

Nicol, A., 1948, Compt. Rend., 226, 253.

Osipov, L. and Ievinš, A., 1954, Latvijas PSR Zinātņu Akad. Vēstis, No. 7, 83.

Osipov, L. and Ievinš, A., 1956, Latvijas Valsts. Univ. Kim. Fak. Zinātniskie Raksti, No. 3, 23.

Oza, T.M. and Walawalkar, B.R., 1945, J. Ind. Chem. Soc., 22, 243.

Robinson, P.L., Smith, H.C. and Briscoe, H.V.A., 1926, J.C.S., 836.

Smith, G.P. and Boston, C.R., 1961, J. Chem. Phys., 34, 1396.

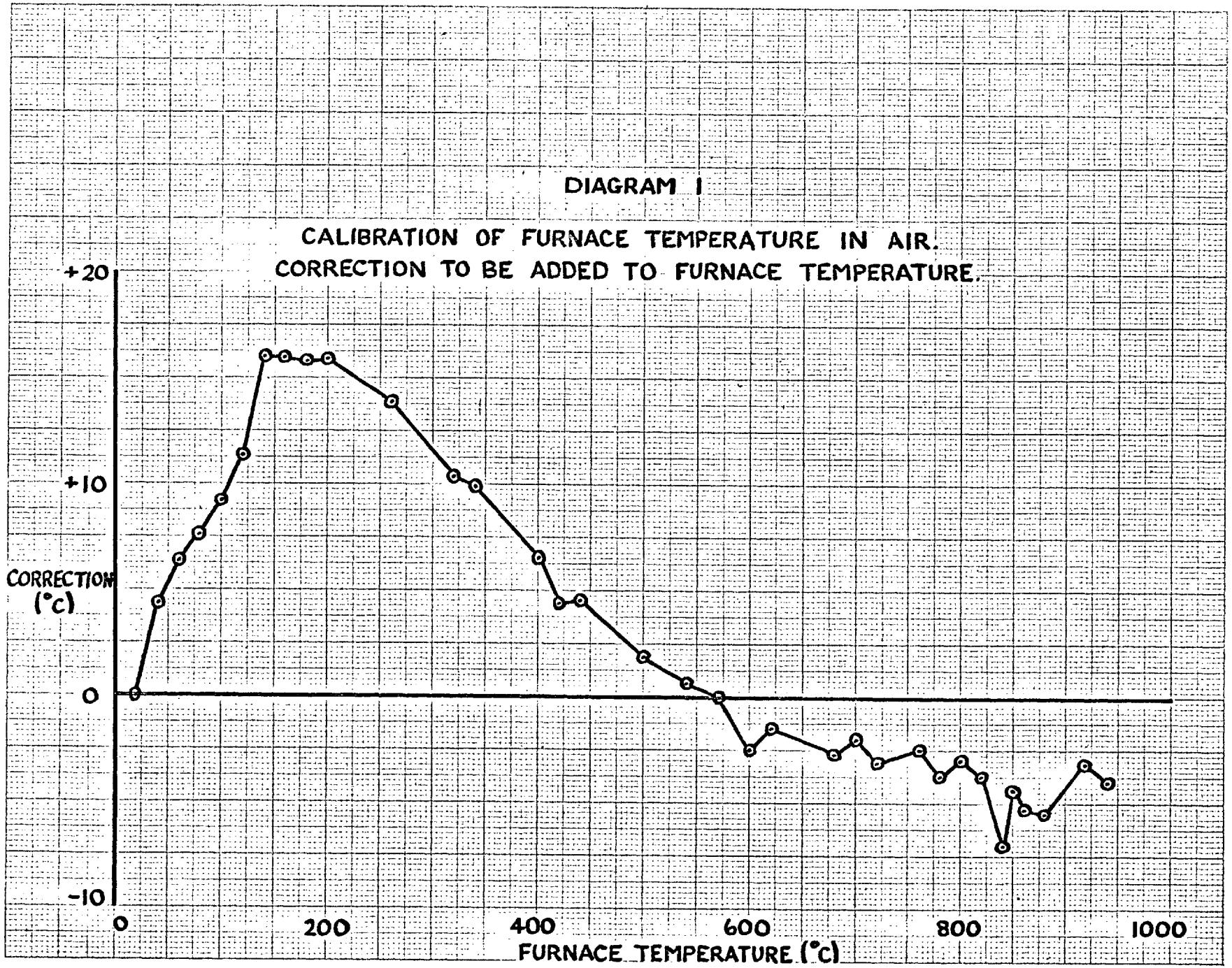

DIAGRAM 1
CALIBRATION OF FURNACE TEMPERATURE IN AIR.
CORRECTION TO BE ADDED TO FURNACE TEMPERATURE.
+20
+10
0
-10
CORRECTION (°C)
0
200
400
600
800
1000
FURNACE TEMPERATURE (°C)

DIAGRAM 2

CALIBRATION OF FURNACE TEMPERATURE IN ARGON.
CORRECTION TO BE ADDED TO FURNACE TEMPERATURE.

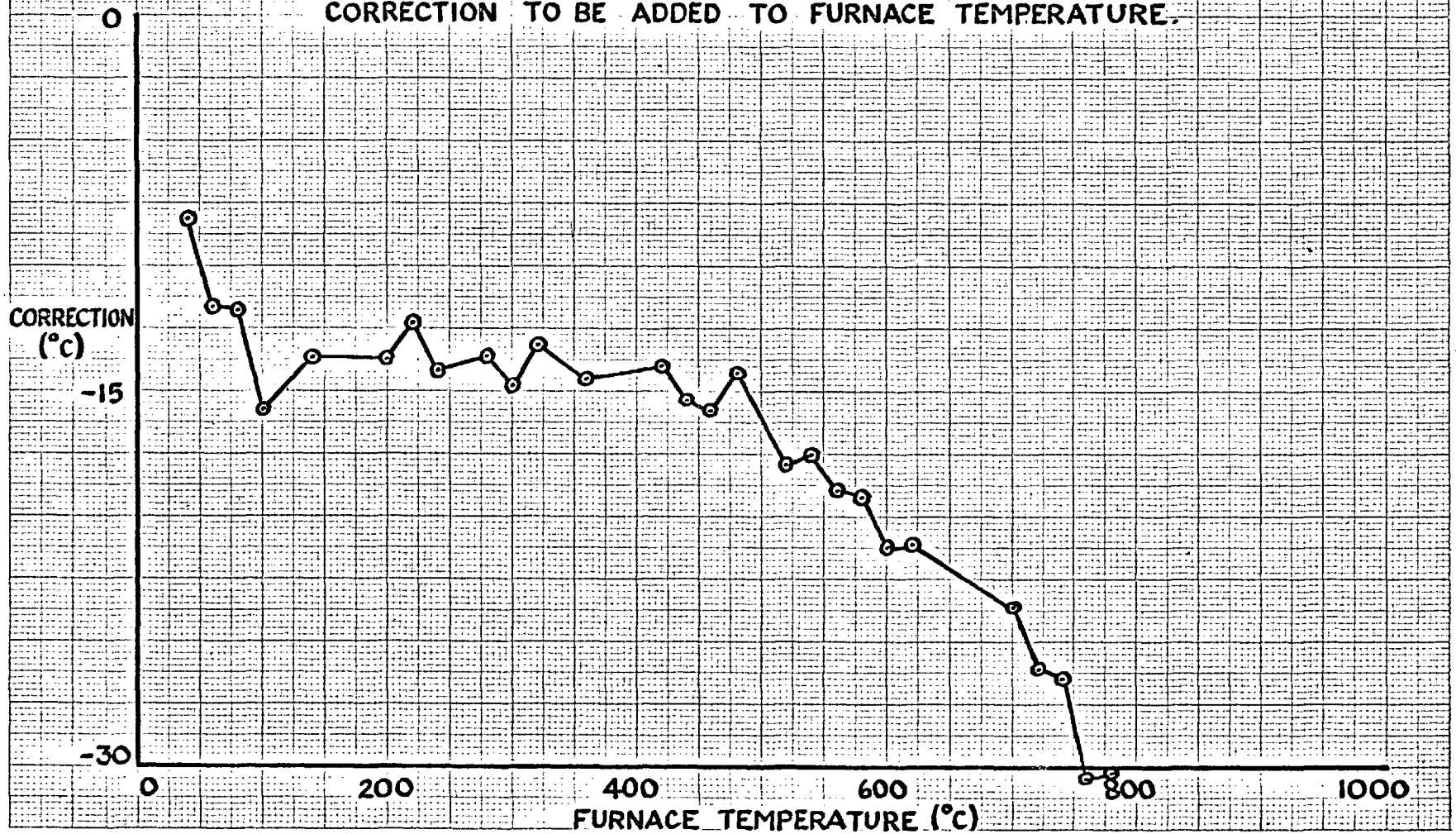


Diagram 3.

Apparatus for the self-heating measurements.

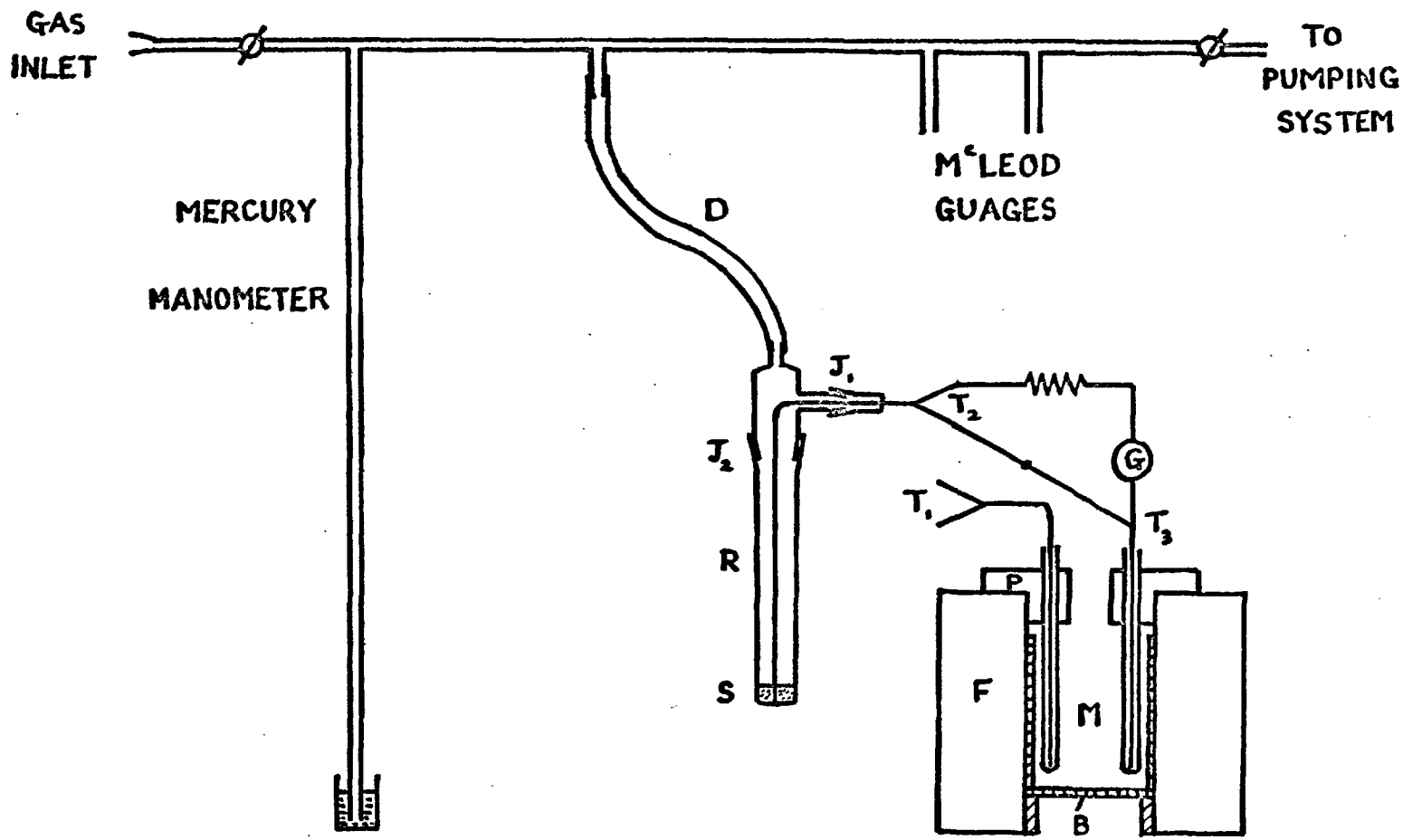
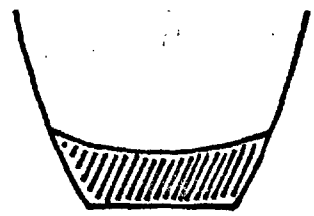


Diagram 4.

a) Concave-shaped melt in the crucible.



b) Variation of the melt formation in the crucible with time.

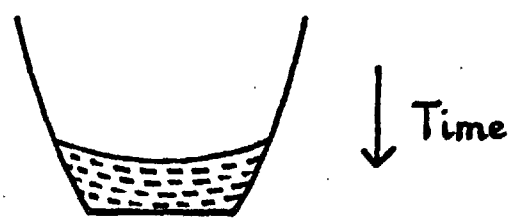


FIGURE 1

THERMAL DECOMPOSITION OF SODIUM NITRATE.

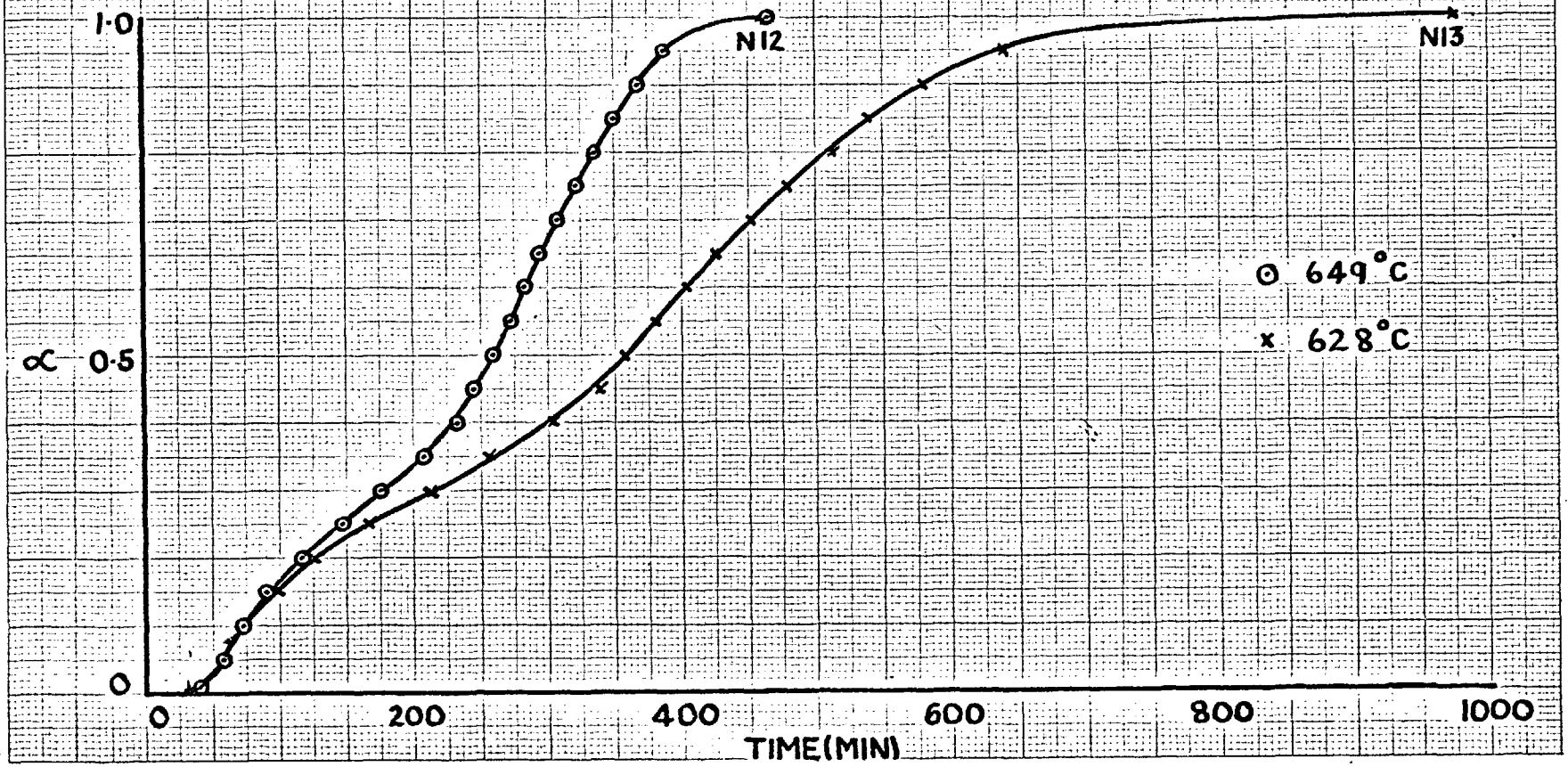


FIGURE 2

THERMAL DECOMPOSITION OF SODIUM NITRATE.
WITH EXTRAPOLATIONS TO SEPARATE KINETICS INTO
2 PARTS AT $\alpha = 0{\cdot}295$.

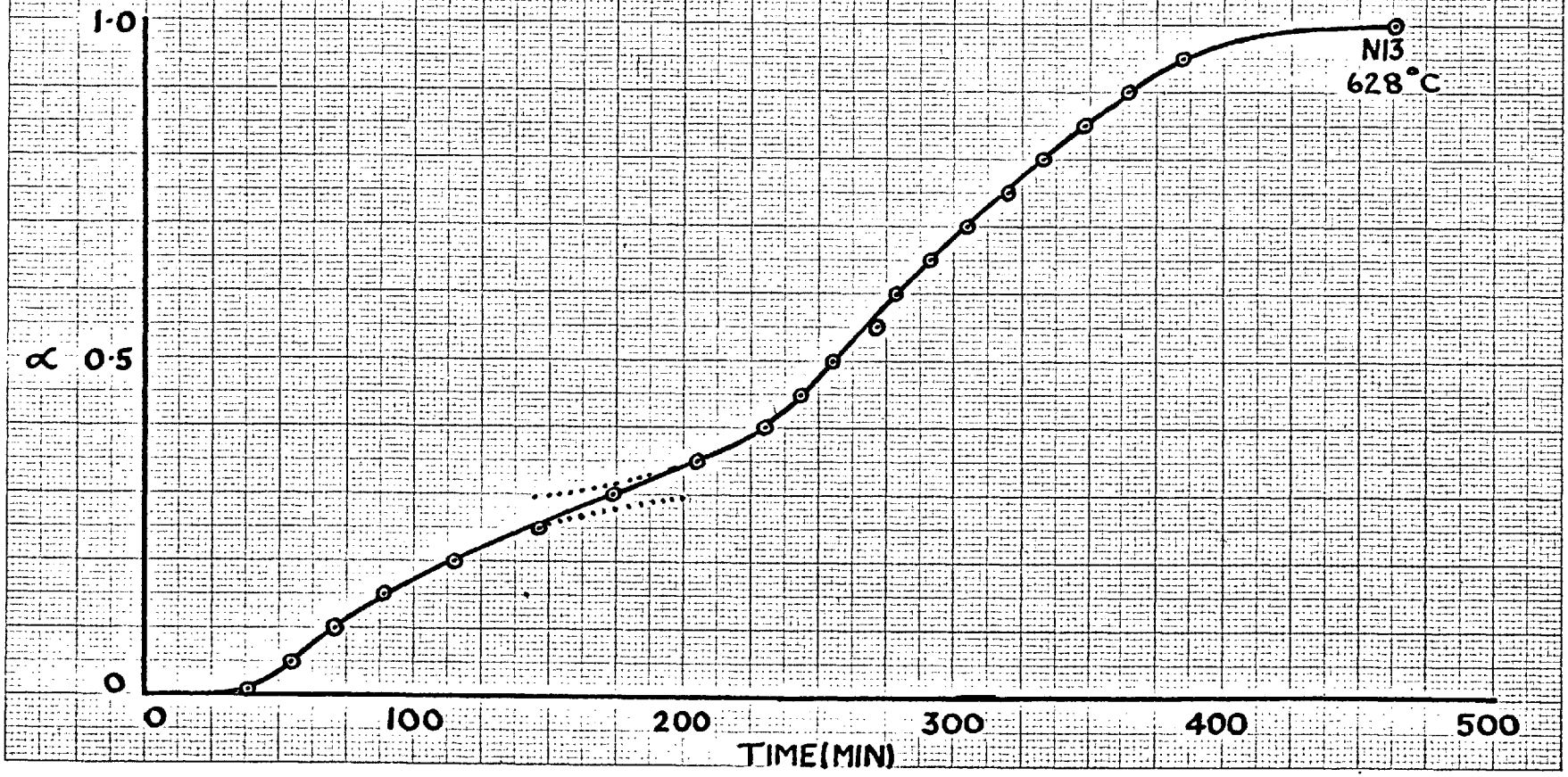


FIGURE 3

THERMAL DECOMPOSITION OF SODIUM NITRATE.

a) $NaNO_3 \rightarrow NaNO_2$; b) $NaNO_2 \rightarrow Na_2O$

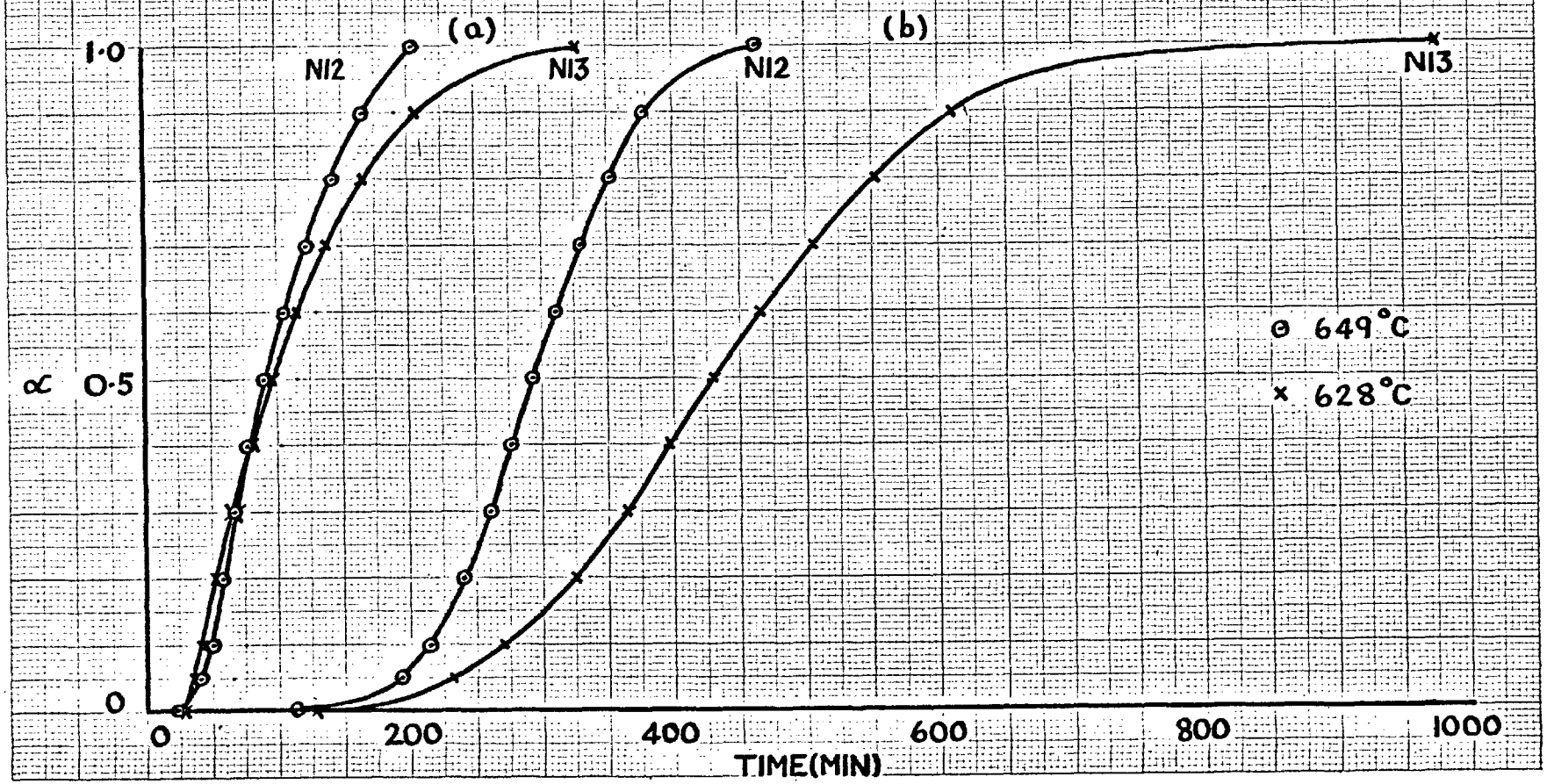


FIGURE 4

THERMAL DECOMPOSITION OF SODIUM NITRATE.
TEST OF THE AVRAMI-EROFEYEV EQUATION WITH n = 3.

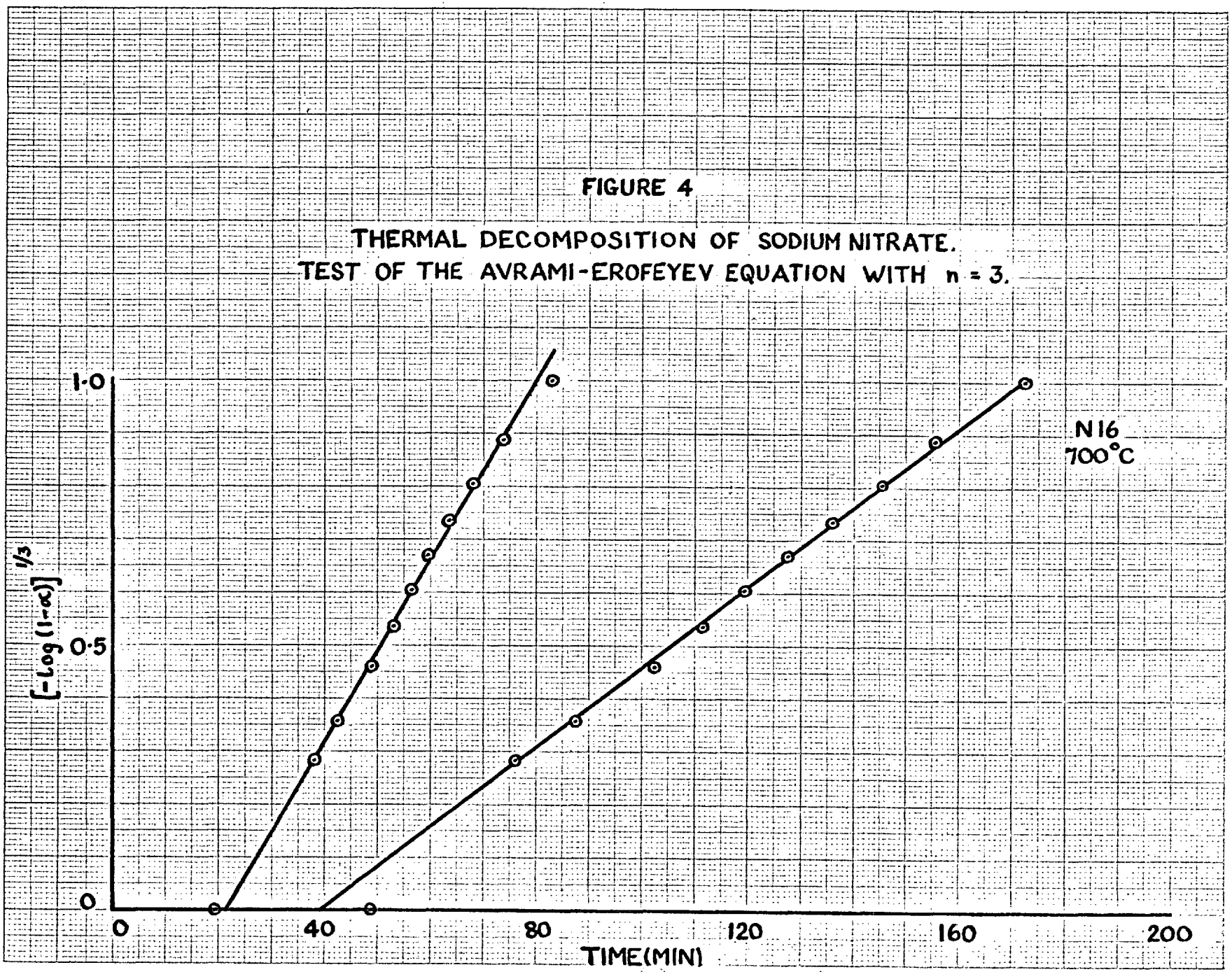


FIGURE 5

THERMAL DECOMPOSITION OF SODIUM NITRATE.
ARRHENIUS PLOT FOR THE NITRATE-NITRITE REACTION.

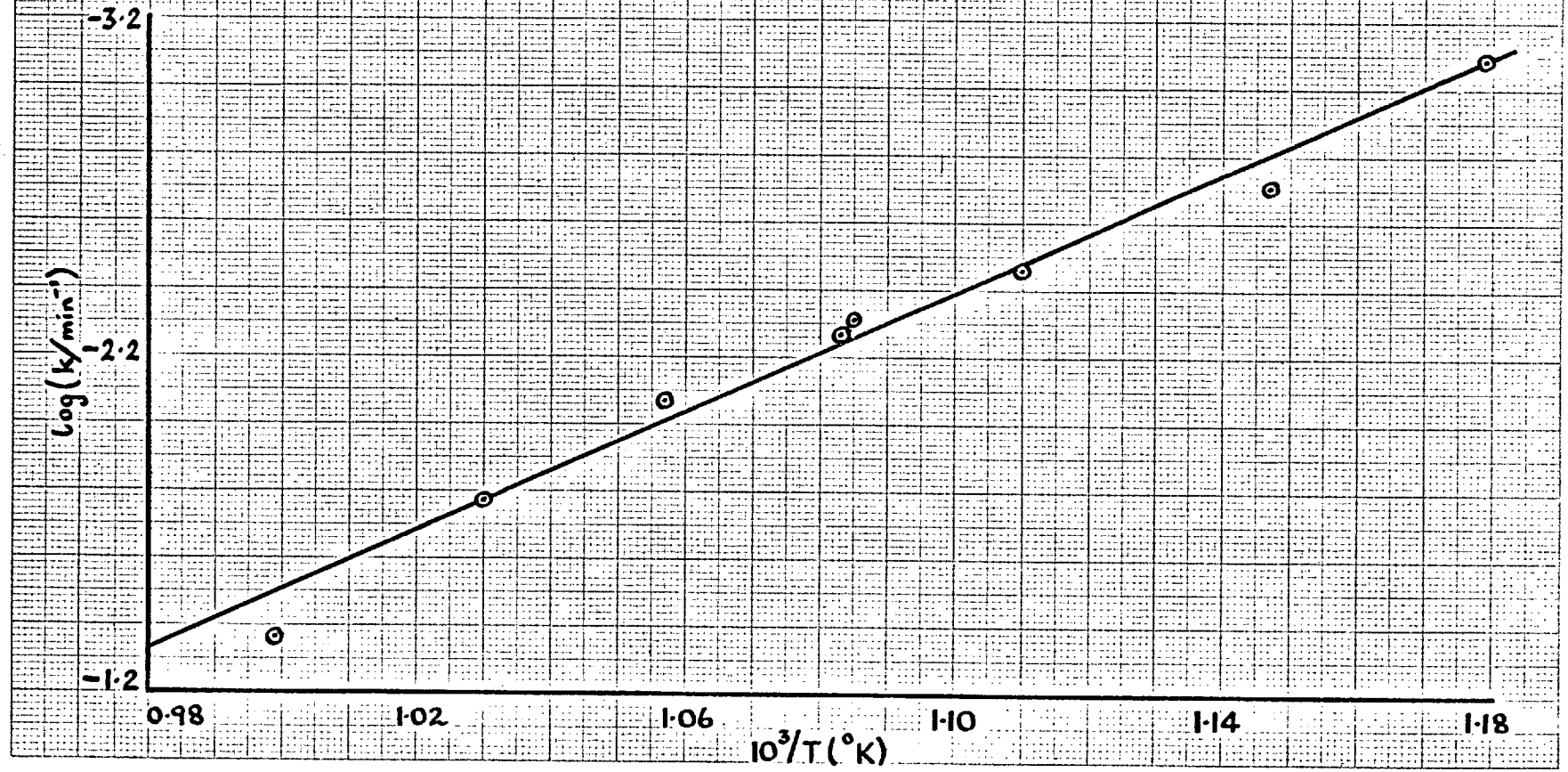


FIGURE 6

THERMAL DECOMPOSITION OF SODIUM NITRATE.
ARRHENIUS PLOT FOR THE NITRITE-OXIDE REACTION.

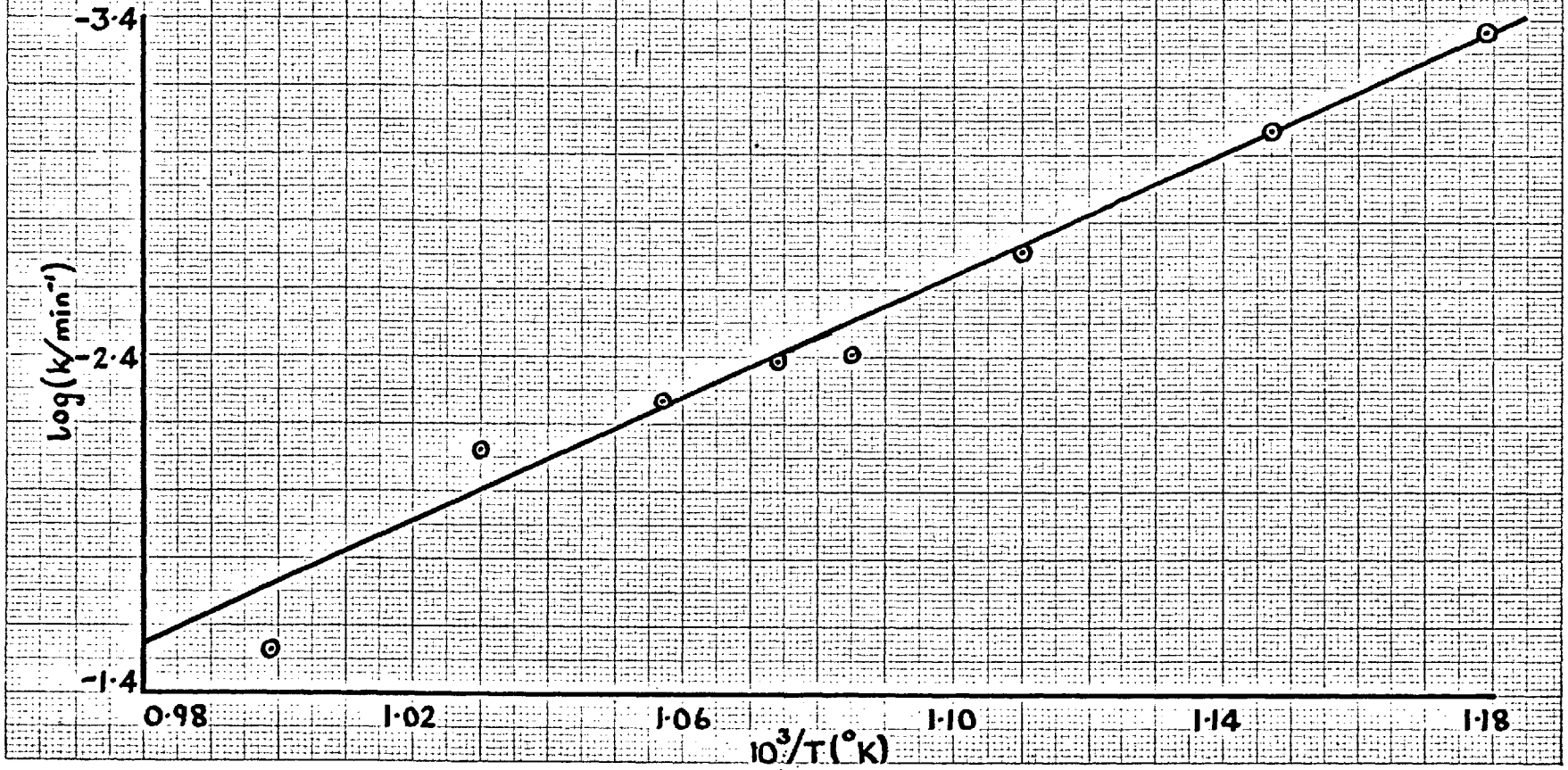


FIGURE 7

THERMAL DECOMPOSITION OF 4·45% Mg + 95·55% $NaNO_3$.

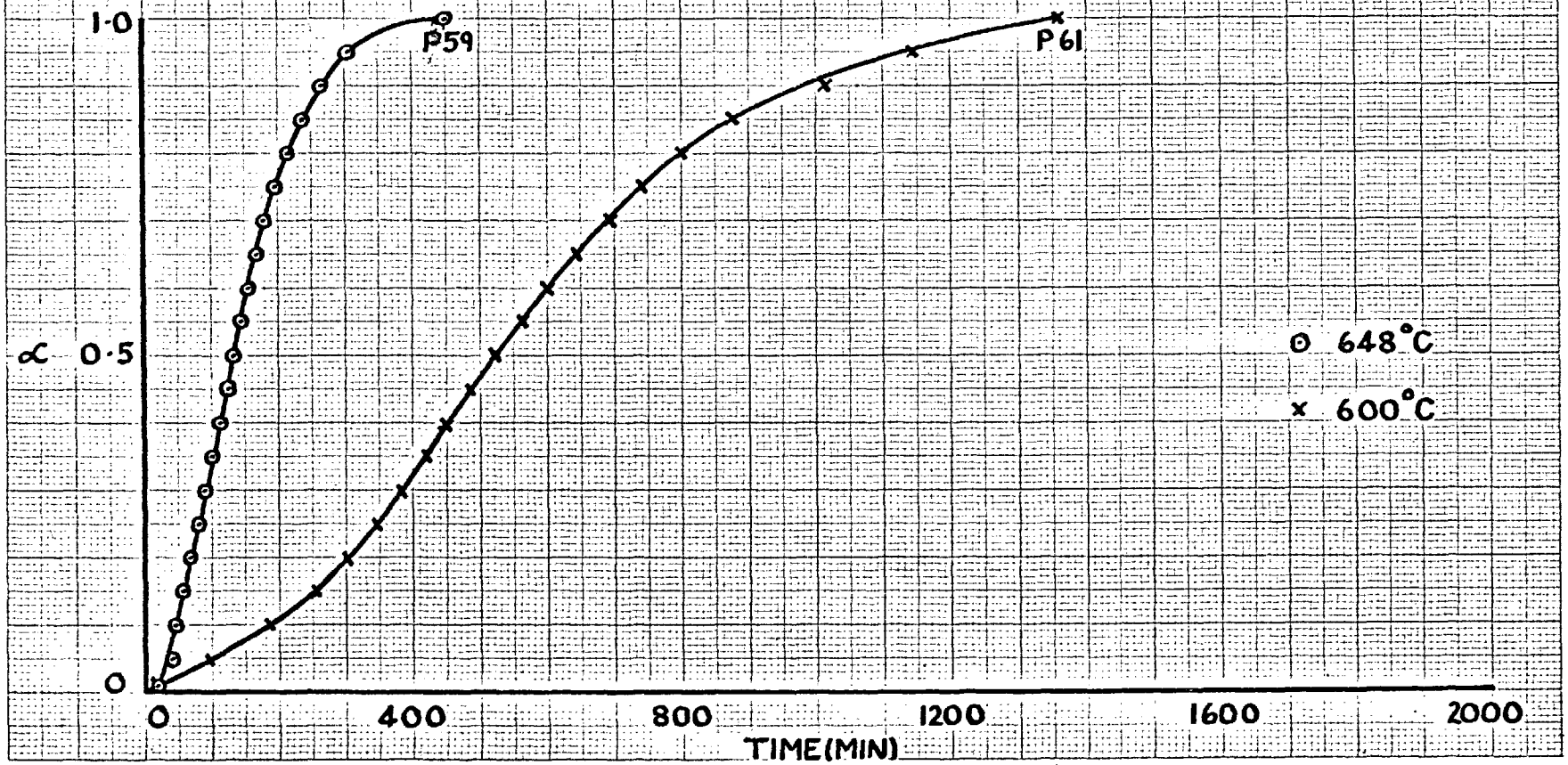


FIGURE 8

THERMAL DECOMPOSITION OF 4·45 % Mg + 95·55 % $NaNO_3$.
TEST OF THE "CONTRACTING AREA" EQUATION.

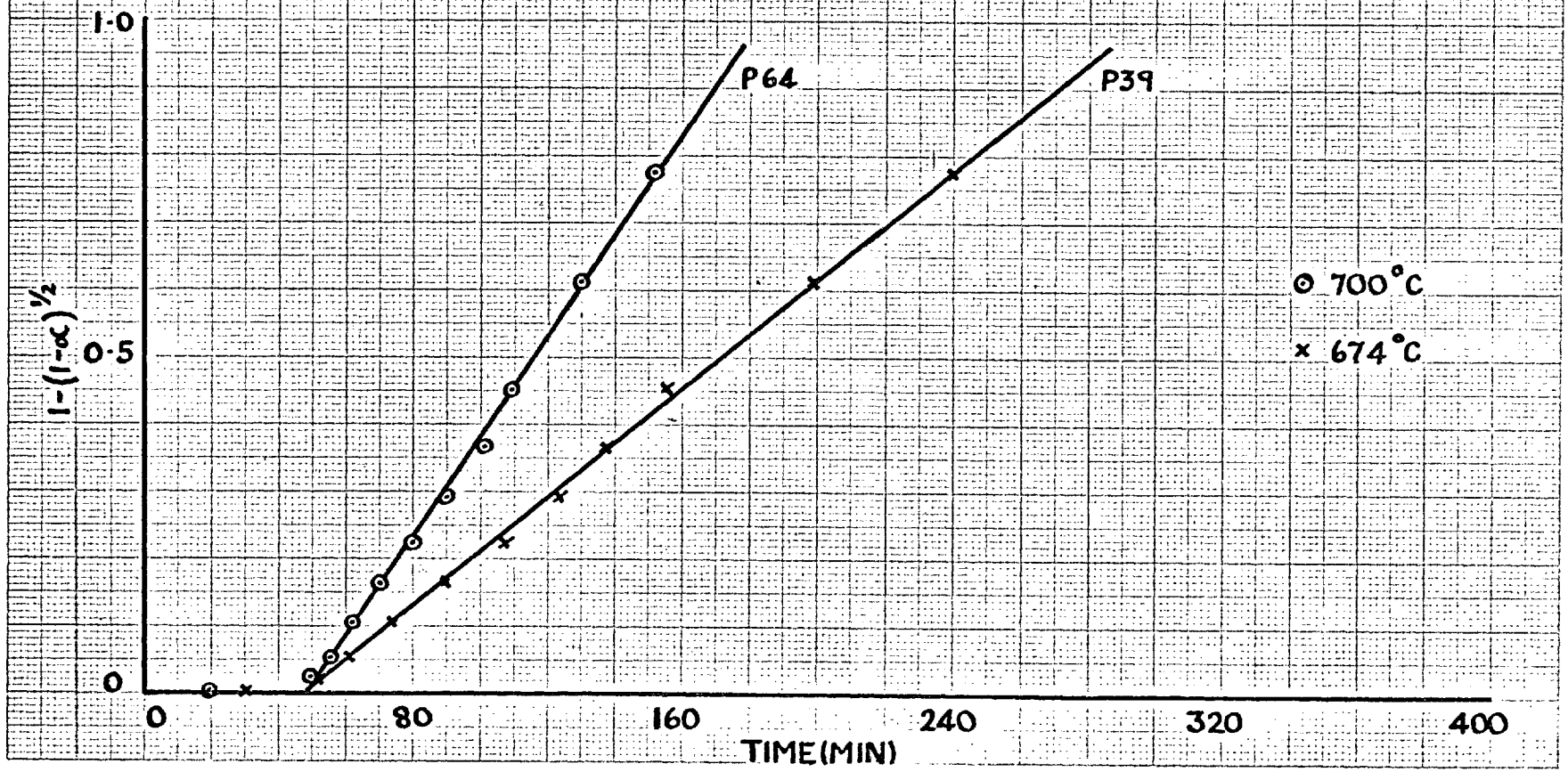


FIGURE 9

THERMAL DECOMPOSITION OF 4·45 % Mg + 95·55 % $NaNO_3$.
ARRHENIUS PLOT.

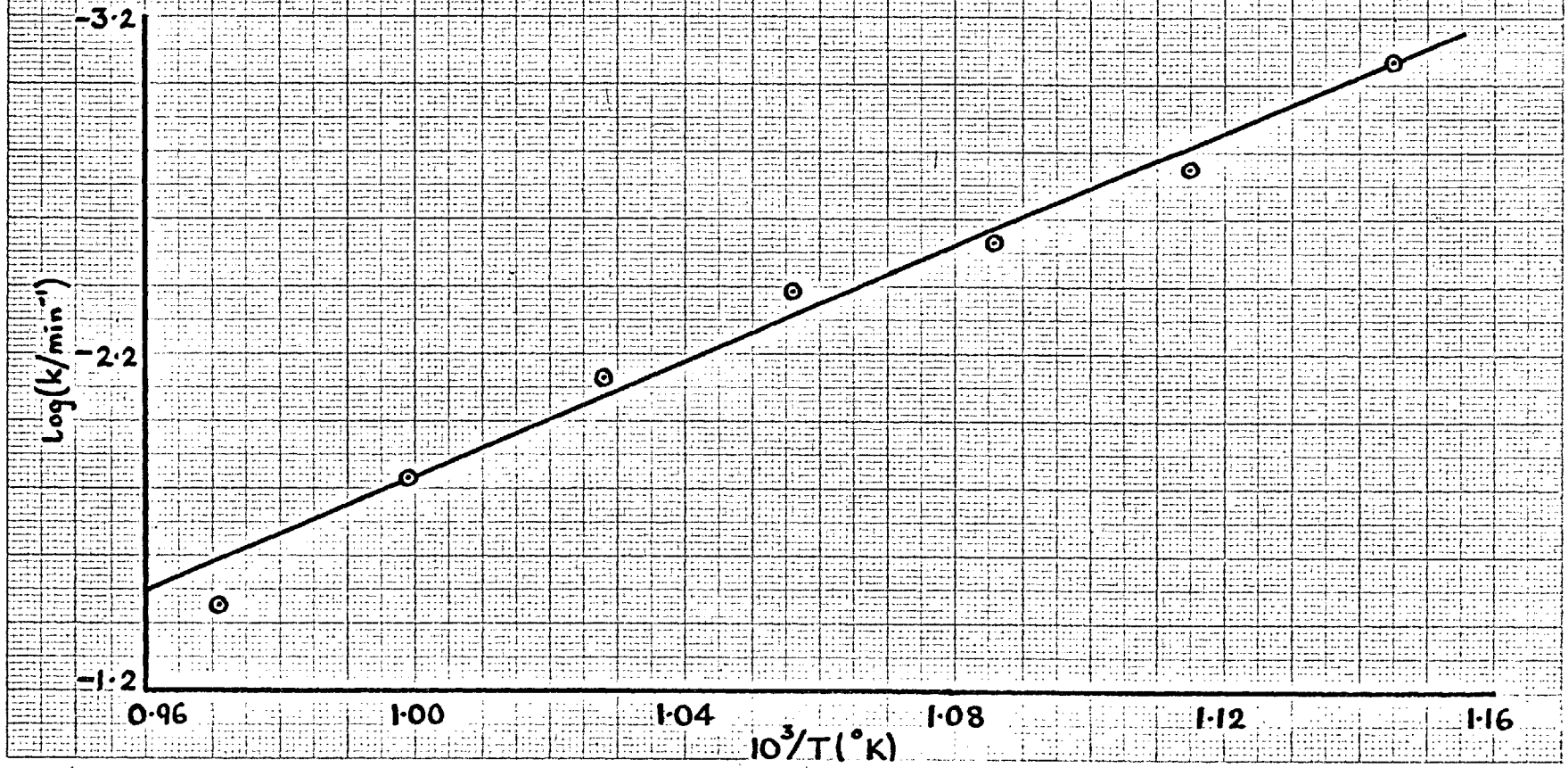


FIGURE 10

THERMAL DECOMPOSITION OF 11·12% Mg + 88·88% $NaNO_3$.

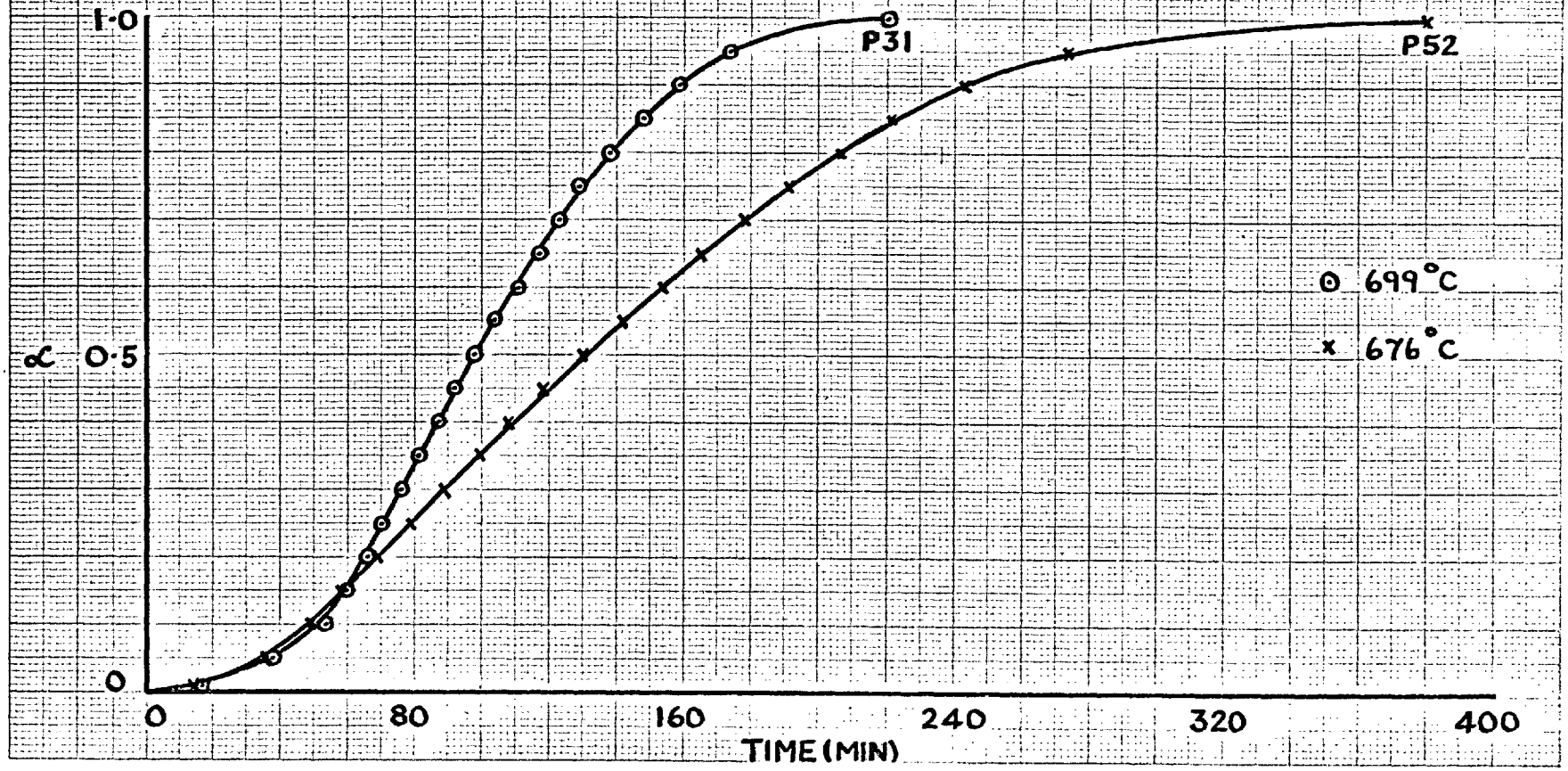


FIGURE 11

THERMAL DECOMPOSITION OF 11·12% Mg + 88·88% $NaNO_3$.
TEST OF THE "CONTRACTING AREA" EQUATION.

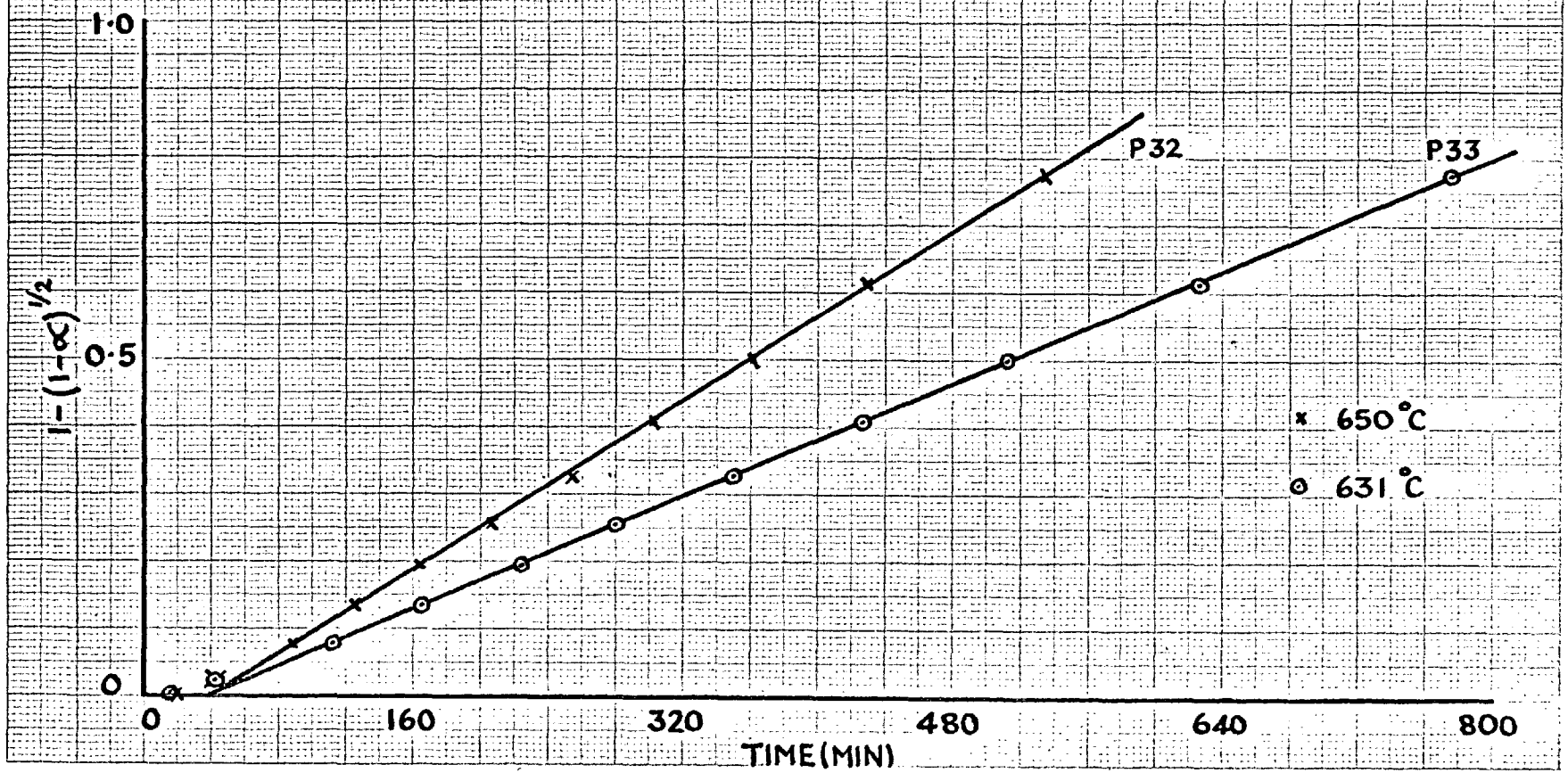


FIGURE 12

THERMAL DECOMPOSITION OF 11·12 % Mg + 88·88 % $NaNO_3$.
ARRHENIUS PLOT.

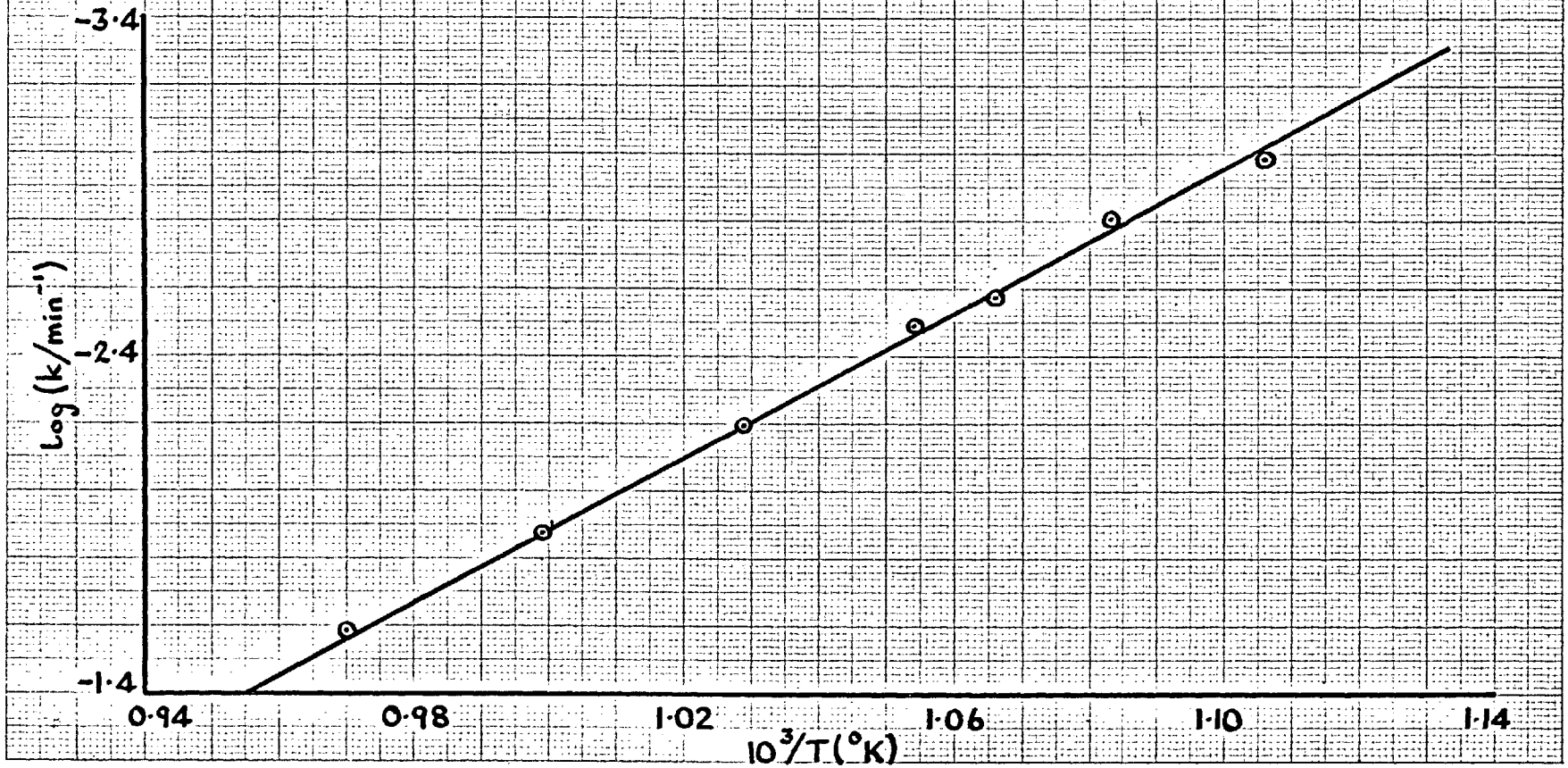


FIGURE 13

THERMAL DECOMPOSITION OF 15·57% Mg + 84·43% $NaNO_3$.

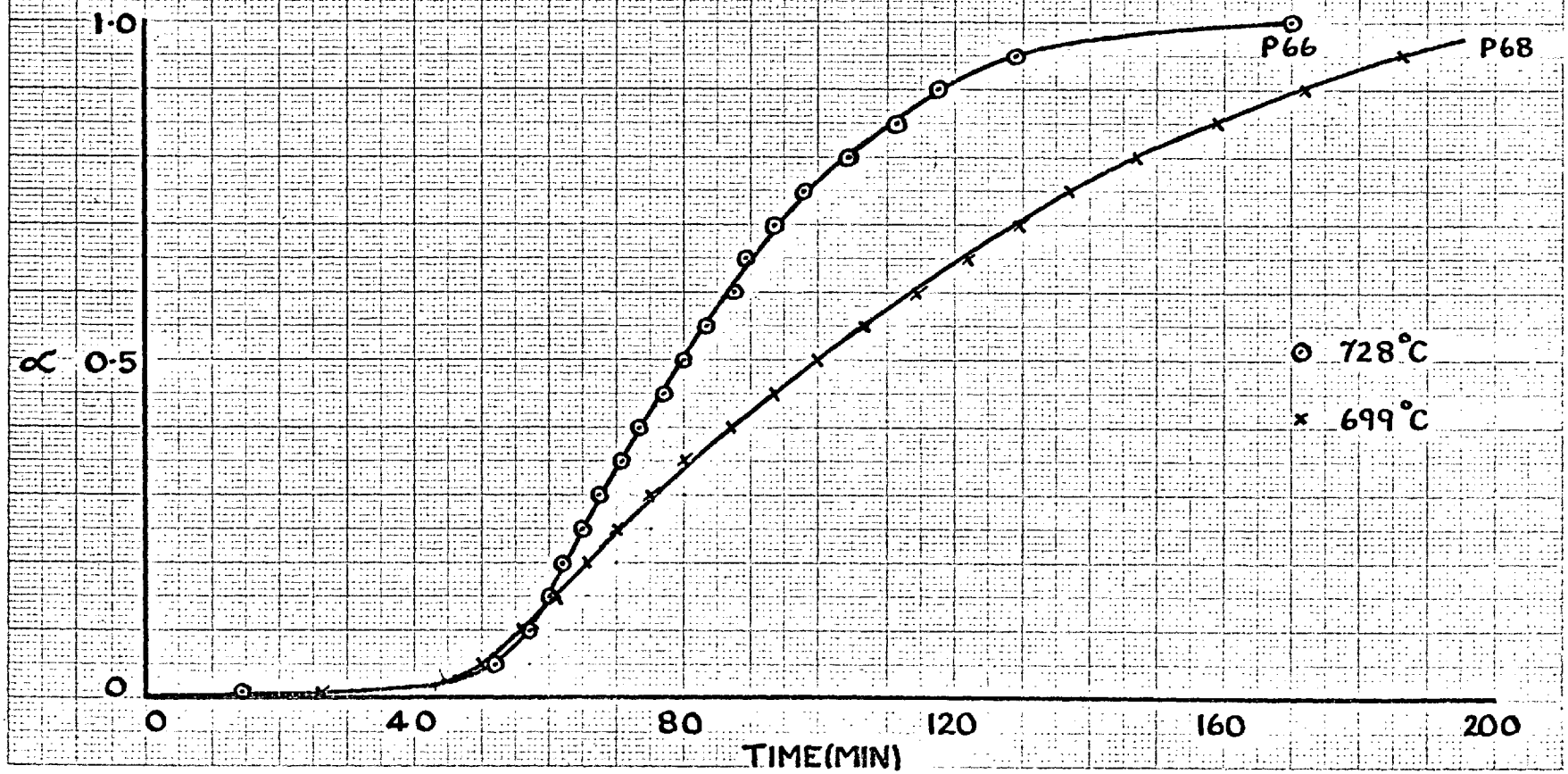


FIGURE 14

THERMAL DECOMPOSITION OF 15·57% Mg + 84·43% $NaNO_3$.
TEST OF THE "CONTRACTING AREA" EQUATION.

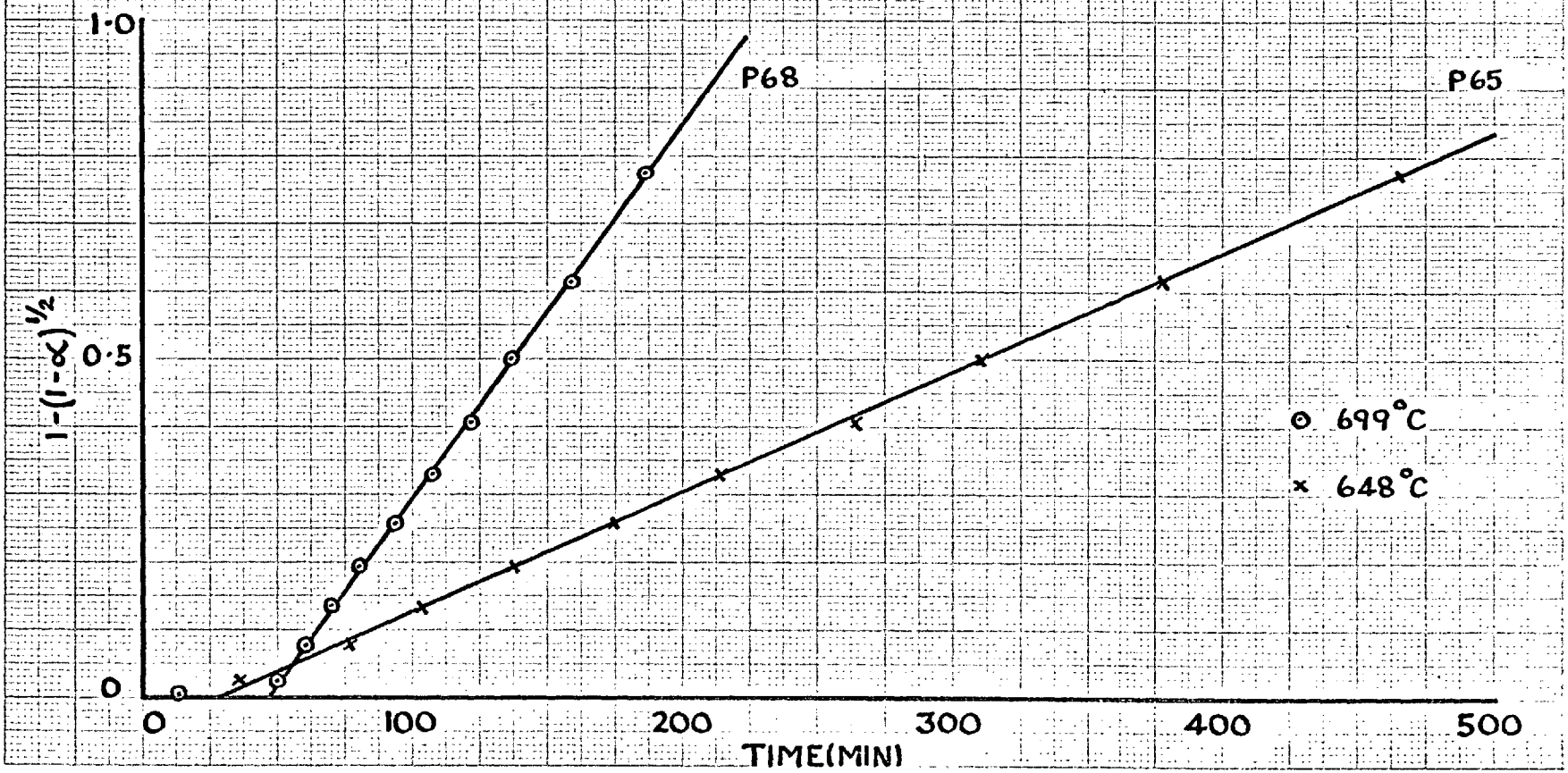


FIGURE 15

THERMAL DECOMPOSITION OF 15·57% Mg + 84·43% $NaNO_3$.
ARRHENIUS PLOT.

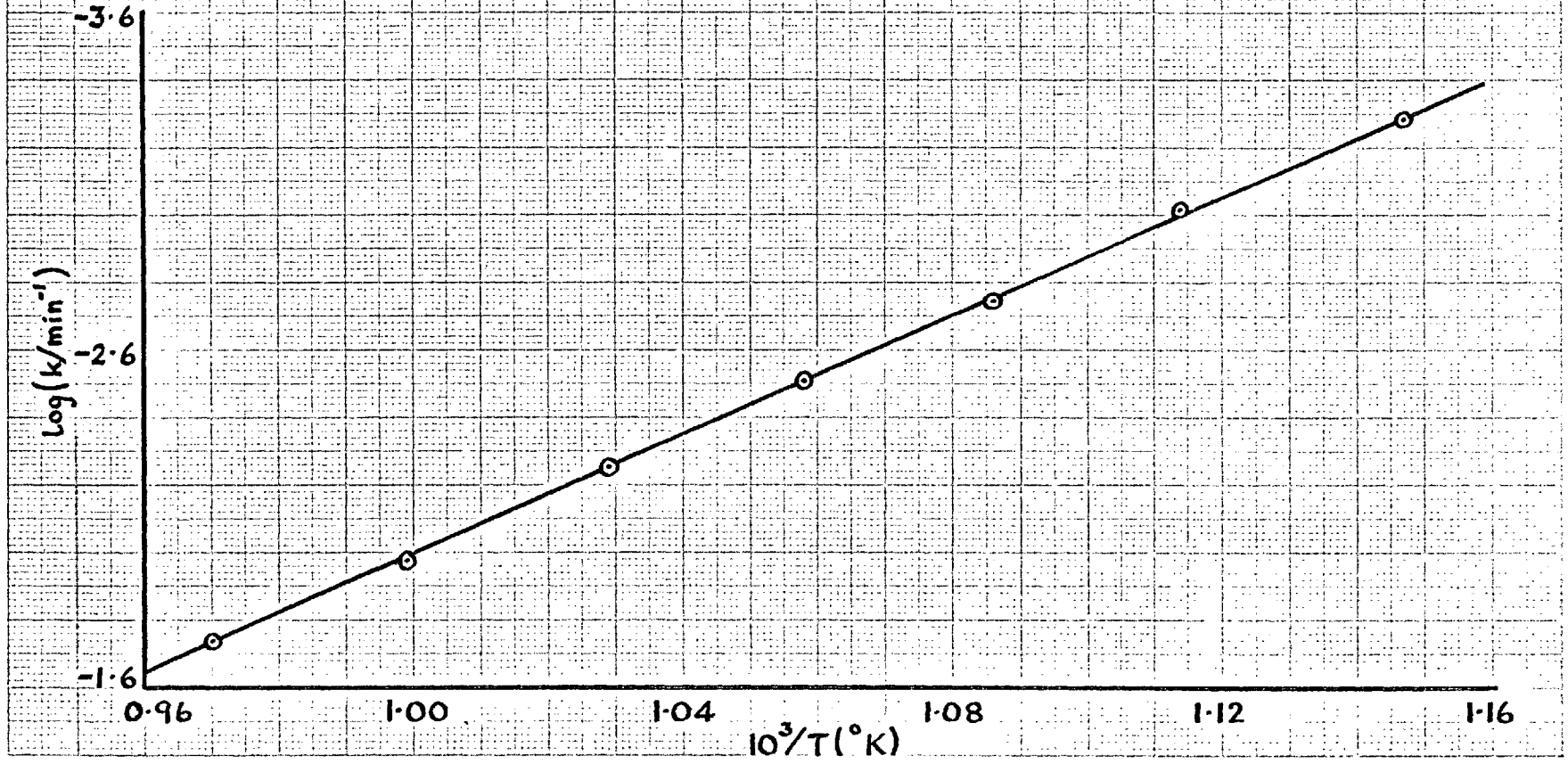


FIGURE 16

THERMAL DECOMPOSITION OF 22·25 % Mg + 77·75 % $NaNO_3$.

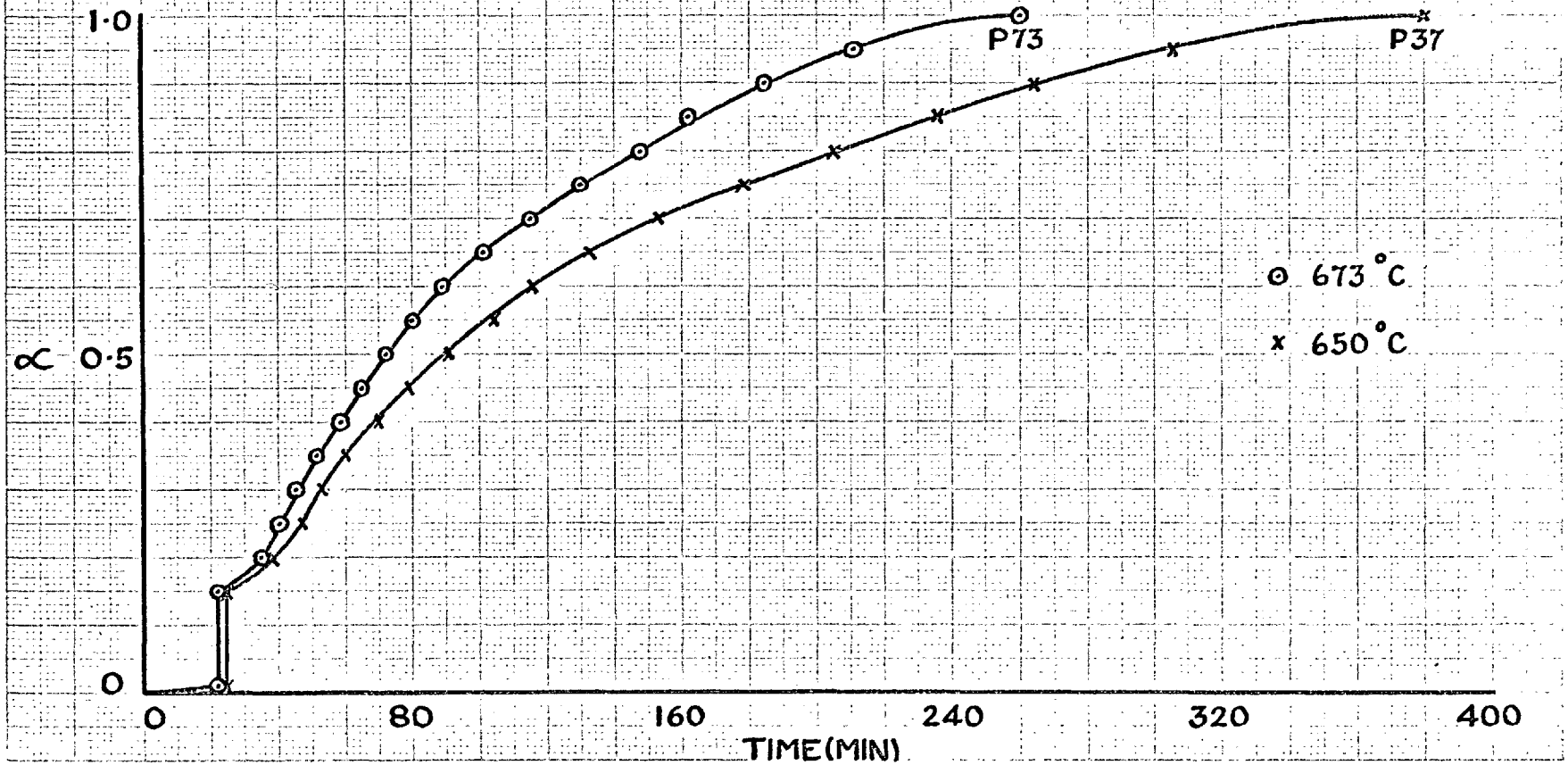


FIGURE 17

THERMAL DECOMPOSITION OF 22·25 % Mg + 77·75 % $NaNO_3$.
TEST OF THE "CONTRACTING AREA" EQUATION.

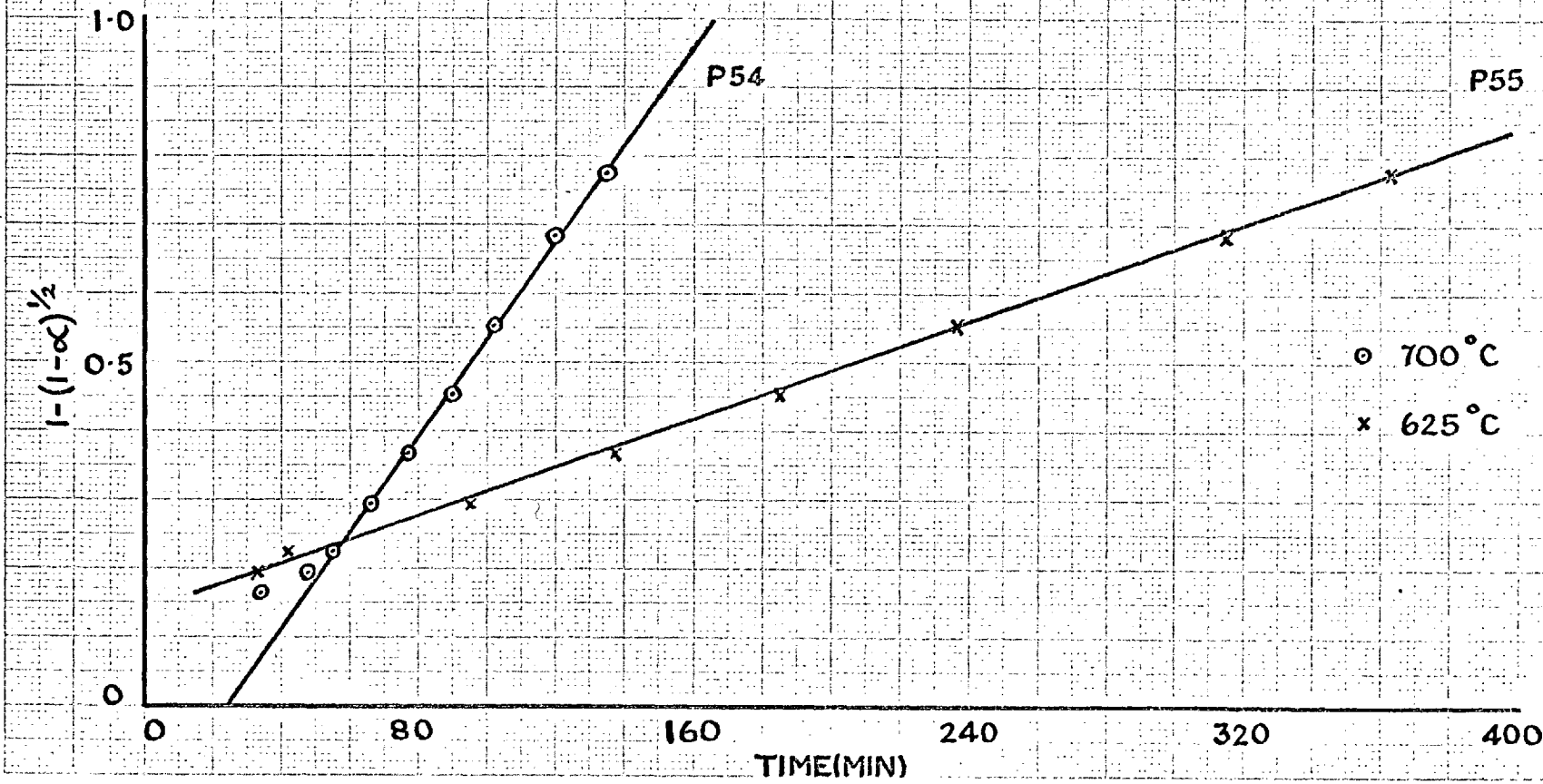


FIGURE 18

THERMAL DECOMPOSITION OF 22·25 % Mg + 77·75 % $NaNO_3$.
ARRHENIUS PLOT.

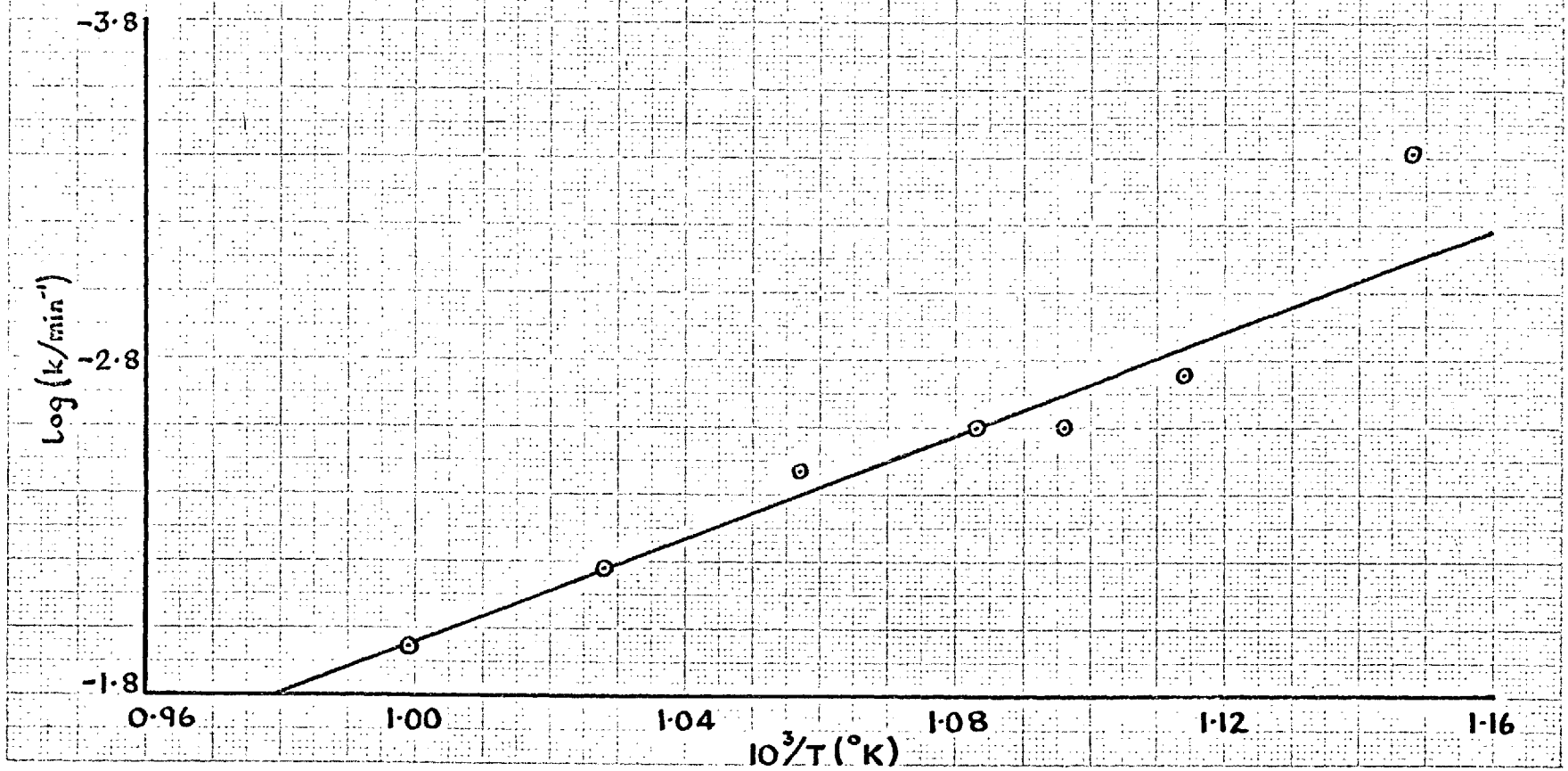


FIGURE 19

THERMAL DECOMPOSITION OF SODIUM NITRATE.

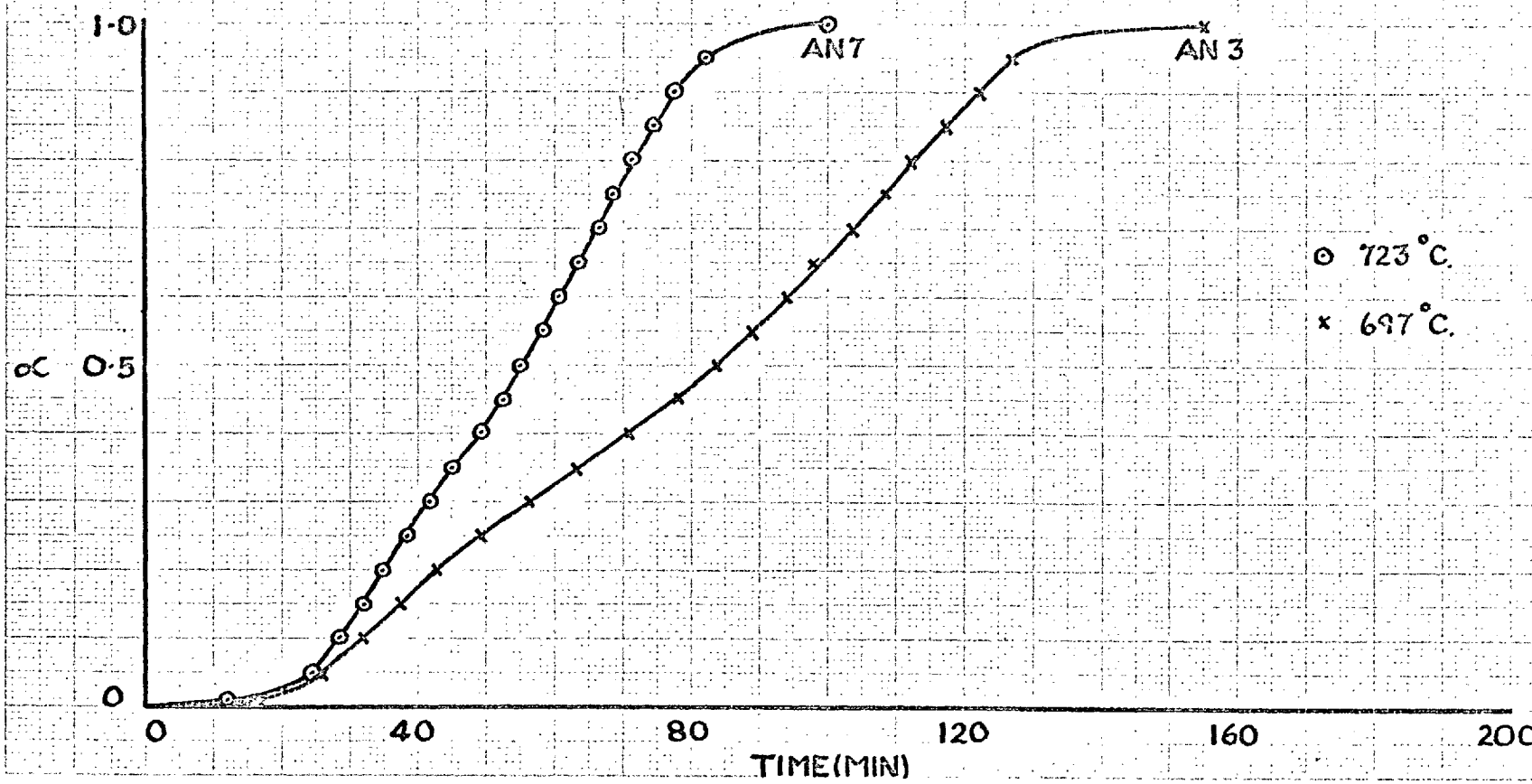


FIGURE 20

THERMAL DECOMPOSITION OF SODIUM NITRATE.

a) $NaNO_3 \rightarrow NaNO_2$; b) $NaNO_2 \rightarrow Na_2O$.

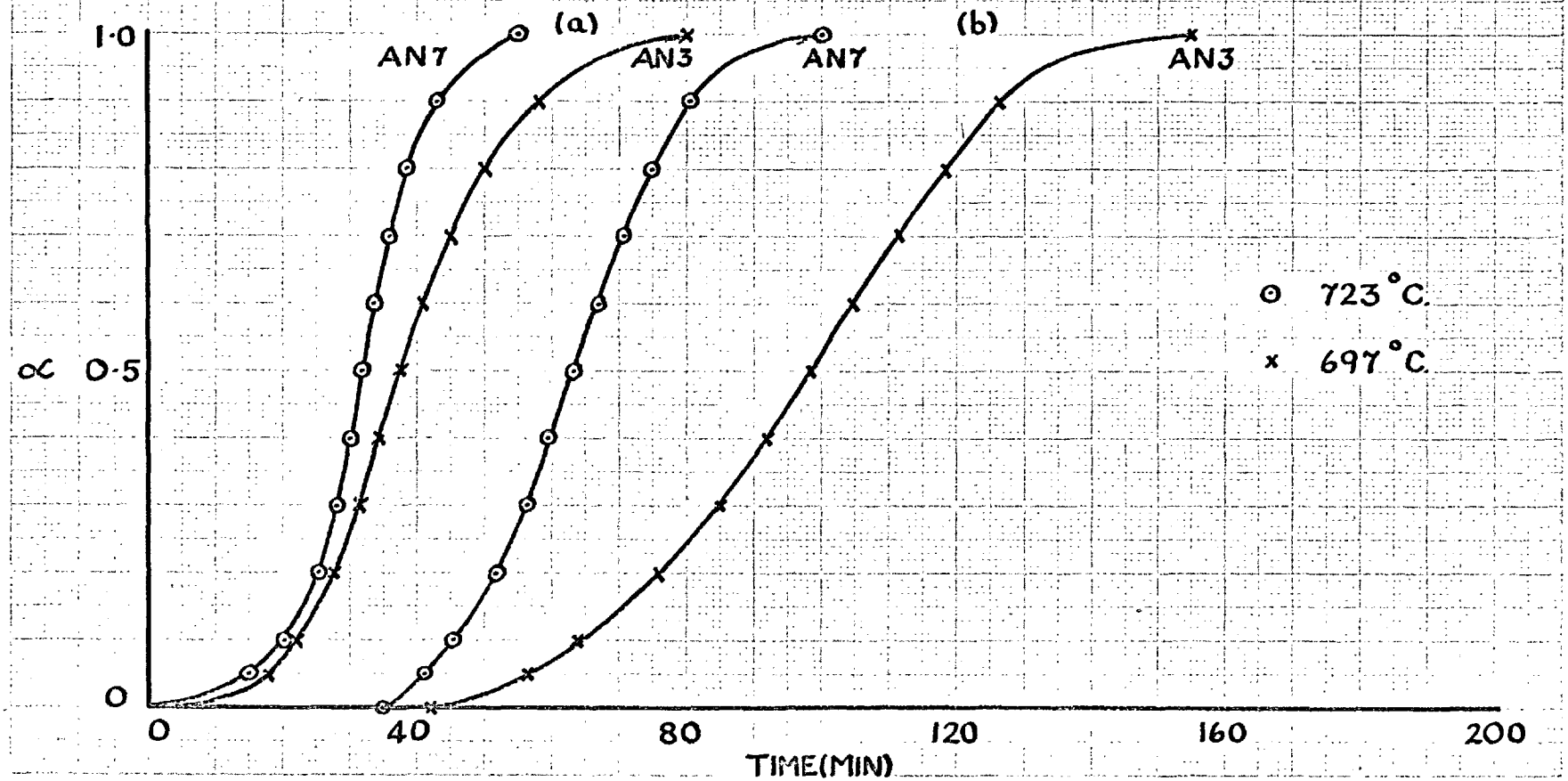


FIGURE 21

THERMAL DECOMPOSITION OF SODIUM NITRATE.
TEST OF THE AVRAMI-EROFEYEV EQUATION WITH n = 3.

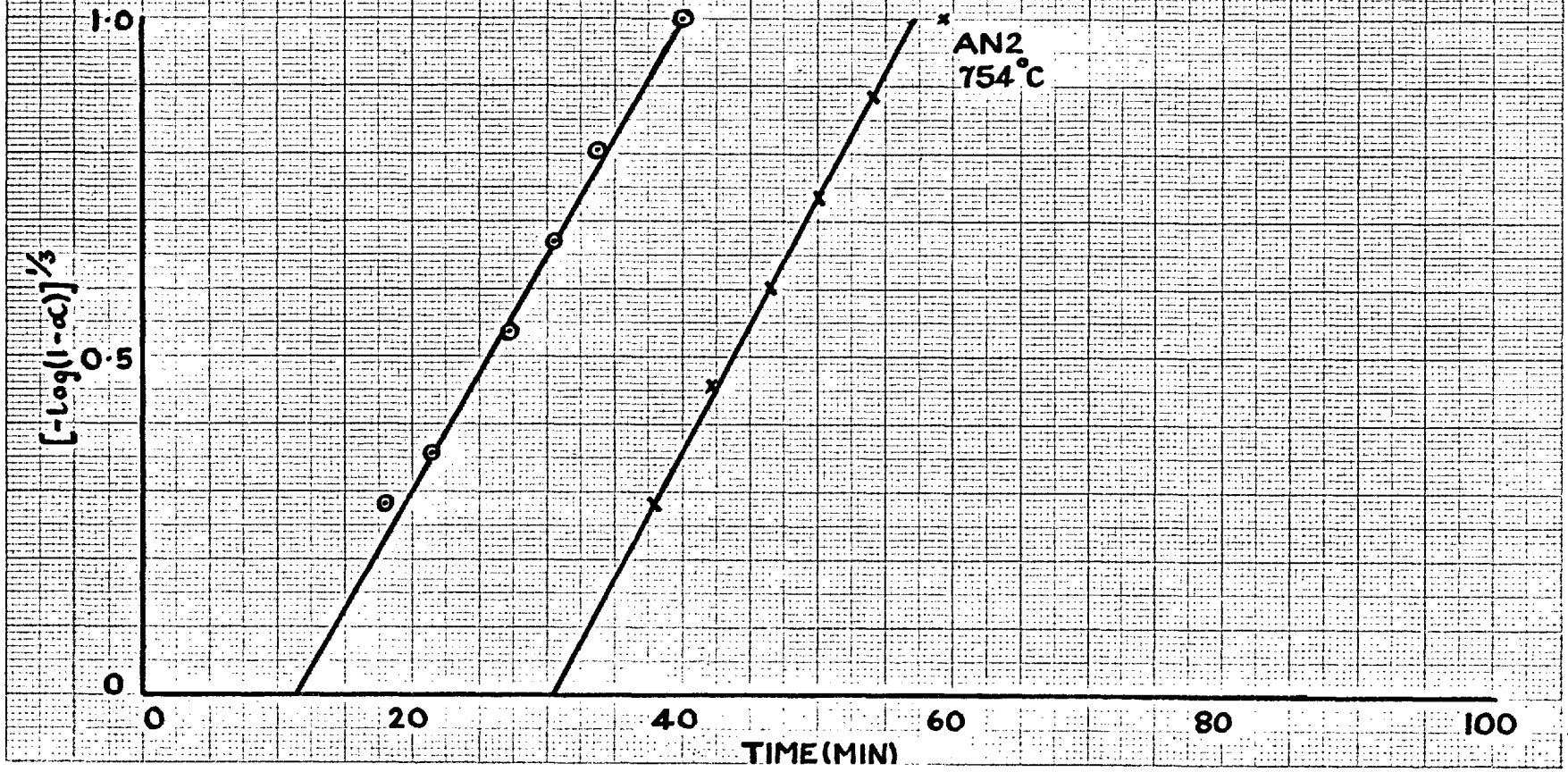


FIGURE 22

THERMAL DECOMPOSITION OF SODIUM NITRATE.
ARRHENIUS PLOT OF THE NITRATE - NITRITE REACTION.

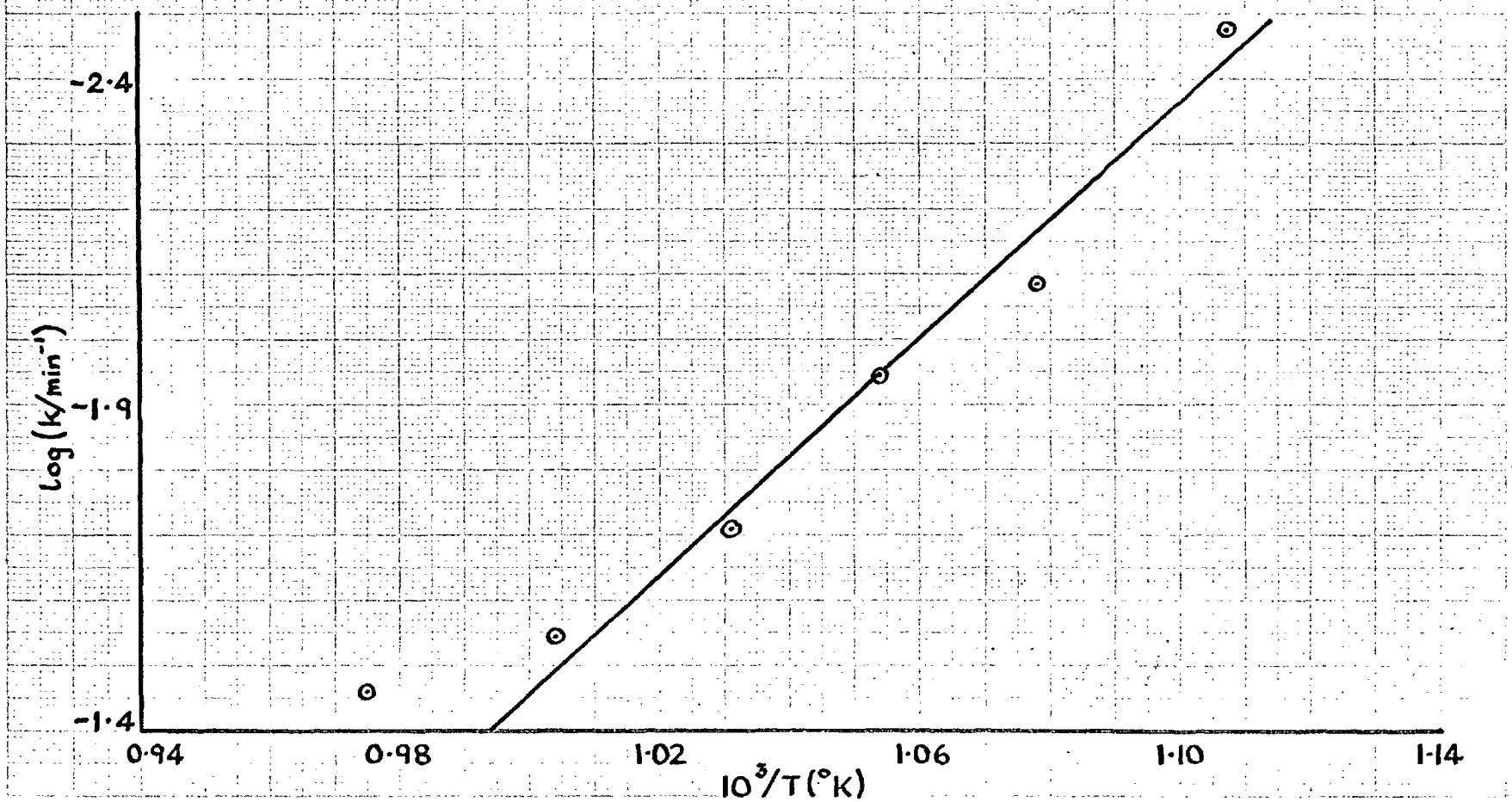


FIGURE 23

THERMAL DECOMPOSITION OF SODIUM NITRATE.
ARRHENIUS PLOT OF THE NITRITE-OXIDE REACTION.

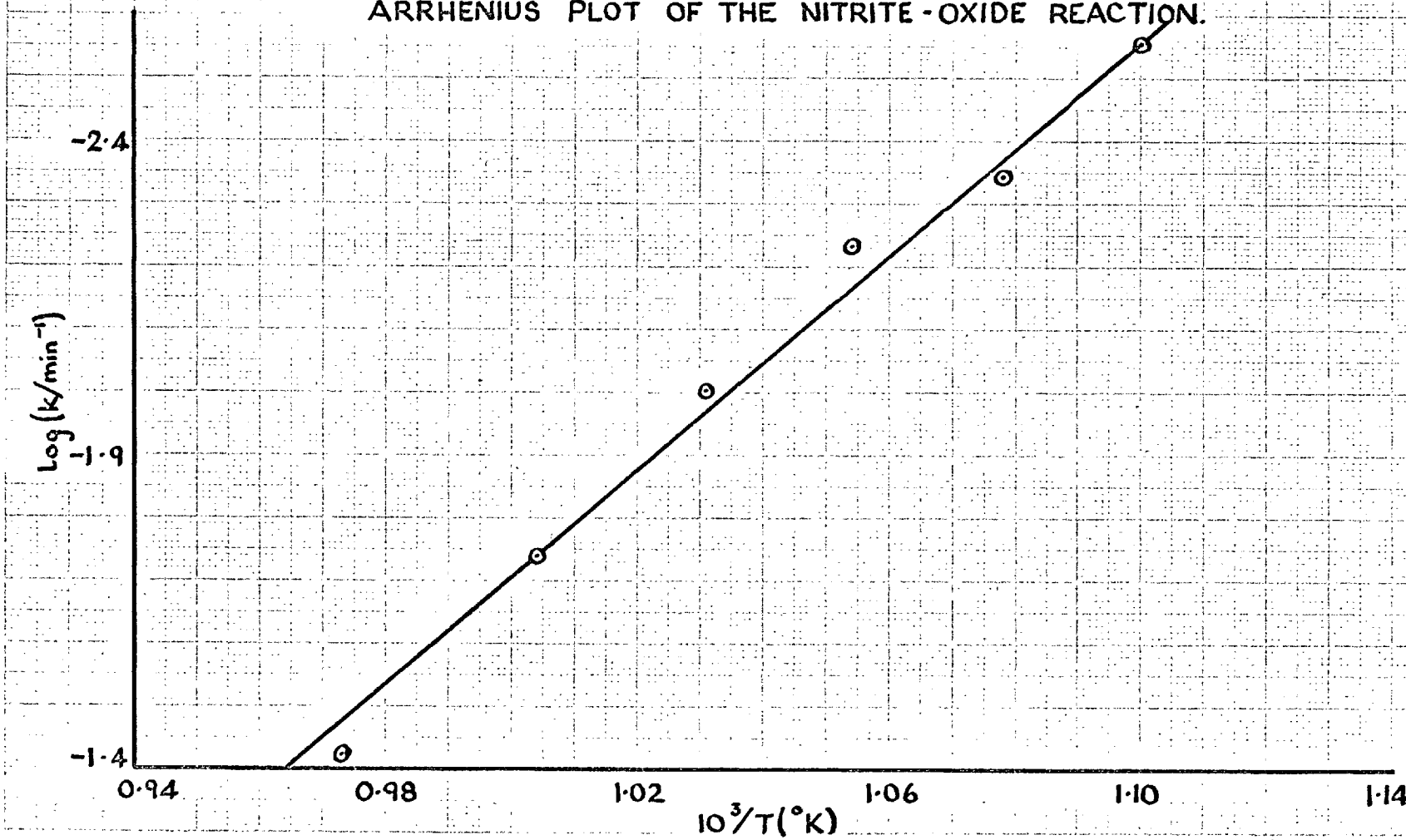


FIGURE 24

THERMAL DECOMPOSITION OF 11·12% Mg + 88·88% $NaNO_3$

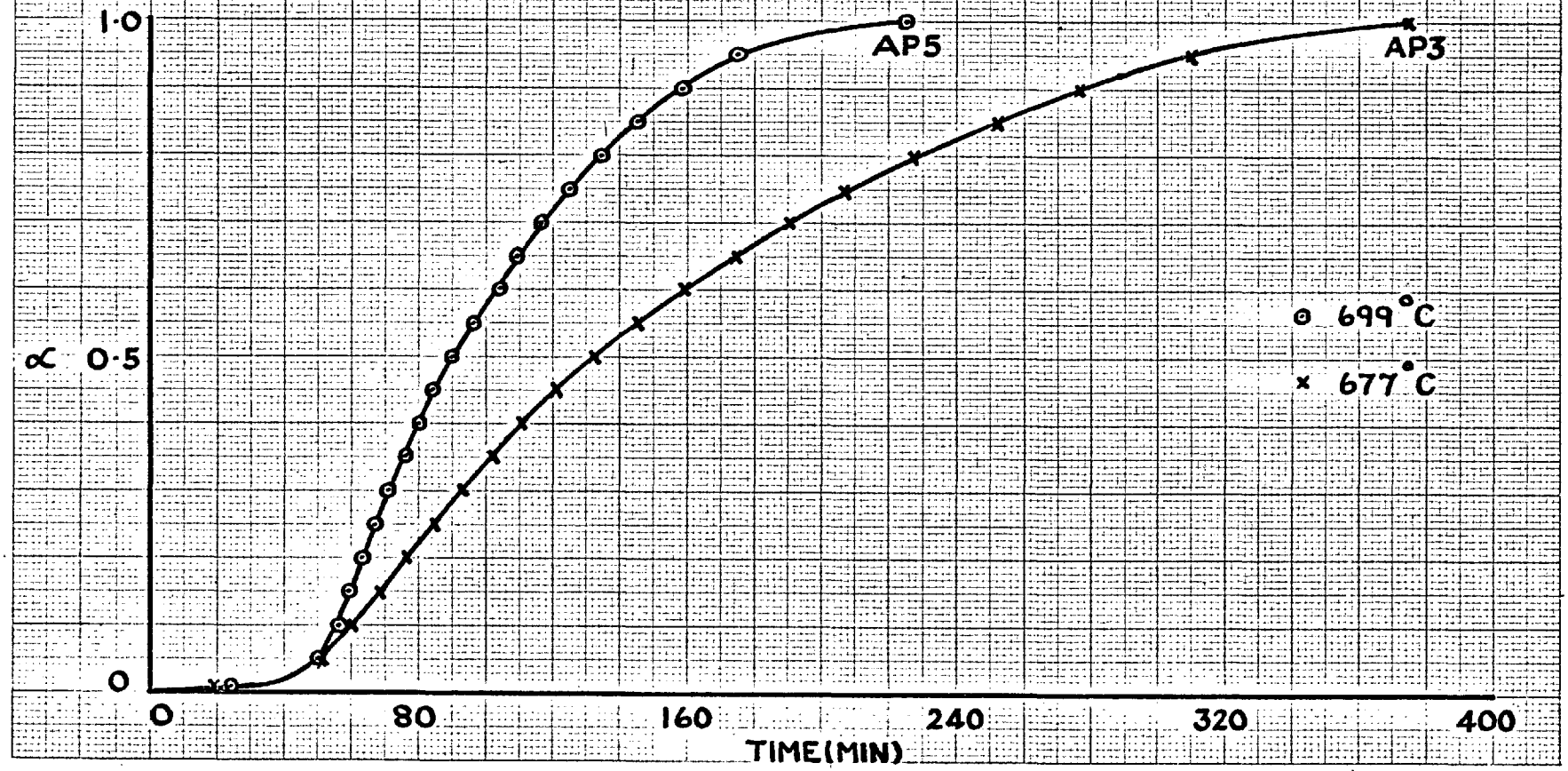


FIGURE 25

THERMAL DECOMPOSITION OF 11·12% Mg + 88·88% $NaNO_3$.
TEST OF THE "CONTRACTING AREA" EQUATION.

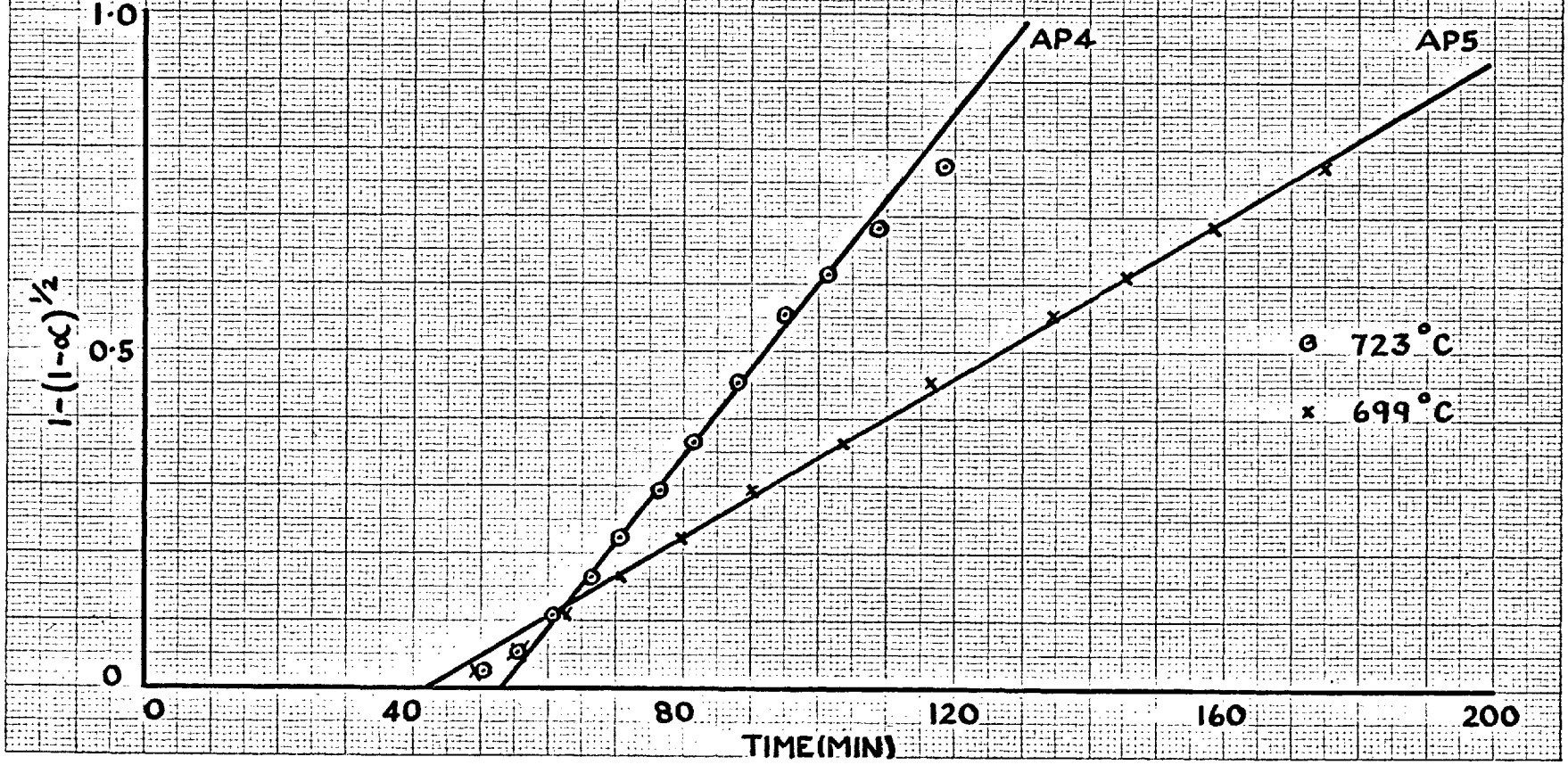


FIGURE 26

THERMAL DECOMPOSITION OF 11·12% Mg + 88·88% $NaNO_3$

ARRHENIUS PLOT

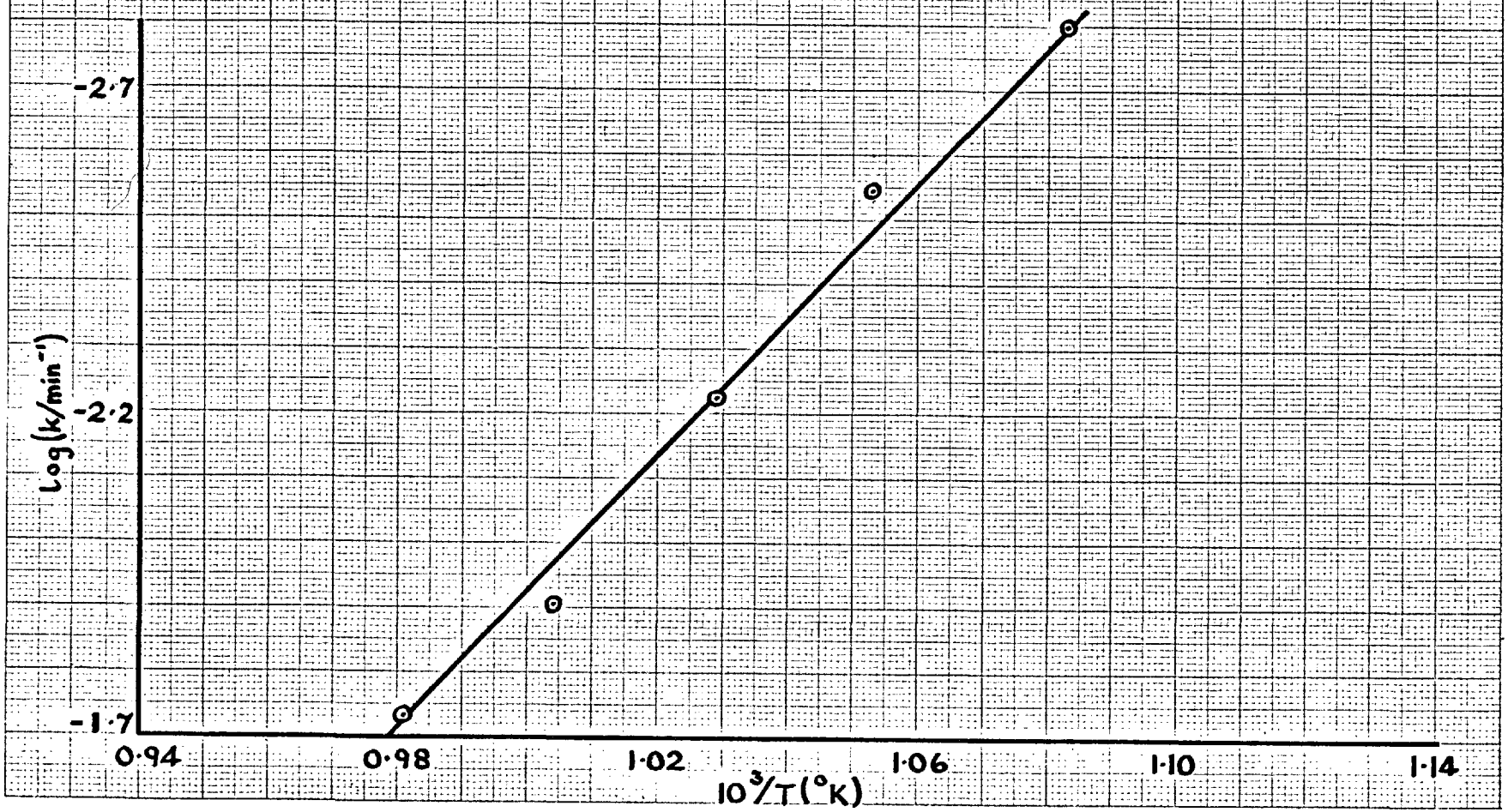


FIGURE 27

THERMAL DECOMPOSITION OF 22·25 % Mg + 77·75 % $NaNO_3$.

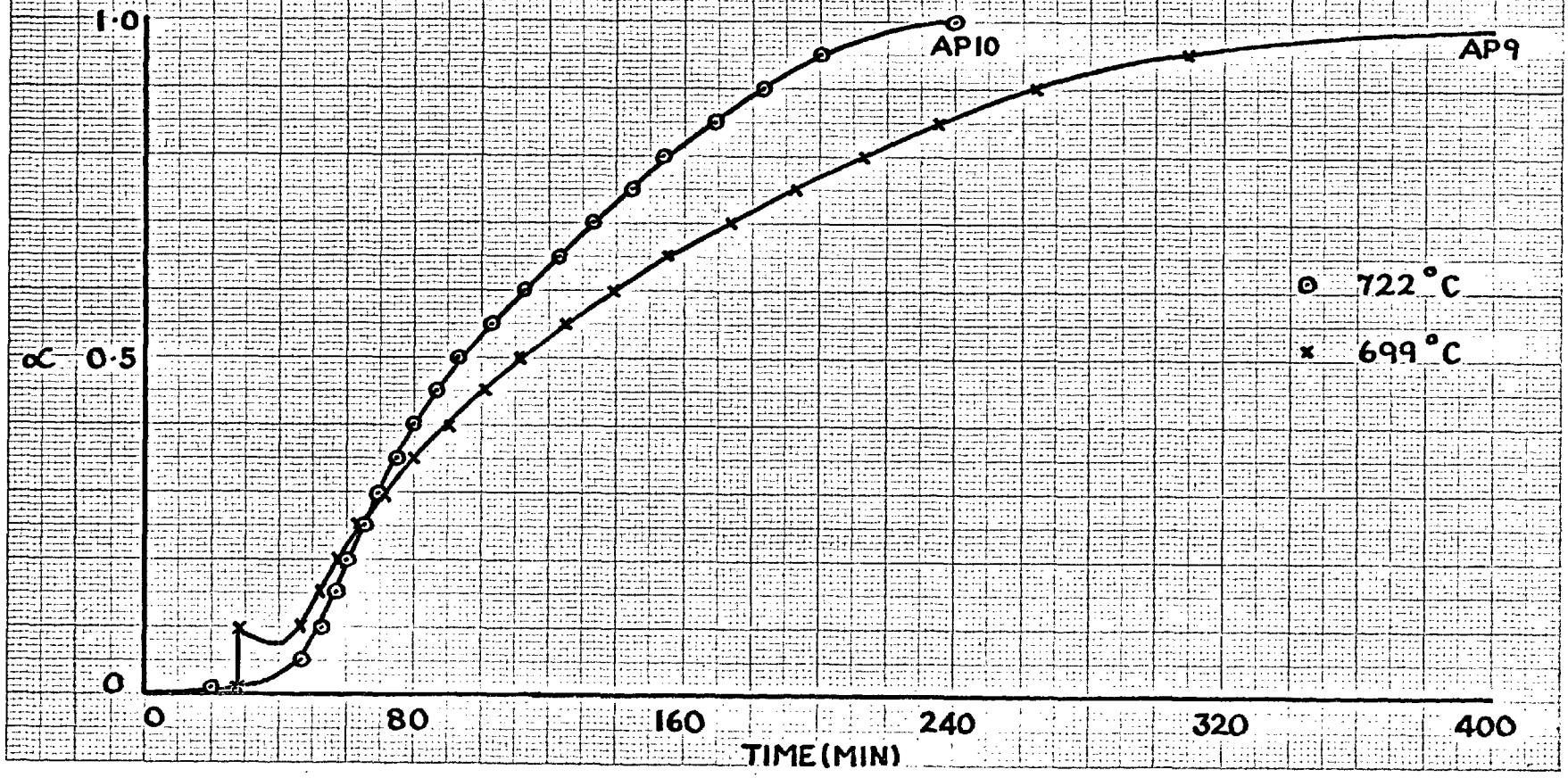


FIGURE 28

THERMAL DECOMPOSITION OF 22·25 % Mg + 77·75 % $NaNO_3$.
TEST OF THE "CONTRACTING AREA" EQUATION.

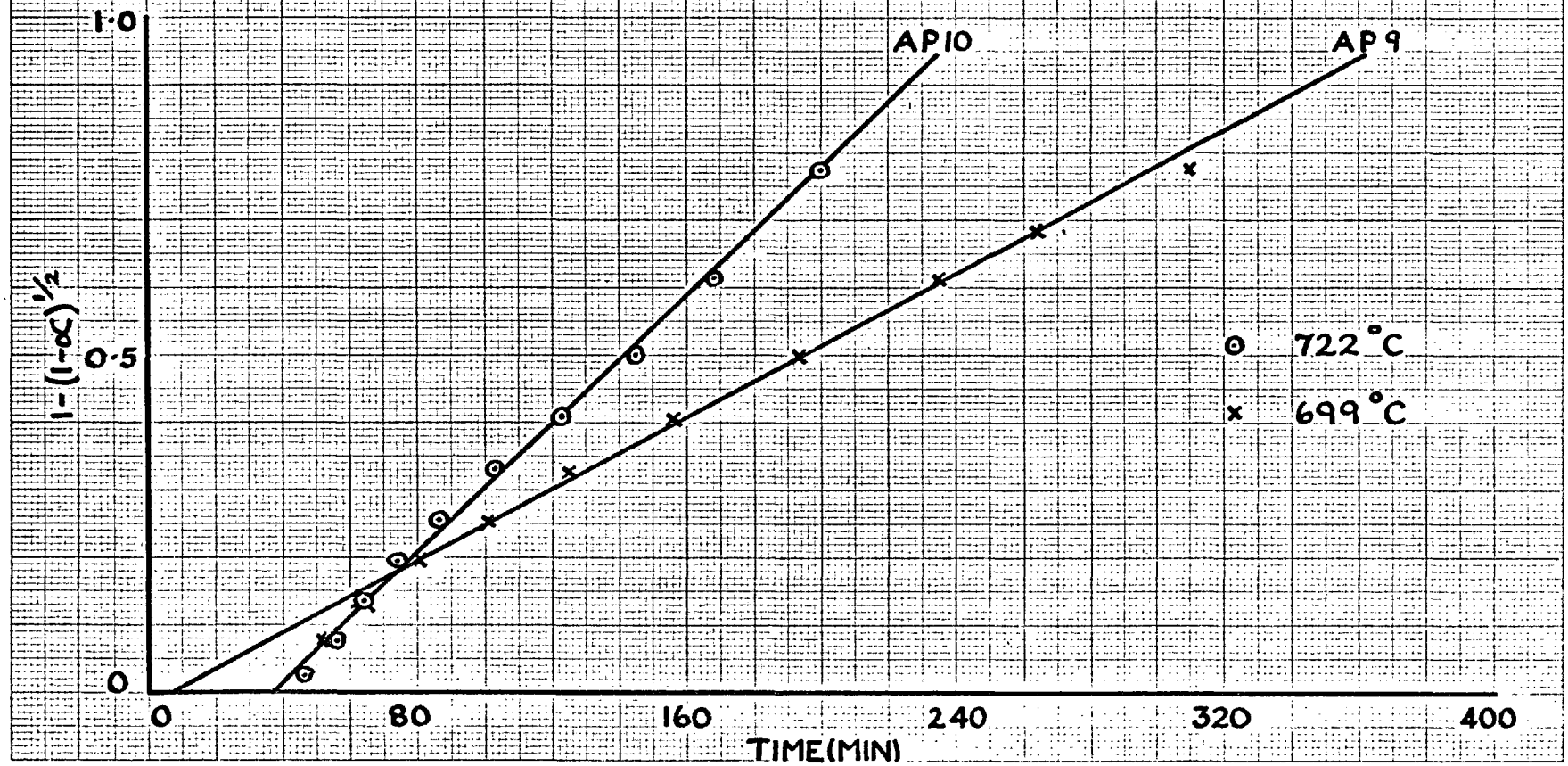


FIGURE 29

THERMAL DECOMPOSITION OF 22·25% Mg + 77·75% $NaNO_3$.

ARRHENIUS PLOT.

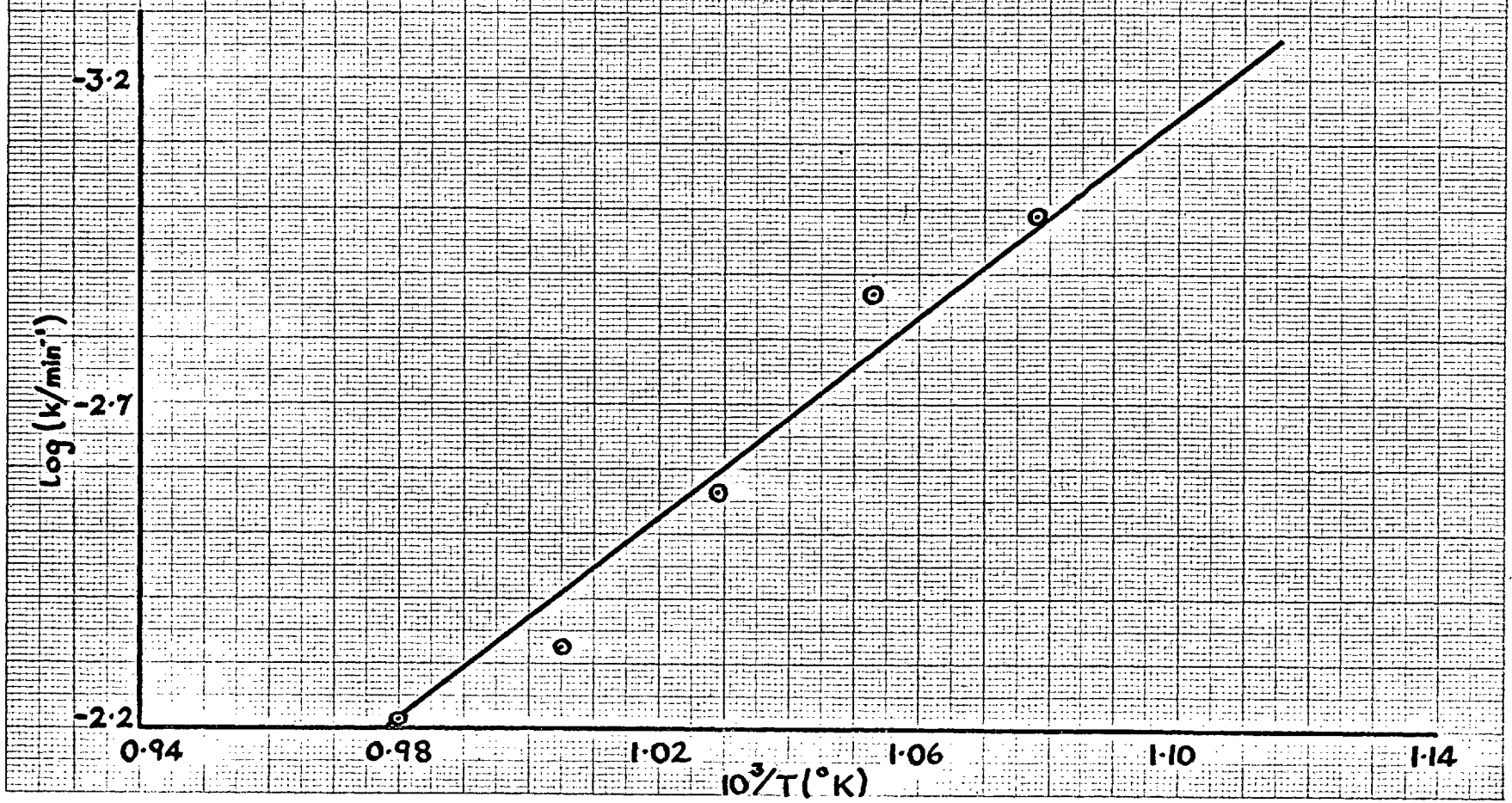


FIGURE 30

THERMAL DECOMPOSITION OF 7·17 % MgO + 92·43 % $NaNO_3$.

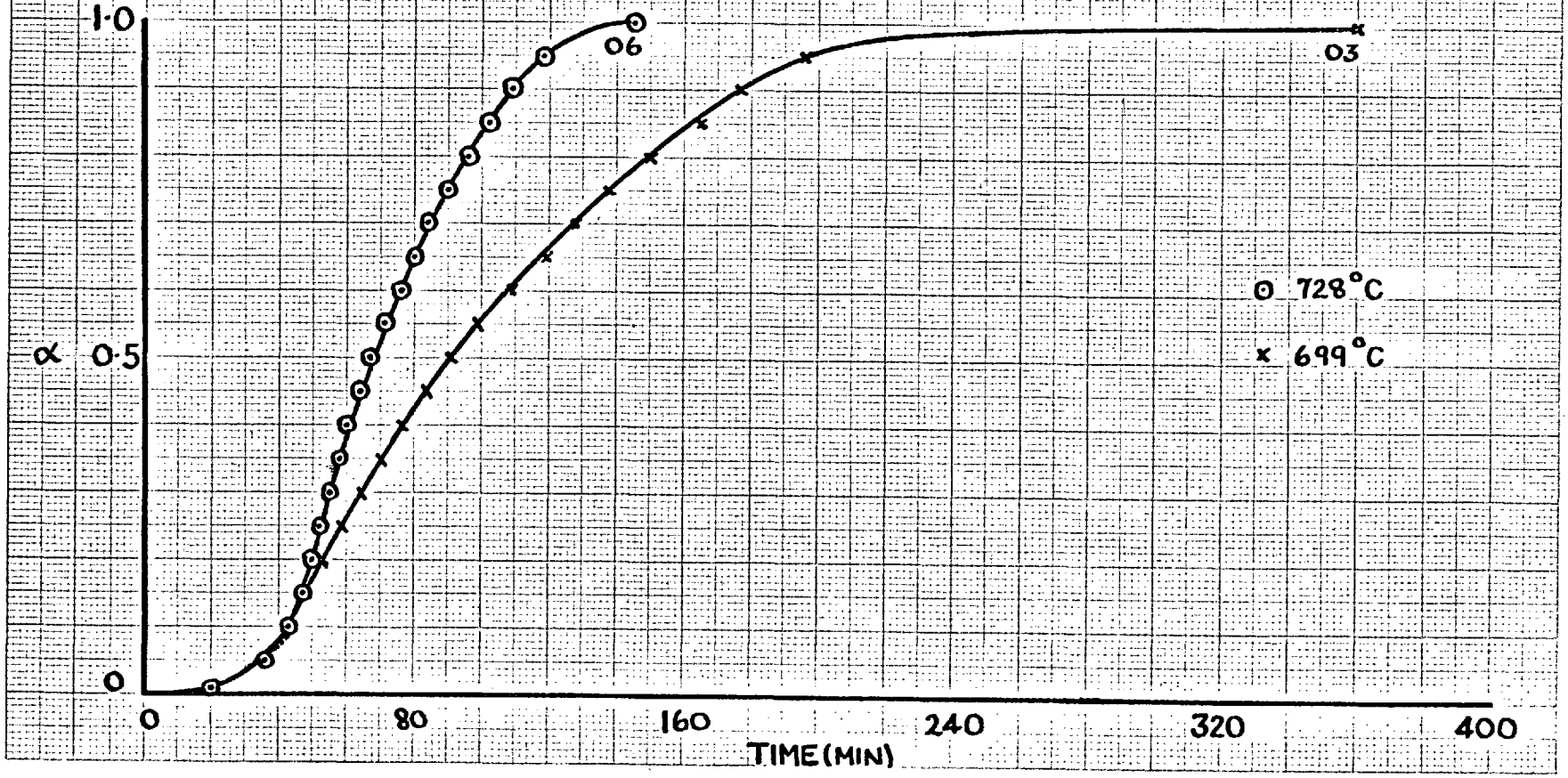


FIGURE 31

THERMAL DECOMPOSITION OF 22·25% MgO + 77·75% $NaNO_3$

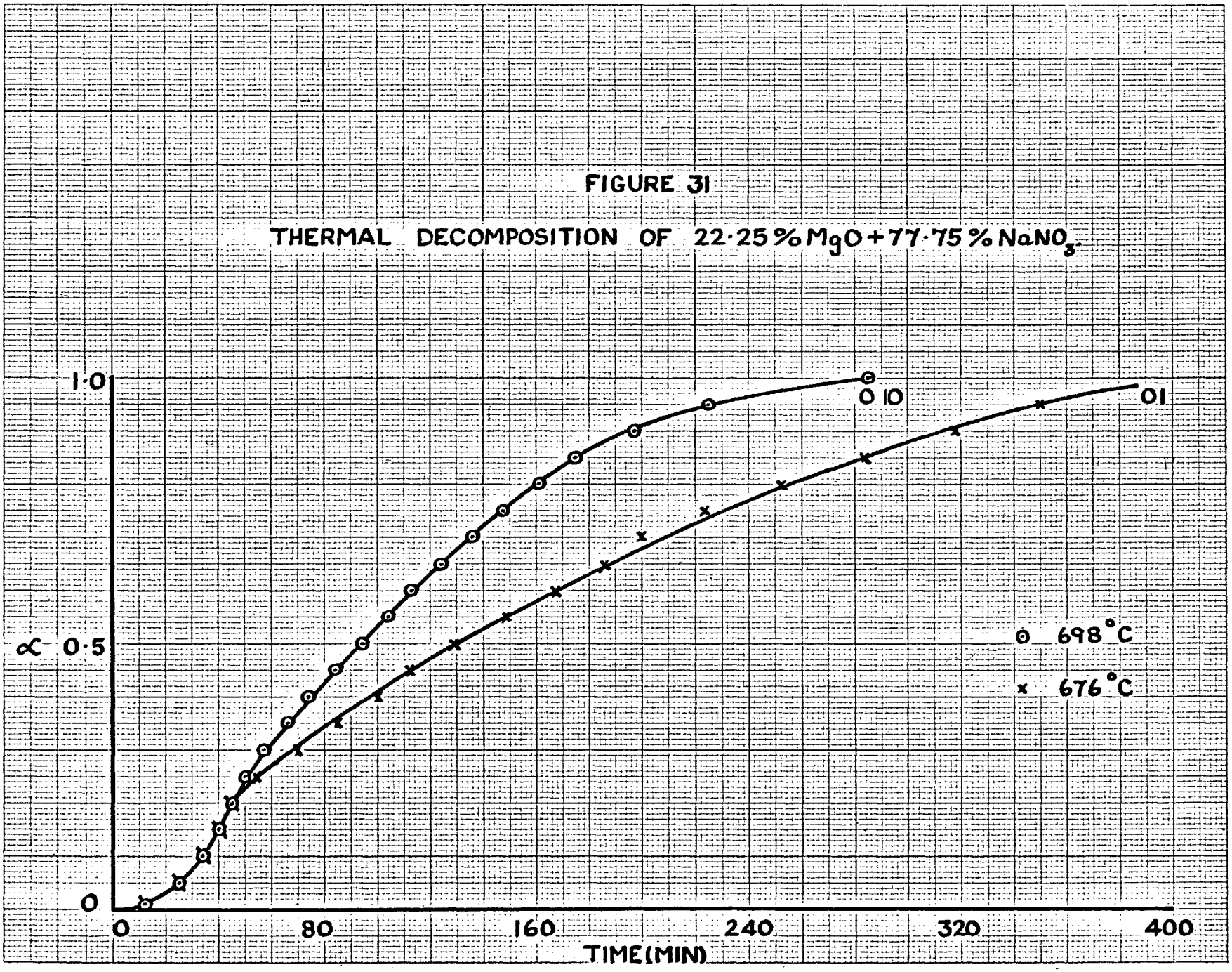


FIGURE 32

PLOTS OF LOG ΔT vs. t FOR SODIUM NITRATE.

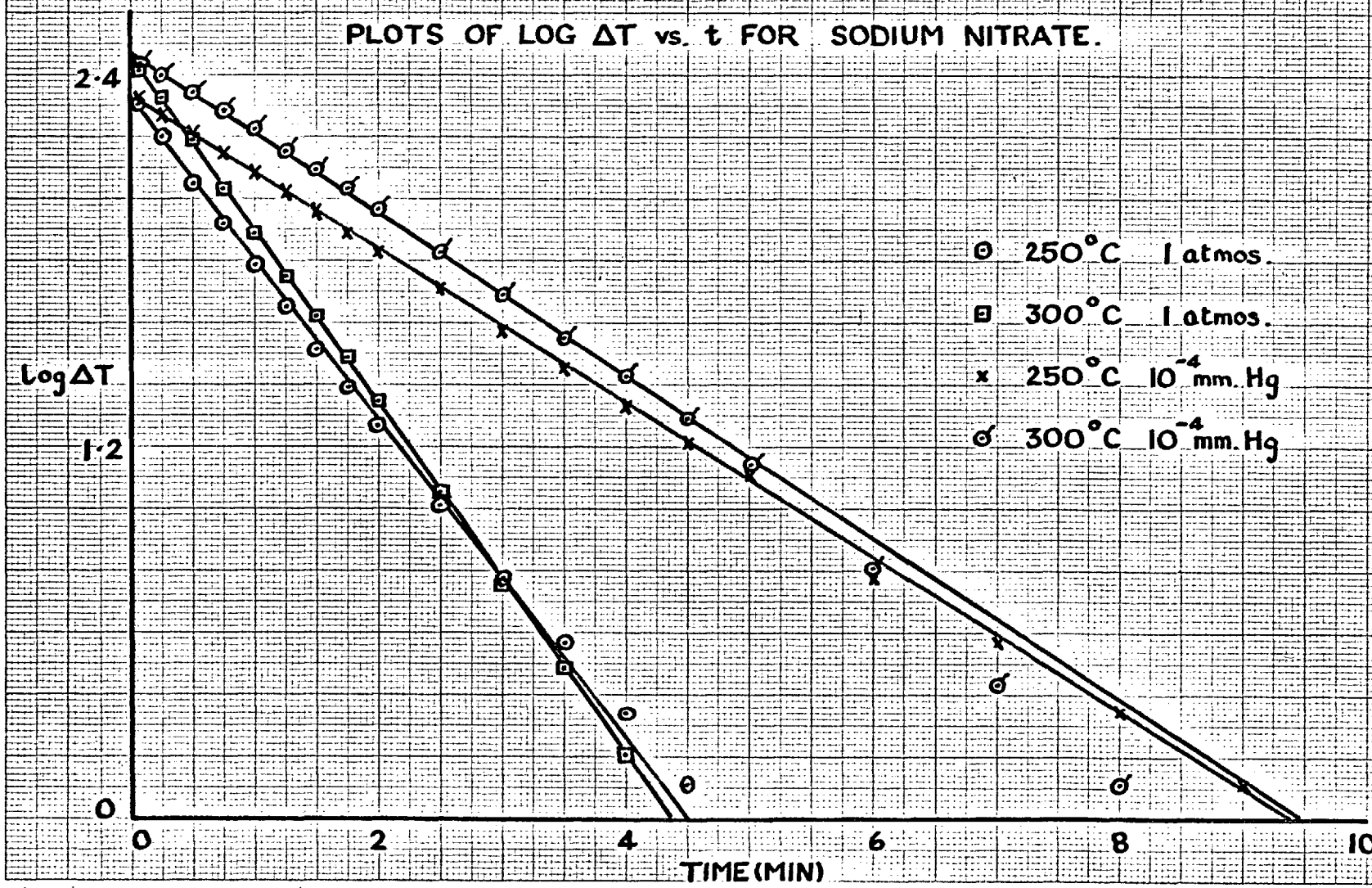


FIGURE 33

TEST OF HEAT-UP EQUATION WITH n = 1, 2 and 3.

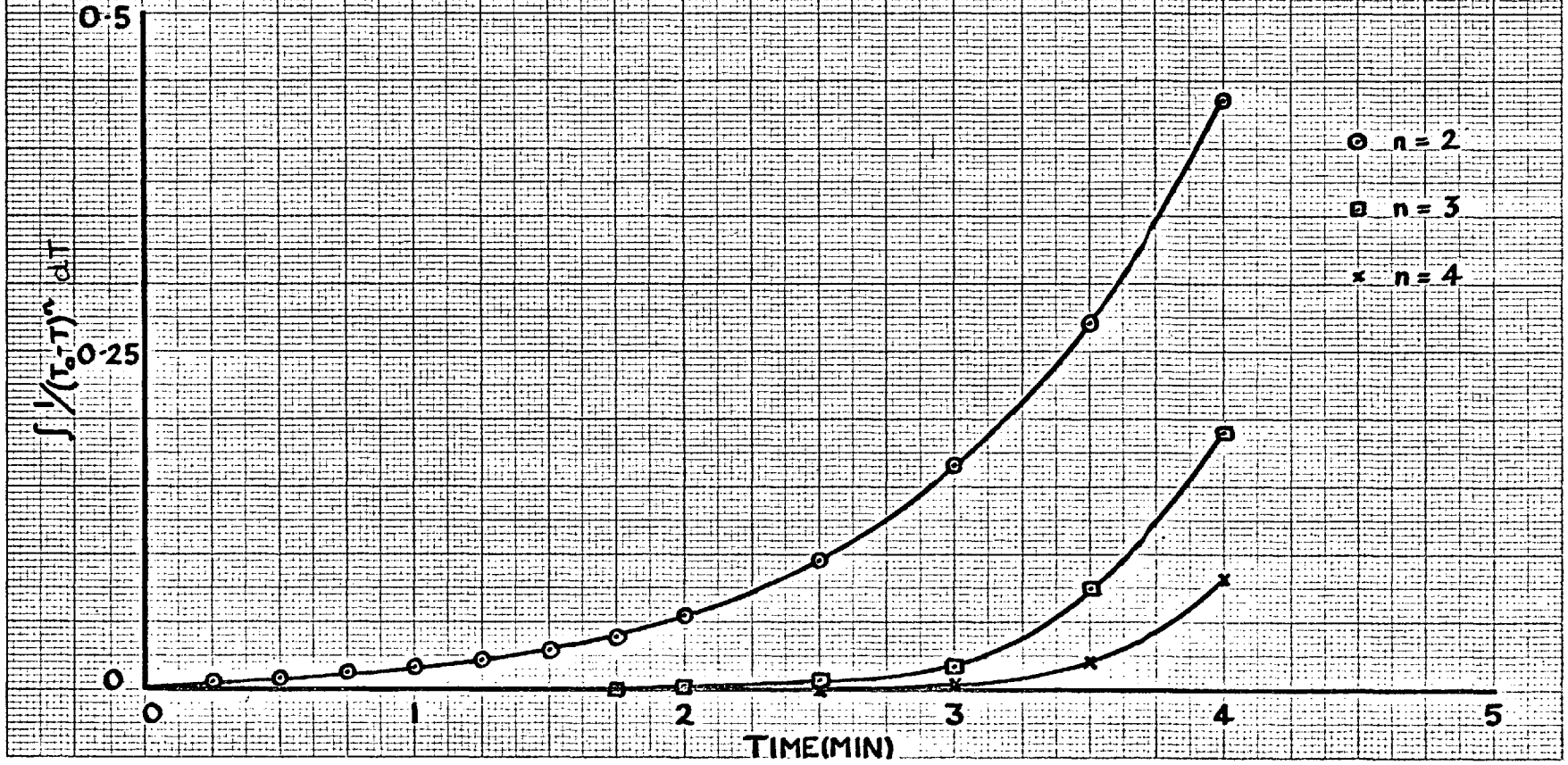


FIGURE 34

COMPARISON OF THE HEAT-UP OF KAOLIN AND SODIUM NITRATE AT 300°C AND ONE ATMOSPHERE PRESSURE.

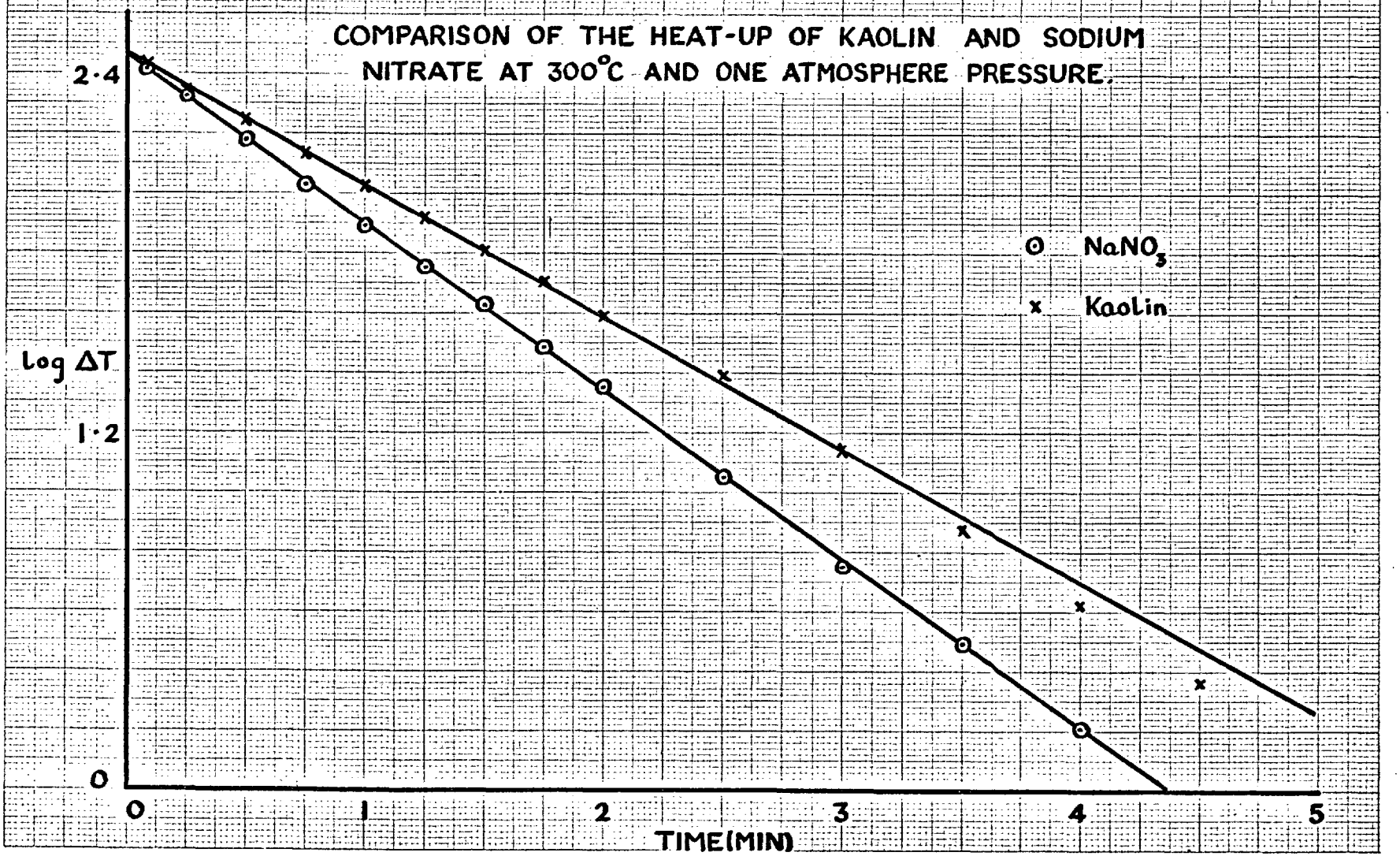


FIGURE 35

COMPARISON OF LOG ΔT vs. t PLOTS FOR SODIUM NITRATE AT TWO TEMPERATURES.

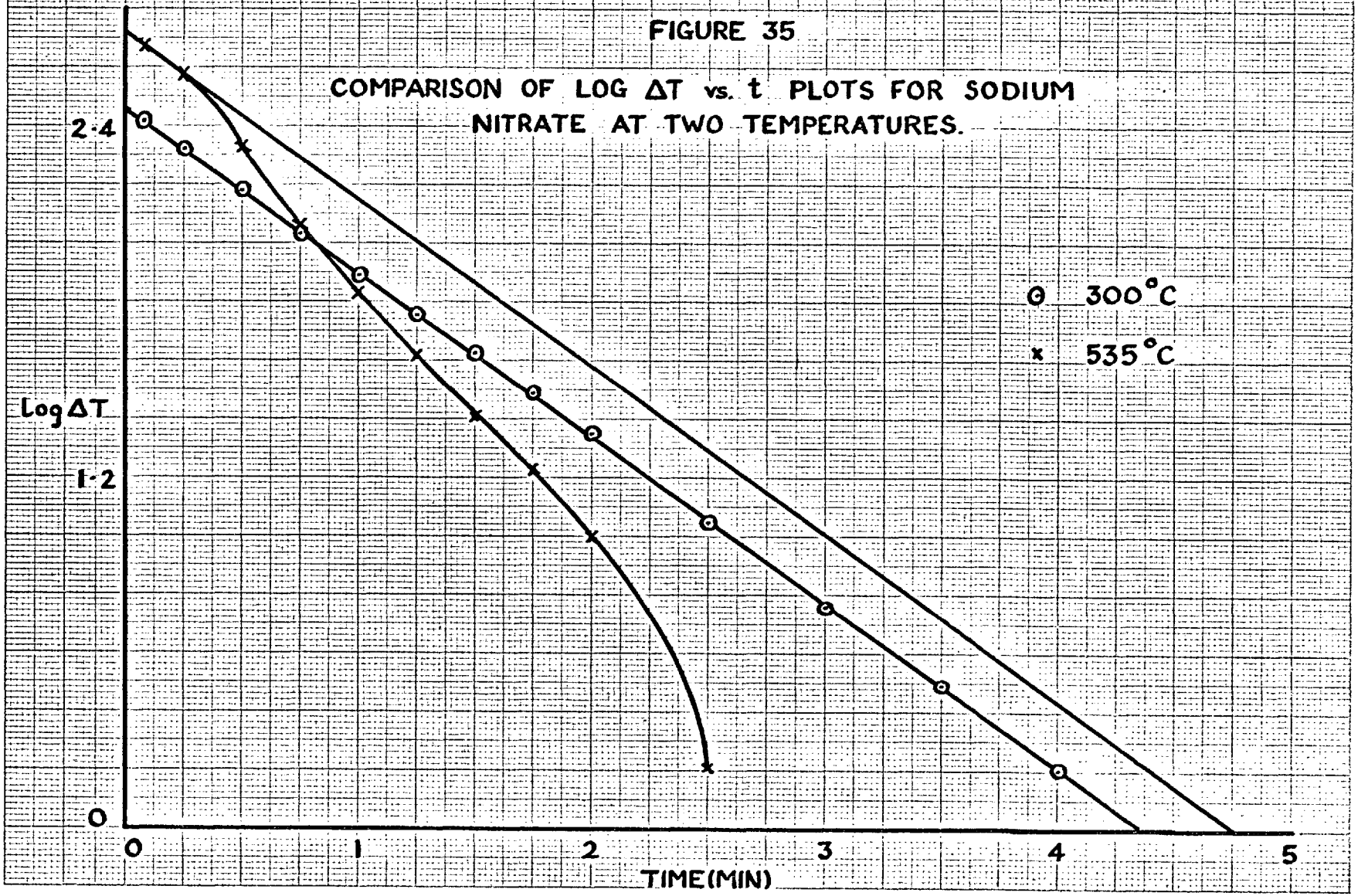


FIGURE 36

LOG ΔT vs. t PLOTS FOR SODIUM NITRATE AND 22·25% Mg + 77·75% $NaNO_3$ AT VARIOUS TEMPERATURES.

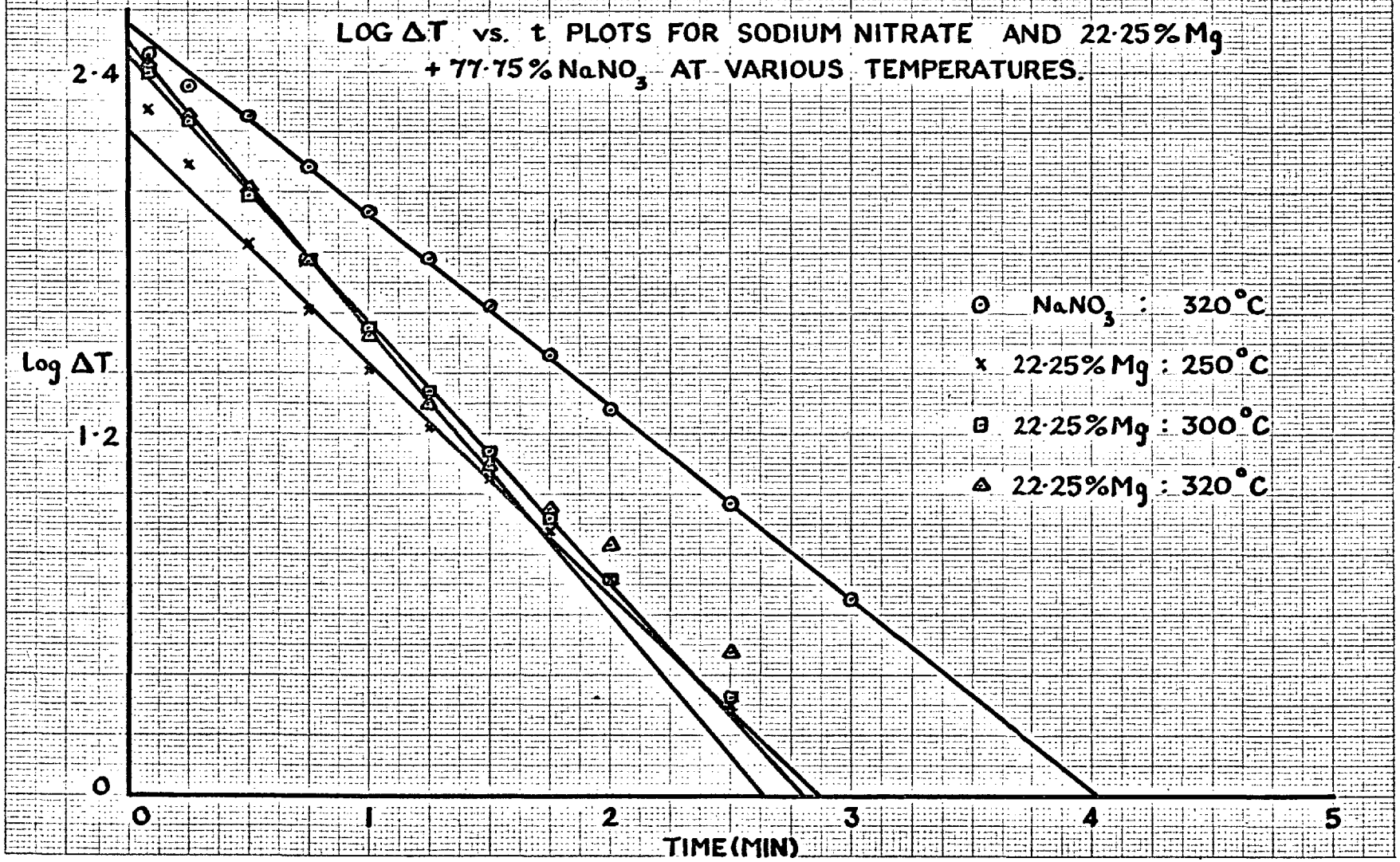


FIGURE 37

SELF-HEATING TEMPERATURES OF SODIUM NITRATE AT ATMOSPHERIC PRESSURE.

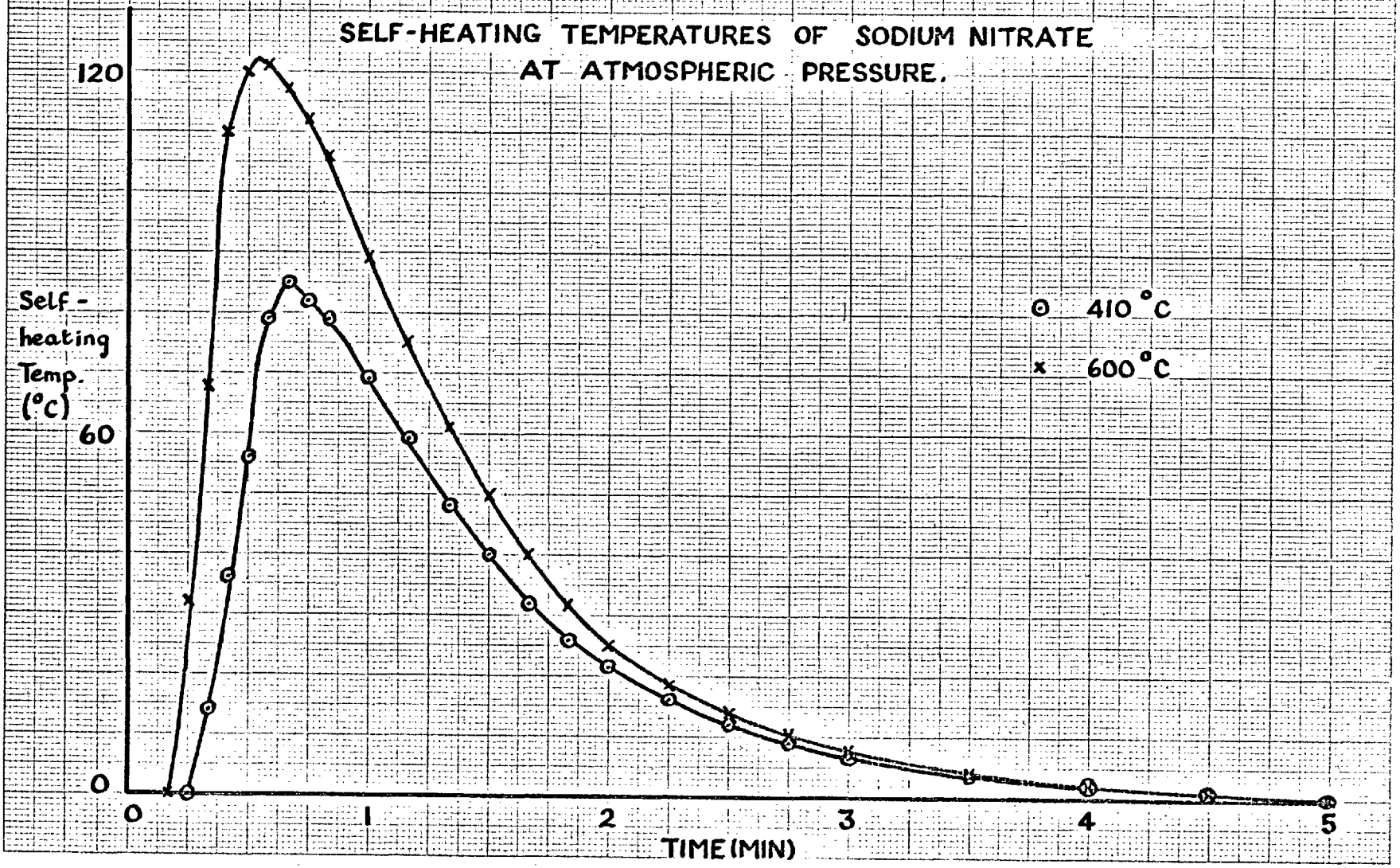


FIGURE 38

SELF-HEATING TEMPERATURES OF 22·25% Mg + 77·75% $NaNO_3$ AT ATMOSPHERIC PRESSURE.

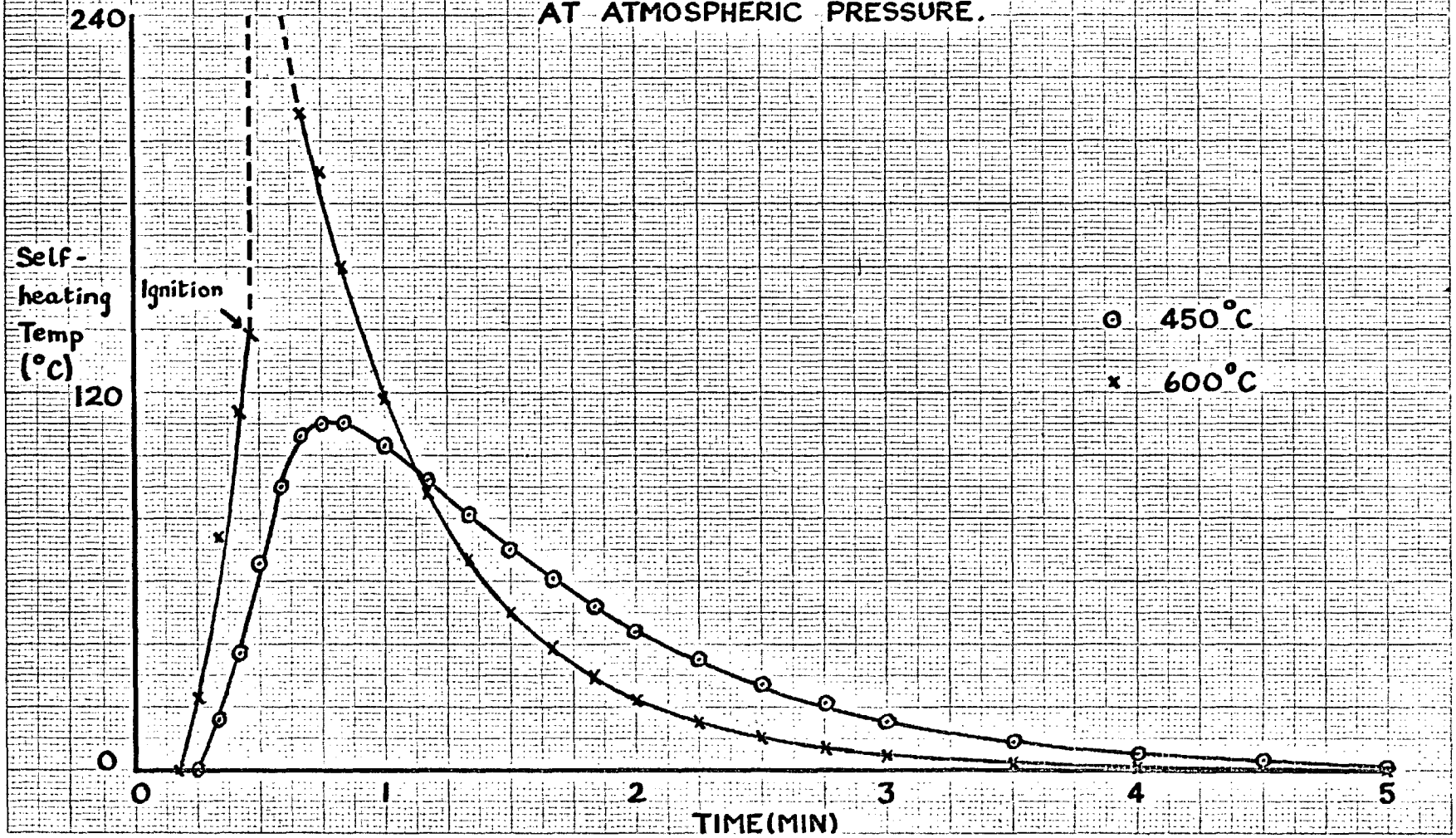


FIGURE 39

SELF-HEATING TEMPERATURES OF SODIUM NITRATE AT 10^{-4} mm.Hg PRESSURE.

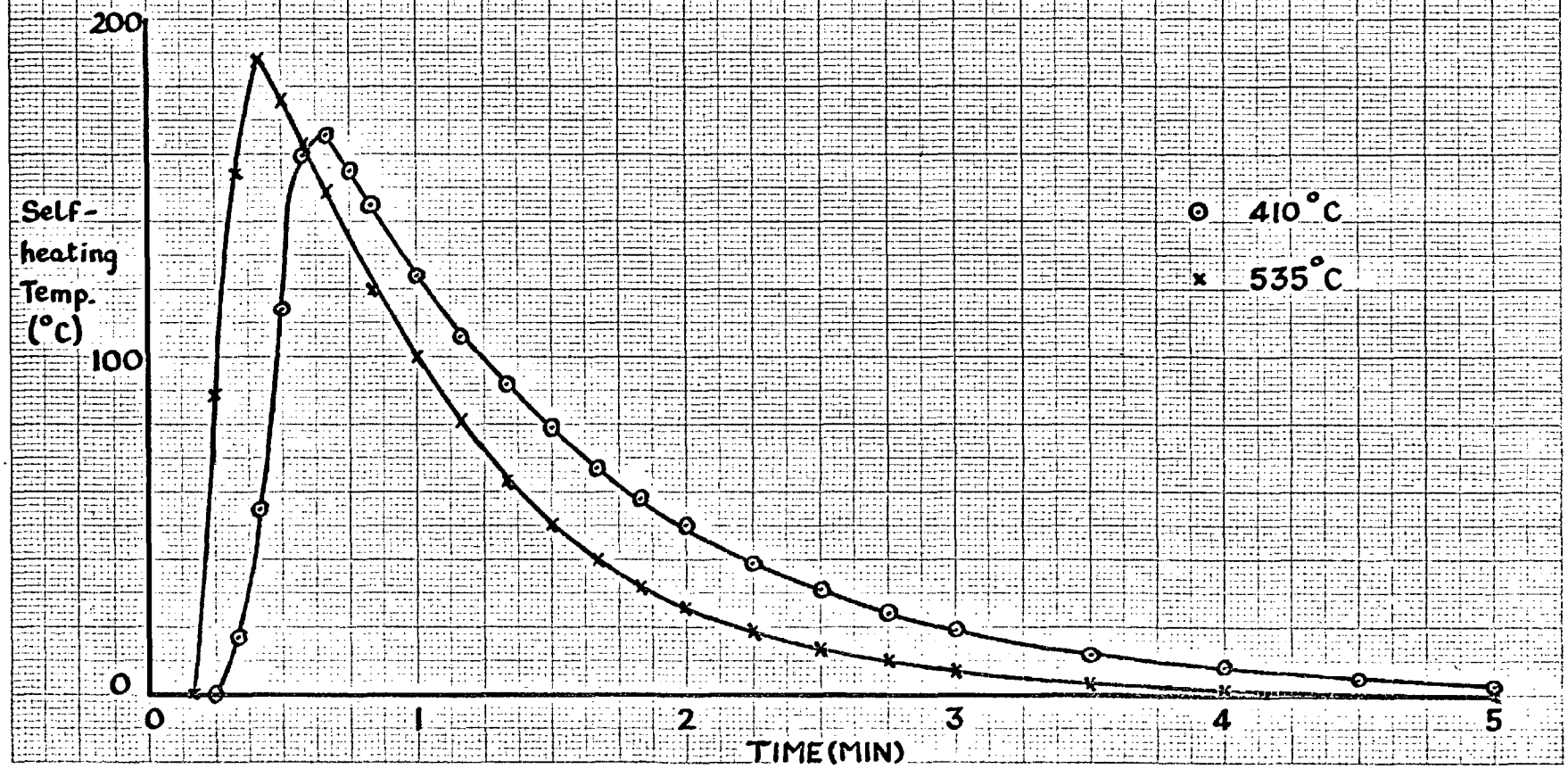


FIGURE 40

SELF-HEATING TEMPERATURES OF 22·25% Mg + 77·75% $NaNO_3$ AT 10^{-4} mm. Hg PRESSURE.

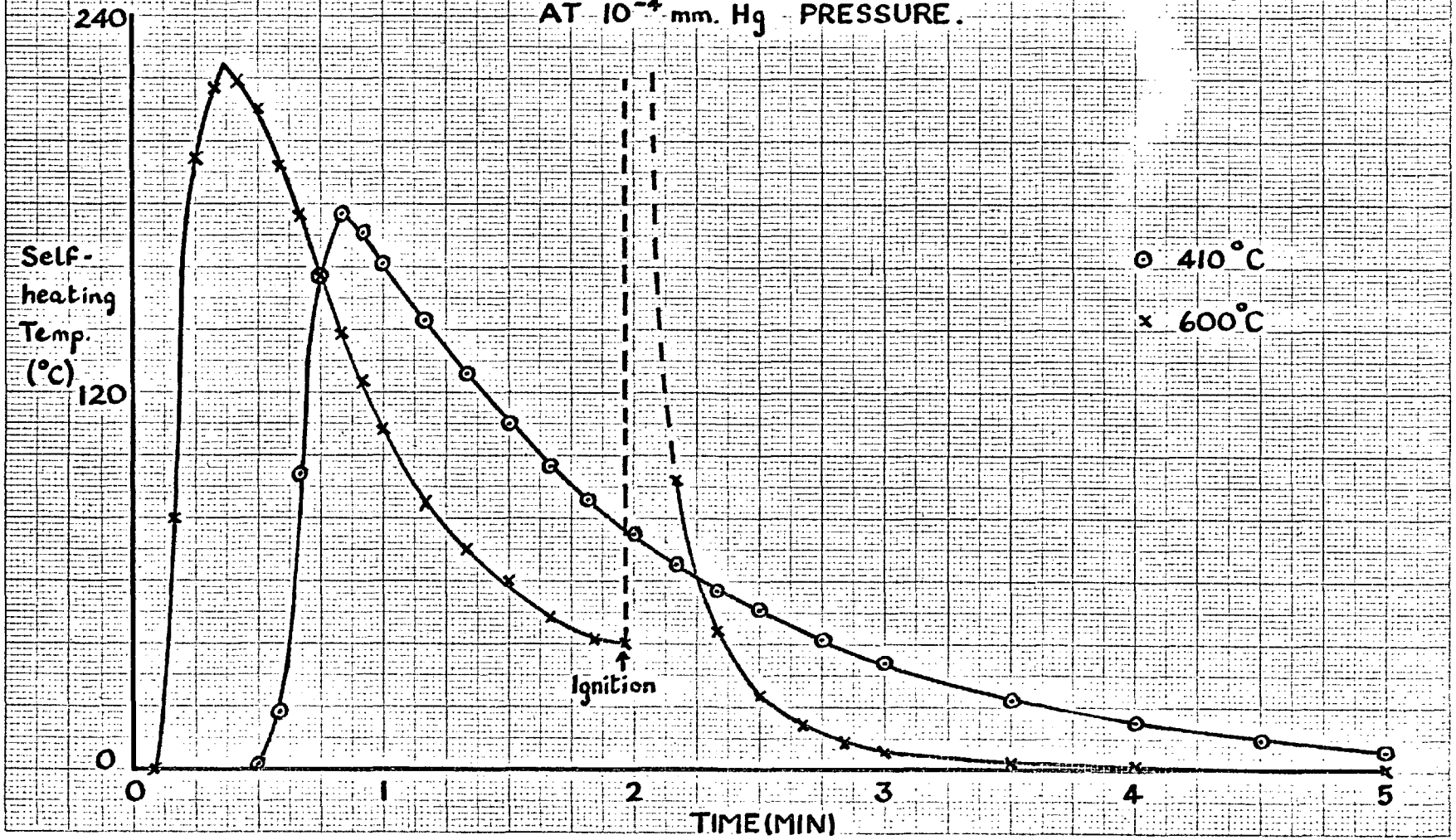


FIGURE 41

VARIATION OF THE ACTIVATION ENERGY WITH MAGNESIUM CONTENT.

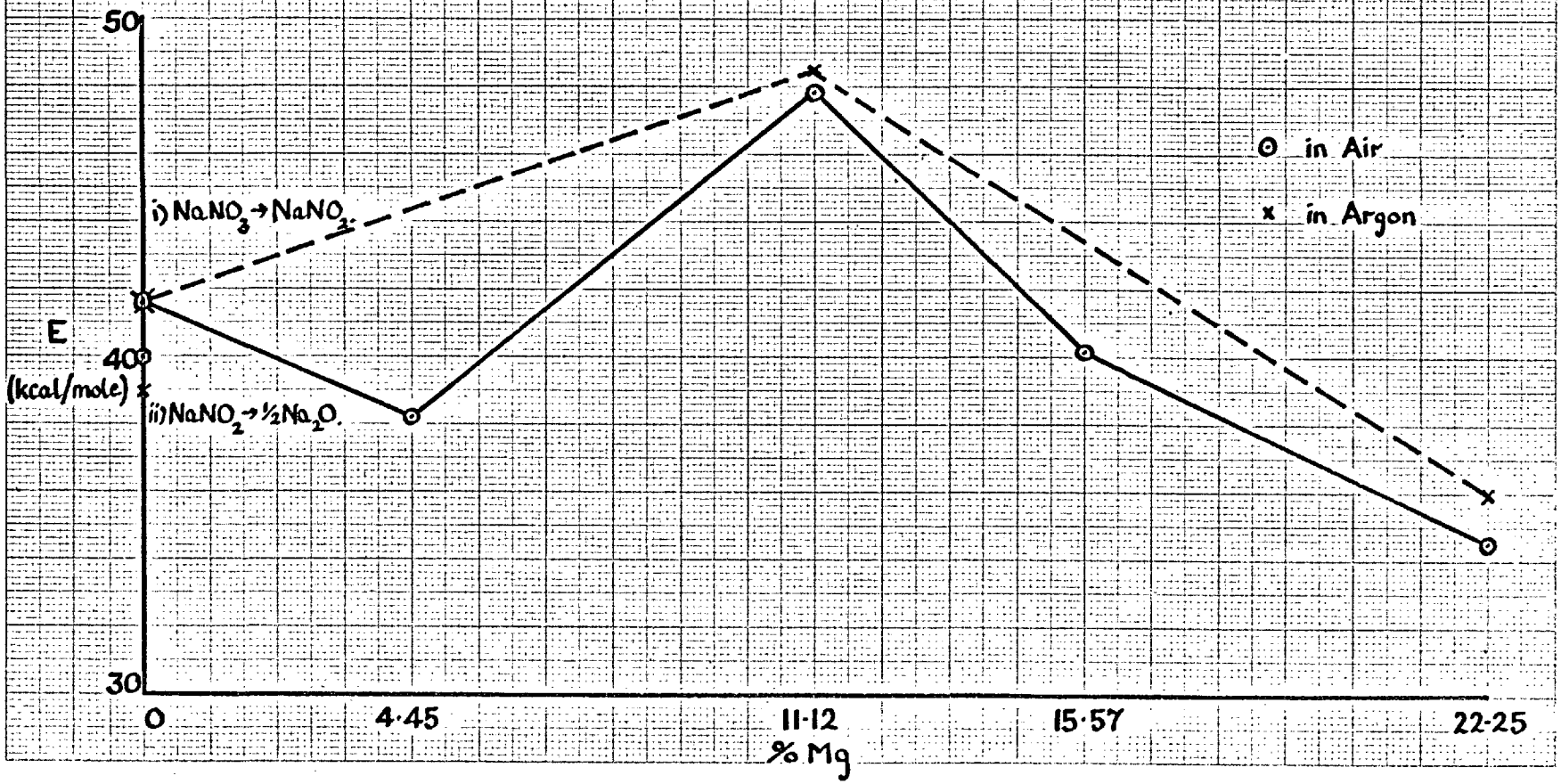


FIGURE 42

VARIATION OF THE PRE-EXPONENTIAL FACTOR WITH MAGNESIUM CONTENT.

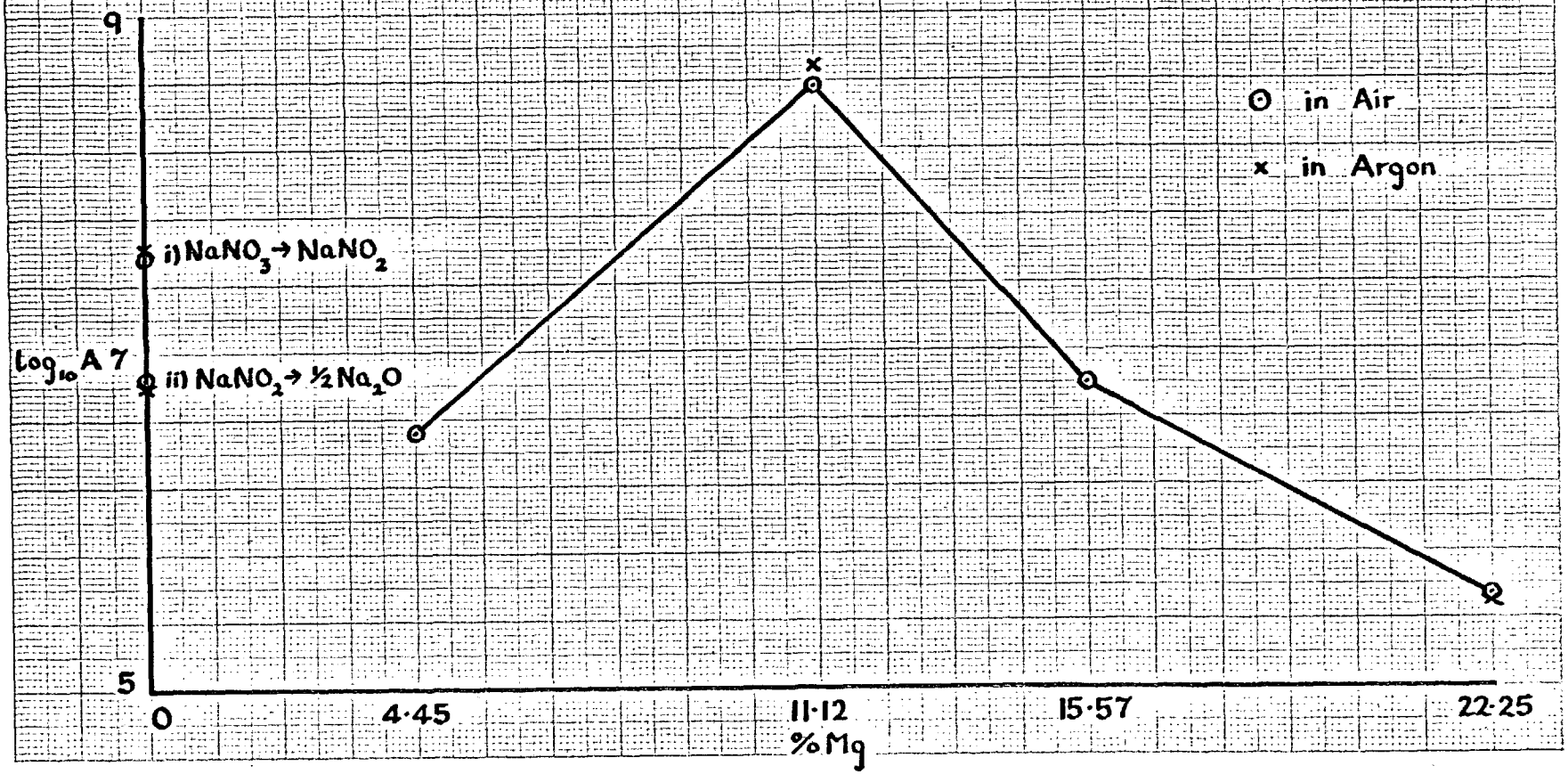


FIGURE 43

VARIATION OF IGNITION TEMPERATURE WITH MAGNESIUM CONTENT.

